Title

Modulators of maladaptive decision-making in methamphetamine dependence: A multimodal neuroimaging approach

Author

Kohno, Milky

Publication Date

2013

Peer reviewed|Thesis/dissertation

UNIVERSITY OF CALIFORNIA

Los Angeles

Modulators of maladaptive decision-making in methamphetamine dependence: A multimodal neuroimaging approach

A dissertation submitted in partial satisfaction of the

requirements for the degree Doctor of Philosophy

in Neuroscience

by

Milky Kohno

2013

ABSTRACT OF THE DISSERTATION

Modulators of maladaptive decision-making in methamphetamine dependence: A multimodal neuroimaging approach

By

Milky Kohno

Doctor of Philosophy in Neuroscience

University of California, Los Angeles, 2013

Professor Edythe D. London, Chair

Methamphetamine (MA) abuse is associated with maladaptive decision-making, particularly when risk and reward are involved. Decision-making deficits are linked to impairments in the neural circuitry underlying cognitive control and the evaluation of reward, especially in dopaminergic brain regions that guide motivated behavior and prefrontal cortical (PFC) regions that modulate them.

However, the mechanism by which dopamine neurotransmission and frontostriatal activity are integrated to affect choices is unclear. MA-dependent individuals exhibit abnormal patterns of activation in the prefrontal cortex and striatum and deficits in markers of dopamine function. The concurrent examination of the dopamine system and brain activation during decision-making may provide a better understanding of the neural systems underlying cognitive

appraisal of risk and reward and identify systems-level biomarkers for maladaptive decision-making in human drug dependence.

To understand the modulators of maladaptive decision-making, the two studies presented here examined the relationships between risky decision-making, brain function, striatal dopamine receptor availability and the intrinsic activity of the mesocorticolimbic network in MA-dependent and healthy control (HC) individuals.

The studies assessed brain activation while subjects performed the Balloon Analogue Risk Task (BART), using functional magnetic resonance imaging (fMRI). In study 1, the relationship between dopamine D2-type receptor availability and risky decision-making was tested. Sixty healthy research volunteers performed the BART while undergoing fMRI, and in a subset of participants, dopamine D2-type receptor availability was measured using $F^{[18]}$ positron emission tomography (PET). The second study examined differences in risk-taking performance and associated activation between MA-dependent and healthy control groups and related differences to intrinsic brain activity of the mesolimbic system using resting-state fMRI.

Study 1 showed that the modulation of activation by level of risk in the dorsolateral prefrontal cortex (DLPFC) during risky decision-making was negatively correlated with striatal D2-type dopamine receptor availability and positively related to total amount earned on the BART. The decision to limit risk and cash out was associated with the modulation of activation in the ventral striatum, which was positively related to striatal D2-type dopamine receptor availability. In addition, both measures were negatively related to the number of risky choices following the choice to cash-out as well as to the total amount earned on the BART.

In study 2, the groups differed in the modulation of activation by levels of risk during risky decision-making where the MA-dependent subjects compared to controls exhibited greater

modulation of activation in the ventral striatum while the healthy controls had greater modulation of activation in the DLPFC. MA-dependent subjects also exhibited greater intrinsic activity in the mesocorticolimbic network compared to healthy control subjects. Furthermore, the intrinsic activity of the mesocorticolimbic system was negatively related to the modulation of activation in the DLPFC during risky decision-making in the MA-dependent group.

The results suggest that the enhanced sensitivity for potential reward and diminished cortical inhibition of reward-driven responses exhibited by MA-dependent subjects may result from the altered relationship between prefrontal cortical activation and functional connectivity of dopaminergic pathways. By combining positron emission tomography, task-based fMRI and resting-state fMRI, these studies help clarify the biological underpinnings and network interactions of risky decision-making in human drug dependence.

The dissertation of Milky Kohno is approved.

J. David Jentsch

Robert M. Bilder

Craig R. Fox

Edythe D. London, Committee Chair

University of California, Los Angeles
2013

Dedication

For my brother, Ray Kohno

May you rest in peace

11/12/1977 - 12/01/2013

TABLE OF CONTENTS

ACKNOWLEDGMENTS

The research described here was funded in part by NIH grants P20 DA022539, R01 DA020726 (EDL), M01 RR00865 (UCLA GCRC), and endowments from the Thomas P. and Katherine K. Pike Chair in Addiction Studies (EDL), and the Marjorie M. Greene Trust. M Kohno was supported by institutional training grant T32 DA 024635 and F31 DA033120-02.

Chapter 3 is a version of Kohno, M., Ghahremani, D.G., Morales, A.M., London ED Risk-taking behavior: Dopamine D2/D3 receptors, feedback, and frontolimbic activity. Cerebral Cortex *August 2013*. The author would like to thank the co-authors and the research director (EDL) for their contributions.

Curriculum Vitae

Education

- University of California, Los Angeles
  PhD candidate Neuroscience (7/29/2011)
  Dissertation: Modulators of maladaptive decision-making in methamphetamine dependence
- University of California Berkeley
  BA Psychology

Research Positions

Laboratory of Dr. Edythe London — **University of California, Los Angeles**
Graduate student researcher — June 01, 2008 – Present

NeuroFocus Inc. — **Berkeley, CA**
Researcher — March 2006- August 2007
Project: Advertising efficacy determined by EEG

Laboratory of Dr. Robert Knight — **University of California, Berkeley**
Research Assistant — March 2004- May 2006
Project 1: EEG multi sensory integration study
Project 2: fMRI study investigating neural plasticity amongst unilateral stroke patients

Teaching Experience

Guest Lecturer: Psychopharmacology, Psych 15	University of California, Los Angeles
Guest Lecturer: Seminars in Addiction	University of California, Los Angeles
Teaching Assistant: Neuroanatomy 101	University of California, Los Angeles
Teaching Assistant: Neuroanatomy 102	University of California, Los Angeles
Mentor: At-risk Youth Service Program	University of California, Berkeley

PUBLICATIONS AND PRESENTATIONS

Publications

1. Berman, SM, Licinio, J., Paz-Filho, G., Wong, M., **Kohno**, M., London, ED: Effects of leptin deficiency and replacement on cerebellar responses to food-related cues. *Cerebellum* February 2013, 12 (1): 59-67.
2. Galvan, A., Schronberg, T., **Kohno, M.,** Poldrack, R.A., London, ED: Greater risk sensitivity of dorsolateral prefrontal cortex in young smokers than in nonsmokers. *Psychopharmacology* May 2013
3. **M. Kohno**, D. Ghahremani, A. Morales, C. Robertson, K. Ishibashi, A. Morgan, M. Mandlekern, E. D. London: Dopamine D2/D3 Receptors, Feedback, and Frontolimbic Activity. *Cereb Cortex.* August 2013.
4. **M. Kohno**, A. Morales, D. Ghahremani, G. Hellemann, E. D. London: Risky decision-making:Prefrontal Function and Mesocorticolimbic Resting-state Connectivity in Methamphetamine Users (manuscript under review)
5. A. Morales, D. Ghahremani, **M. Kohno**, E. D. London: Cigarette Exposure, Dependence and Craving are Related to Insula Structure in Young Adult Smokers (manuscript under review)

6. A.C. Dean*, **M. Kohno***, G. Hellemann, E. D. London: Childhood Maltreatment and Amygdala Connectivity in Methamphetamine Dependence (manuscript in preparation)

Abstracts

1. **M. Kohno,** A. Morales, D. Ghahremani, E. D. London (2013) Risky decision-making: Prefrontal Function and Mesocorticolimbic Resting-state Connectivity in Methamphetamine Users. Nanosymposium at SFN 43th Annual Meeting
2. **M. Kohno,** A. Morales, D. Ghahremani, E. D. London (2013) Strength of corticostriatal resting state connectivity linked to prefrontal activation during risky decision-making in controls but not in methamphetamine dependence. OHBM conference
3. **M. Kohno**, D. Ghahremani, A. Morales, E. D. London (2012): Risky decision-making: The relationship between neural activation and white-matter microstructure. OHBM conference
4. **M. Kohno**, D. Ghahremani, A. Morales, E. D. London (2012): Risky decision-making: Frontolimbic activation, dopamine receptors, and recent experience. SFN 42th Annual Meeting
5. **M. Kohno**, A. Morgan, E. D. London (2011) Faulty decision-making in methamphetamine dependence is associated with abnormal reward valuation and disruptions in white matter integrity in the reward circuitry. SFN 41th Annual Meeting
6. **M. Kohno**, A. T. Morgan, E. D. London (2011) Methamphetamine use and impulsivity, the relationship between self-report and behavior. College on Problems of Drug Dependence 69th Annual Meeting.
7. **M. Kohno** (2010) Maladaptive Decision-Making in Addiction. "Lecture for Seminars in Addiction Psychiatry, UCLA"
8. **M. Kohno**, A. Morales, E. D. London (2010) Cigarette exposure associated with abnormal white matter development in adolescent smokers. Abstract for poster presentation, Society for Neuroscience 40th Annual Meeting
9. **M. Kohno**, D. Ghahremani, A. Galvan, E. D. London (2010) The influence of prior experiences on neural activity during risk taking in methamphetamine users. OHBM conference
10. **M. Kohno (2010)** Cigarette exposure associated with abnormal white matter development in adolescent smokers. Nicotine and Nicotinic Receptors in Addiction Research & Treatment Symposium oral presentation
11. **M. Kohno** (2009) Risky decision-making: An fMRI study. UCLA Addiction symposium oral presentation
12. **M. Kohno**, D. Ghahremani, A. Galvan, E. D. London (2009) Neural correlates of risky decision-making in methamphetamine dependence. Society for Neuroscience Annual Meeting 41st Annual Meeting

Academic and Professional Honors

- 2005-2007 – Mentor of the year award- Youth Service Program Berkeley California
- 2004-2006 – Dean's list honors, University of California, Berkeley
- 2007-2010 - Achievement Rewards for College Scientists– Scholarship in Academic Excellence
- 2008-2010 - University of California, Los Angeles - Quality of Graduate Education Award
- 2009- Frontiers in Addiction Research: NIDA Mini-Convention Travel Award
- 2010-2011 - National Institute of Health (T90 DA023422) - Neuroimaging Training Fellowship
- 2011- Brain Research Institute, UCLA – Society for Neuroscience Travel Award
- 2011-2012 - National Institute of Health (T32 DA024635) -Translational Neuroscience of Drug Abuse Fellowship
- 2012-2013 - National Institute of Health- Ruth L. Kirschstein National Research Service Award (NRSA)

CHAPTER 1
INTRODUCTION

METHAMPETAMINE DEPENDENCE

Prevalence and Societal Costs

Amphetamine type stimulants, such as ecstasy and methamphetamine (MA), now rank as the most commonly abused drugs worldwide, second only to cannabis (UNODC, 2011). According to the 2008 National Survey on Drug Use and Health (NSDUH; SAMHSA, 2007), lifetime prevalence of MA use in Americans aged 12 and older exceeded 13 million individuals (5% of the population), with past-year users exceeding 1.3 million (0.5% of the population); of those, nearly 320,000 individuals used it in the past month. Data from the 2007 Monitoring the Future survey further show that 1.8%, 2.8%, and 3.0% of 8th, 10th, and 12th graders, respectively, have tried MA in their lifetime, and NSDUH (2005) data suggest that MA is prominent across socio-economic and cultural subgroups, age groups, and gender.

MA dependence is associated with numerous adverse and costly consequences. The cost of MA abuse has been associated with a number of medical, social, and criminal justice consequences, including cost associated with premature death, crime, lost work productivity, environmental damage and health care.[1-3] Admissions to treatment for MA use disorders in 2009 and 2010 exceeded admission rates for all other substances, including alcohol[4, 5]. However, with no approved pharmacological interventions for MA dependence, behavioral therapies are currently the only intervention strategies for MA addiction but show only modest effects.

Behavioral and Cognitive Deficits in MA dependence

Individuals who abuse MA often exhibit disturbances in mood and emotional processing. Early abstinence is associated with mood disorders [6, 7], along with high levels of depression and anxiety during early abstinence [8-11]. In addition, MA abuse is often associated with irritability, interpersonal sensitivity, and uncontrolled anger [11]. A combination of these negative mood states likely contribute to maladaptive decision-making strategies that are frequently observed in MA-dependent individuals[12, 13 14].

Poor decision-making is a characteristic of substance dependence and has been implicated as factor in the initiation and maintenance of drug abuse[15]. In this regard, a hallmark of drug addiction is the persistence of drug self-administration despite the risk of adverse consequences. A growing literature supports a role for risky decision-making in the development and maintenance of addictive behavior. For example, among individuals who abuse amphetamine, risk-taking is positively associated with the length of drug abuse[16], and among those who abuse heroin, the severity of dependence is positively associated with risky behaviors[17]. In laboratory tests of decision-making, individuals who abuse substances exhibit a greater propensity for risk-taking compared to matched-controls[18-20].

In addition to risky decision-making, impairments in the temporal discounting of rewards may contribute to relapse, where long-term benefits of abstinence are discounted for the more immediate rewarding effects of drugs. The Delay Discounting Task[21] models this potential contributor to addiction by presenting the participant with choices that require comparisons of different reward magnitudes across different delay periods. The task measures an individual's rate of discounting a reward as a function of time, and individuals with drug abuse disorders consistently choose smaller, sooner rather than a larger, later reward compared to healthy

individuals[22]. Neuropsychological testing has also identified impairments in executive functioning in MA users [23, 24], specifically in abstract thinking, mental flexibility [25, 26], impulsivity [27, 28], response inhibition [29, 30], sustained attention [31], attentional control [30], verbal and nonverbal fluency [32], and verbal and working memory [33, 34].

Together the data show that MA-dependent individuals have impairments in executive functioning, which may contribute to the maintenance of addiction. Despite high rates of attrition and relapse [35, 36], cognitive behavioral therapy, contingency management, and motivational interviewing [37, 38] are the only available treatment options for MA dependence. Behavioral therapies targeting specific cognitive domains could aid in the adaptation of behavior; however, without a better understanding of the neural systems underlying the cognitive appraisal of reward and consequences, the success of behavioral therapies may be limited.

Brain Function in MA dependence

fMRI Studies of Decision-making

As frontal and striatal regions and their interconnections play a critical role in integrating motivational and cognitive processes to produce optimal behavior, frontostriatal impairments may contribute to maladaptive decision-making in MA-dependent individuals. In tasks that assess decision-making in the presence of varying likelihoods of risk and reward magnitude, MA-dependent subjects take longer to make decisions and use suboptimal decision strategies[16]. Consistent with the reports that chronic MA use results in changes in biological markers of neuronal function in cortical areas[39], and changes in dopamine transporter and receptor density in subcortical areas[40], stimulant users show impairments in prefrontal and striatal activation during risky decision-making. A meta-analysis of studies that have examined risky decision-making in

individuals with substance use disorders found that drug users consistently show impairments in the striatum and in the orbital frontal, dorsolateral prefrontal, medial frontal and anterior cingulate cortices [41]. Specifically, poly-drug users exhibited hyperactivity of the ventral medial frontal, right frontopolar, and superior frontal cortex during risky decision-making[42] while performing the Iowa Gambling Task. Similarly, cocaine-dependent individuals showed less activation than controls in the medial prefrontal cortex and right dorsolateral prefrontal cortex (DLPFC) and the striatum when making risky decisions[43]. On a different task of risky decision-making, drug-dependent individuals show less activation in the nucleus accumbens and medial prefrontal cortex[44]. Not only is the activation of frontal and striatal systems central to decision-making, the degree of activation in these regions has been associated with relapse to MA use. An fMRI study of decision-making using a 2-choice prediction task, found that activation of the insula and the dorsolateral prefrontal, parietal, and temporal cortices was predictive of maintained abstinence from MA, with lack of activation predictive of relapse[45]. Together, the studies suggest that frontal and striatal impairments may underlie maladaptive decision-making in MA dependence and may contribute to the maintenance of addiction.

Another component of risky decision-making is the subjective value of a reward and its associated risk and latency. An fMRI study using the Delayed Discounting Task associated the propensity for smaller more immediate rewards to the abnormality in neural recruitment of the left dorsolateral prefrontal cortex and intraparietal sulcus[22]. While control subjects showed increasing BOLD signal with more difficult choices, MA users showed recruitment that was similar for both easy and difficult choices[22]. Another study found similar results, where controls compared to MA users exhibited greater activation in DLPFC as well as in the ACC and caudate[46]. The results suggest that inefficient decision-making in MA-dependent individuals may

represent stimulus-bound behavior due to impairments in frontal and parietal activation.

Outcome and Feedback on Decision-making Processes

Studies of decision-making focus on neural networks associated with anticipation of a reward and delivery of reinforcements [47, 48]; however, only a limited number of studies have examined the role of outcome and feedback on subsequent decision-making. In a decision-making task that involves uncertainty, administered to a healthy control sample, the activation of the superior temporal gyrus is preferentially associated with the selection of an action if the previous trial resulted in a positive outcome [49], and the activation of the insula was associated with the probability of selecting a safe response following a punished trial[50]. In a study examining win–stay/lose–shift strategies, controls showed greater success-related patterns of neural activation in orbitofrontal, dorsolateral prefrontal and anterior cingulate cortices than MA-dependent individuals, while MA-dependent individuals showed hypoactivation in these regions irrespective of reward[51]. These results suggest that MA-dependent individuals are less sensitive to losses than healthy controls and point to impairments in the neural mechanism responsible for risk-prediction signals [52] and reinforcement learning[53].

Cerebral Glucose Metabolism

Studies examining brain glucose metabolism using [^{18}F]fluorodeoxyglucose (FDG) in MA-dependent individuals have found metabolic abnormalities in brain regions subserving decision-making. For example, relative glucose metabolism was 12 % less in the caudate and 6% less in the putamen in abstinent (2 weeks- 35 months) MA users than in control subjects[54]. Metabolic abnormalities were also found in abstinent (4-7 days) MA users in limbic and paralimbic cortices. Compared with controls MA users exhibited less relative regional glucose metabolism in the ACC and insula but greater relative regional glucose metabolism in the

amygdala, ventral striatum, and orbital frontal cortex.[55] One study found changes in cerebral glucose metabolism over the first month of abstinence in MA-dependent users, suggesting that long-term effects of chronic use may be obscured in the first weeks of abstinence. [56] Together the studies suggest that recovery is region specific and vary as a function of abstinence.[56] Alterations in cerebral metabolism in MA users may reflect active gliosis [54], as glia cells exhibit greater metabolic activity than neurons and inflammation is associated with high glucose metabolism [57].

Brain Structure

Evidence also points to MA-related structural deficits in both cortical and subcortical brain regions. High-resolution MRI scanning and surface-based computational image analyses has been used to determine structural differences along the cortical surface and in the hippocampus between 22 MA users and 21 healthy control subjects [58]. MA users exhibited less gray matter volume in the cingulate, limbic, and paralimbic cortices compared to healthy controls. A deficit was also observed in the gray matter volume of the right inferior frontal gyrus but this effect did not retain statistical significance after correction for multiple comparisons. A different study confirmed frontal structural deficits in MA users with the finding of lower gray matter density in the right middle frontal gyrus, which was positively correlated with errors on the Wisconsin Card Sorting Task[59]. In contrast, one study showed that abstinent (10-330 days of abstinence from MA-dependent) MA users exhibited greater cortical volumes than healthy control subjects[60]. Differences in subcortical volume has also been shown between MA-dependent and healthy individuals. Abstinent MA-dependent abusers were found to have larger bilateral volumes of the caudate, nucleus accumbens[60], putamen and globus pallidus[60, 61] in comparison with healthy controls. Greater subcortical gray matter volumes in MA users

compared to controls may reflect a compensatory response to chronic MA-induced neuronal injury followed by reactive gliosis [62].

Although these studies show structural abnormalities in MA-dependent individuals, cigarette smoking was not accounted for. Given that smoking has been associated with lower gray matter density in the PFC, dorsal ACC and the right cerebellum [63], the greater prevalence of cigarette smoking in the MA-dependent than the control group in the aforementioned studies may account for some of the structural differences. A study comparing gray matter volume in non-cigarette smokers, cigarette smokers and MA users found that both control smokers and MA-dependent smokers exhibited less gray matter volume in the orbitofrontal cortex and caudate nucleus compared with non-cigarette smokers [64]. In comparison with control smokers, MA-dependent smokers had smaller gray-matter volumes in frontal, parietal and temporal cortices [64]. Taken together, the evidence points to widespread prefrontal cortical and striatal deficits in MA-dependent individuals, spanning regions implicated in decision-making and reward processing.

BIOLOGICAL EFFECTS OF METHAMPHETAMINE

Pharmacology and Mechanism of Action

Psychostimulants exert multiple effects in the central nervous system by increasing cytoplasmic and extracellular concentrations of dopamine, as well as other monoamines including serotonin, norepinephrine, epinephrine, and histamine[65]. Among stimulants, MA is unique in its pharmacokinetic and pharmacodynamic properties. The methyl group on the molecule renders methamphetamine more lipid-soluble than amphetamine and facilitates the transport of the substance across the blood–brain barrier and stabilizing against enzymatic degradation by monoamine oxidase (MAO)[65]. Methamphetamine potentiates dopaminergic neurotransmission by enhancing dopamine release and inhibiting its reuptake[65]. By virtue of

similarity in chemical structure to dopamine and other monoaminergic transmitters, MA enters the nerve terminal through dopamine transporter (DAT), norepinephrine transporter (NAT) or serotonin 5-HT transporter (5-HTT)[66] (Fig. 1.1).

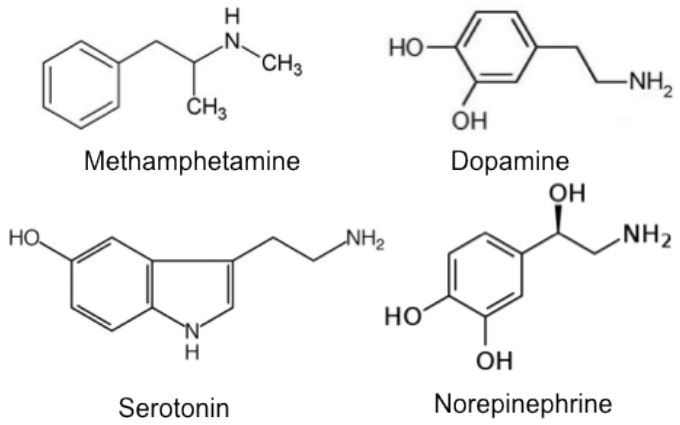

Figure1.1 Chemical structures of methampetamine, dopamine, serotonin and norepinephrine.

The dopamine system: A target of MA action

Dopamine, along with norepinephrine and serotonin, is one of a series of amine neurotransmitters within the brain. Dopamine synthesis originates from the amino acid precursor tyrosine, which is transported through blood-brain barrier into the dopamine neuron. The rate-limiting step in dopamine synthesis is the conversion of tyrosine to L-dihydroxyphenylaline (L-DOPA) by the enzyme tyrosine hydroxylase. L-aromatic amino acid decarboxylase then converts L-DOPA to dopamine[67].

MA substantially elevates intracellular dopamine levels[65] by interacting with dopamine synthesis, packaging and release in the dopaminergic terminal. Within the cell, vesicular monoamine transporter 2 (VMAT2) transports monoamines from cellular cytosol into synaptic vesicles [68, 69]. MA inhibits the activity of VMAT2 resulting in the transportation of dopamine out of the vesicles and into the intracellular space. MA also interferes with the activity of

monoamine oxidase to degrade excess intracellular dopamine[67], and increases the expression of tyrosine hydroxylase[67], the rate-limiting step in dopamine biosynthesis (Fig. 1.2). The reversal of DAT function by MA releases intracellular dopamine into the synaptic cleft, and the blockade of DAT prevents dopamine reuptake[70]. The results are high concentrations of extracellular dopamine, and hence increased dopaminergic activity.

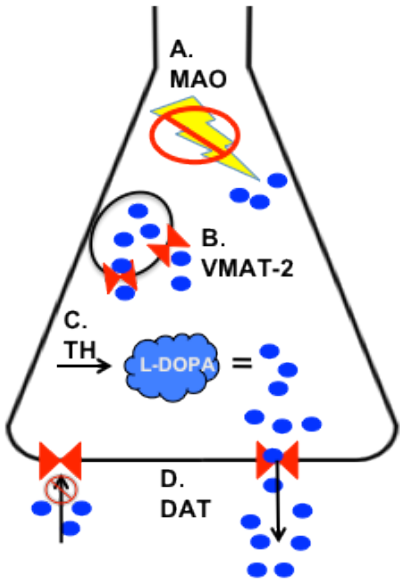

Figure 1.2 Actions of methamphetamine. A) MA limits the degradation of intracellular dopamine by inhibiting MAO activity. B) MA reverses VMAT-2 function and dopamine is transported out of the vesicles rather than into them. C) MA enhances expression of tyrosine hydroxylase D) MA reverses DAT function, where dopamine is released into the synaptic cleft, and reuptake is inhibited.

Methamphetamine and Synaptic Dopamine

Although research has strongly suggested that increased dopamine transmission significantly contributes to the reinforcing effects of psychostimulants [71], it is noteworthy that cocaine has higher affinity for the 5-HT transporter than other monoamine transporters, whereas amphetamines have stronger affinity for the norepinephrine transporter[72] than for other monoamine neurotransmitter transporters. The reinforcing properties of stimulants, however, are correlated with their affinities for the dopamine transporter but not for the serotonin or norepinephrine transporters[73]. Moreover, depletion of dopamine in the nucleus accumbens, but not of forebrain norepinephrine[74], markedly attenuates self-administration of cocaine or d-amphetamine[75-80]. Self-administration of stimulants increases extracellular dopamine levels in the nucleus accumbens, which decline between infusions. In order to maintain extracellular dopamine above a threshold

level, the decline in accumbens dopamine levels is thought to promote drug self-administration [81, 82].

MA-induced Abnormalities of the Dopamine System

Dopamine G Protein-coupled Receptors

Dopamine receptors are a class of G protein-coupled receptors with dopamine as the primary endogenous ligand for these receptors. There are at lease five subtypes of dopamine receptors and are designated D1 through D5. Based on sequence homology and pharmacology of these receptors, dopamine D1 and D5 receptors are classified as D1-type while D2-type dopamine receptors include the D2, D3, and D4 subtypes [83-85]. Pharmacological studies indicate that both D1-type and D2-type dopamine receptors play critical roles in psychostimulant reinforcement[86, 87]. Self-administration studies show that rats and non-human primates self-administer full D1- type agonists, and systemically administered D1- type antagonists decrease the reinforcing efficacy of cocaine[88-92]. Similarly, D2-type agonists are self-administered by rats and non-human primates[93-96], and D2-type antagonists also reduce cocaine and d-amphetamine reinforcement[78, 95-98].

Dopamine D2-type receptor availability has been used as a biomarker for the investigation of postsynaptic dopamine function in human MA abusers. Using PET with [^{11}C]raclopride, a study comparing abstinent MA users to controls showed that MA users had lower levels striatal D2-type receptor availability in the caudate (16%) and putamen (10%).[99] Similarly, lower levels of D2-type receptor availability in the caudate (16.1%), putamen (12.6%) and nucleus accumbens (8.4%) have also been shown in abstinent MA users using [^{18}F]fallypride, a radioligand with affinity for D2-type receptors[100]. A longitudinal study examining the effects of abstinence on D2-type receptor availability was conducted on MA-

dependent participants at baseline, after six months of abstinence and again after nine months of abstinence[101]. During early withdrawal, MA users had lower D2-type receptor availability than controls in the caudate[101]. Low levels of baseline D2-type receptor availability in caudate and putamen were associated with the ability to remain abstinent while participating in an intensive outpatient drug rehabilitation program, where MA users with low baseline D2-type receptor availability relapsed during the nine-month follow-up period[101].

Dopamine D3 receptors also have a role in mediating behavioral responses to psychostimulant drugs. A number of studies using D3-knockout mice suggest that one function of the D3 receptor is to modulate behaviors by inhibiting activation of dopamine D1 and D2 receptors[102]. Low doses of amphetamine produce greater conditioned place preference in D3-knockout mice than wild types[103], and D3-knockout mice exhibit heightened locomotor responses to cocaine, amphetamine and morphine[104]. In addition, a selective D3 receptor antagonist, NGB 2904 produces an exaggerated amphetamine-induced locomotor activity in wild type but not D3-knockout mice[104]. Furthermore, high doses of NGB 2904 stimulate spontaneous locomotion in wild type mice but not D3-knockout mice. These findings are consistent with an inhibitory role for D3 receptors in psychostimulant-induced hyperactivity.

One in vivo neuroimaging study of human MA dependence has investigated D3 receptor density using the radioligand, [^{11}C]-(+)-propyl-hexahydro-naphtho-oxazin ([^{11}C]-(+)-PHNO). Although [^{11}C]-(+)-PHNO lacks absolute specificity for D3 receptors, it does have higher differential binding at this receptor subtype. The study showed that MA users compared to healthy controls exhibited greater binding in the substantia nigra, a region with high expression of D3 receptors and in regions that express both D2 and D3 receptors such as the globus pallidus and ventral pallidum. MA users, however exhibited less binding in D2-rich striatal regions

compared to controls, which may be attributed to low striatal D2-type receptor availability associated with MA use. As highly selective D3 receptor antagonists attenuates drug seeking, self-administration, and cue- and stress-induced reinstatement, the authors conclude that the upregulation of D3 receptors in MA-dependent individuals may contribute to the addicted state in humans.

Dopamine Transporter

MA reverses the function of the dopamine transporter (DAT), and several research groups have investigated the presynaptic terminals of dopaminergic neurons in MA users. A study that examined dopamine terminal density using [^{11}C]WIN-35,428, a DAT ligand, found that abstinent (mean of 3yrs) MA users had DAT levels that were 23% less in the caudate and 25% less in the putamen compared to controls[40]. Lower levels of DAT were also detected using [^{11}C]d-threo-methylphenidate in abstinent (> 11 months) MA users compared to the controls in the caudate 27.8% and putamen 21.1% [105]. Lower levels of DAT have also been found in the nucleus accumbens, DLPFC and amygdala[106, 107]. In these studies, levels of DAT were negatively related to duration of MA use and severity of psychiatric symptoms[106, 107]. Preliminary results in 5 MA abusers indicate a recovery of DAT with prolonged abstinence. Abstinence for a year or greater compared to abstinence of 6 months or less showed a 19% and 16% increase DAT levels in the caudate and putamen, respectively[108].

Vesicular Monoamine Transporter

PET studies have also examined the density of vesicular monoamine transporters (VMAT2), which are responsible for the redistribution of dopamine from synaptic vesicles to the cytosol in MA users[109]. The results from these studies have been mixed. One study found no group differences in VMAT2 binding using [^{3}H]dihydrotetrabenazine (DTBZ) in MA users

compared to controls[110]. Using the ligand [^{11}C]dihydrotetrabenazine, another group showed that MA users had 10% less binding than healthy controls[111]. A third study comparing MA users to controls found greater ligand binding in the caudate, putamen and ventral striatum in MA users[112]. Postmortem studies showed no differences in VMAT levels between MA users and non-drug users[110], and inconsistencies in imaging results may, in part, be explained by differences in the duration and severity of drug use between patient populations[112]. Alternatively, the results may reflect differences in neuronal recovery, as the duration of abstinence varied across studies. VMAT binding using PET may, therefore be a useful tool to detect dynamic changes in vesicular dopamine levels.[112]

NEURAL ADAPTATIONS IN THE MESOCORTICOLIMBIC NETWORK

Mesotelencephalic Dopamine System

Although distinct dopaminergic cell groups have been identified in the midbrain, hypothalamus, and olfactory bulb, most findings support the conclusion that addictive drugs share the common property of enhancing the effect of midbrain dopamine function[113]. The mesotelencephalic dopamine systems consists of dopamine neurons located in the midbrain nuclei of the substantia nigra (SN), the ventral tegmental area (VTA), and the midbrain reticular formation[114]. Broadly, the midbrain dopamine system is separated into the functionally distinct systems.

Nigrostriatal Dopamine System

Dopaminergic projections from substantia nigra to the striatum form the nigrostriatal pathway. Dopamine is released from proximal dendrites in the substantia nigra pars compacta and from distal dendrites of nigrostriatal neurons of the substantia nigra pars reticulata[115, 116]. Dopamine released in the pars compacta can act at D2-type autoreceptors located on soma and

dendrites of nigrostriatal neurons to reduce firing rates[114]. Neurons of the substantia nigra pars compacta provide dopaminergic innervation to striatum. Striatal outputs are all GABAergic inhibitory neurons. The striatum projects to the medial and lateral segments of the globus pallidus as well as to the substantia nigra pars reticulata. As the substantia nigra pars reticulata provide inhibitory inputs to GABAergic inhibitory neurons in the thalamus [117, 118], the disinhibition of the dorsomedial nucleus of the thalamus results in the excitation of prefrontal motor neurons. As such the nigrostriatal system is critical in motor function and the dysfunction in this system underlies Parkinson's disease [119, 120].

Mesocorticolimbic Dopamine System

The mesocortical circuit originates in the VTA of the midbrain and projects to the nucleus accumbens, the amygdala, the hippocampus and the medial prefrontal cortex cortices[113, 121, 122]. Signaling in this pathway is primarily dopaminergic; however, glutamatergic and GABAergic signaling play an important modulatory role in the activity of VTA dopaminergic neurons. Dopaminergic neurons are the principle neurons in the VTA, however 20% of neurons are GABAergic. GABAergic neurons synapse on dopaminergic cells within the VTA but also projects to limbic regions. The VTA also receives GABAergic afferents from the nucleus accumbens and ventral pallidum. It is speculated that the inhibition of GABAergic interneurons results in the disinhibition of dopamine cells and enhance firing frequency[114]. The VTA also receives glutamatergic projections from the medial prefrontal cortex, pedunculopontine and the subthalamic nucleus. Glutamate release from prefrontal projections play a critical role in N-methyl-Daspartate (NMDA) dependent firing of dopaminergic neurons in the VTA[123]. Stimulation of NMDA receptors activates the dopaminergic neurons that project to the prefrontal

cortex while stimulation of non-NMDA receptors activate dopaminergic neurons that project to the nucleus accumbens[124, 125].

There is considerable overlap in the VTA neurons that form the mesolimbic and mesocortical pathways. These systems, therefore, are often considered in combination as the mesocorticolimbic pathway[126]. The mesocorticolimbic pathway contributes to drug craving, drug withdrawal, and compulsive drug-taking behaviors[121, 127]. As microinjections of dopamine antagonists into the terminal regions of the mesocorticolimbic but not the nigrostriatal dopamine system block the reinforcing effects of stimulant drugs[128], the mesocorticolimbic system seems to be the primary neurobiological substrate of addiction[113].

Neural Adaptations Associated with Stimulant Action

Excess dopamine neurotransmission caused by stimulants induces epigenetic and neuroplastic changes that lead to altered neuronal morphology and cell signaling in the mesocorticolimbic system. Activation of dopamine receptors results in the activation of protein kinase (PKA). The phosphorylation of receptor subtypes or transcription factors by PKA lead to an increase or decrease of the transcription of downstream genes[129]. Dopamine receptors and other G-protein coupled receptors undergo complex processes of desensitization and down-regulation after short-term exposure to stimulants[130]. Dopamine receptor desensitization can occur through the phosphorylation by several types of protein kinases which promote the internalization of receptors[131]. G-protein receptor kinases (GRKs), which phosphorylate only the agonist-bound form of the receptor lead to the sequestration of the receptor resulting in desensitization[132]. The phosphorylation of receptors can also directly lead to reduced coupling of G proteins[131] or indirectly by reducing the expression of the α subunit of the G_i protein[133].

Stimulant-induced Changes in RGS9-2 Expression

Alterations in dopamine receptor G-protein coupling following chronic cocaine exposure have been associated with the dysregulation of other proteins that modulate the α subunit[131]. RGS proteins modulate heterotrimeric G-protein function through the stimulation of GTPase activity that is intrinsic to G protein α subunits[134]. RGS proteins attenuate or terminate G protein-mediated signaling. Levels of the gene variant RGS9-2 are highly expressed in striatal regions and the olfactory tubercle, with very little expression in other brain regions. RGS9 expression is found on the medium spiny projection neurons in the striatum[135], and can alter dopaminergic neurotransmission in striatum. Chronic administration of cocaine increases RGS9-2 immunoreactivity in the nucleus accumbens and dorsal striatum[136], and RGS9-2 overexpression decreases sensitivity to dopamine D2-type receptor activation[136]. Stimulant-induced changes of RGS9-2 expression, therefore, may mediate the functional changes in dopaminergic signaling seen in addiction.

Stimulant-induced Epigenetic Expression

Dopamine receptor activation can also activate cAMP-dependent protein kinases (PKA) leading to the phosyphorylation of the transcription factor, cAMP response element binding protein (CREB)[137]. The activated CREB protein then binds to cAMP response elements (CRE), thereby increasing or decreasing the transcription of the downstream genes[129]. CREB regulates the transcription of a number of genes including, c-fos[138] the neurotrophin BDNF (brain-derived neurotrophic factor)[139], and tyrosine hydroxylase[140, 141].

Stimulant-induced Expression ΔFosB

Stimulant-induced expression of ΔFosB is thought to mediate the transition to addiction, as changes in ΔFosB overlap with the pattern of changes in the nucleus accumbens induced by chronic cocaine administration[142]. Stimulant use leads to a reduction in lysine

dimethyltransferase, G9a, which mediates histone methylation and is regulated by the transcription factor ΔFosB. Chronic stimulant use leads to ΔFos accumulation in the nucleus accumbens. The overexpression of ΔFosB leads to a reduction in G9a thereby reducing dimethylation of histones and altering gene expression in the nucleus accumbens[142]. Reductions in G9a are associated with an increase in dendritic spines of neurons in the nucleus accumbens and an increase in cocaine-seeking behavior[142].

Stimulant-induced changes in Glutamate Receptors

Ionotropic glutamate receptors such as α-amino-3-hydroxy-5-methyl-4-isoxazolepropionic acid (AMPA) and *N*-methyl-D-aspartate (NMDA) receptors that mediate fast excitatory glutamate transmission, and metabotropic glutamate receptors (MGlu) that mediate slower, modulatory glutamate transmission contribute to the alterations in glutamatergic transmission seen with long term drug use[130]. Adaptations of glutamate transmission in the nucleus accumbens are critical for the expression of addictive behaviors, such as drug-seeking and sensitization[143]. Specifically, release of glutamate in the projection from the PFC to the nucleus accumbens provokes reinstatement of drug seeking in animals trained to self-administer cocaine[144]. In addition, enhanced glutamate release during cocaine exposure lead to enduring post-synaptic structural changes in the nucleus accumbens, including enhanced dendritic spine density and dendritic branching on medium spiny neurons[144]. These morphological changes are associated with both the degree of cocaine intake and the development of behavioral sensitization to cocaine[145-149].

ΔFosB mediates the synthesis of AMPA glutamate receptors[130]. An increase in glutamate receptor subunit, GluR1, in the VTA is associated with stimulant-induced increases in ΔFosB[150], and is implicated in the enhanced responsiveness of VTA neurons to AMPA glutamate receptor

stimulation following chronic stimulant exposure[151]. The role of AMPA receptors in addiction is further established by studies showing that the over expression of specific AMPA receptor subunits by viral-mediated gene transfer within the VTA sensitizes animals to the reinforcing effects of morphine[150]. Neurons of the nucleus accumbens also show altered expression of glutamate receptor subunits[151, 152] and an increase in the responsiveness to glutamate[60]. In addition, administration of AMPA glutamate receptor antagonists in the nucleus accumbens prevent drug- and cue-induced reinstatement[153, 154].

Neuroadaptations are also seen in NMDA receptors and NMDA-mediated glutamatergic signaling. Activation of dopamine D1 receptors by stimulant drugs can potentiate NMDA receptor function through the phosphorylation of the NR2B subunit of NMDA receptors[155]. The phosphorylation of NMDA receptors leads to the trafficking of NMDA receptors to the postsynaptic membrane and redistribution of receptors across the dendritic spines[156]. In response to psychostimulants, the upregulation and distribution of NMDA receptors may mediate enhancements of NMDA receptor currents and NMDA receptor-dependent potentiation of AMPA receptor currents in the striatum[157]. This view is in line with results showing that repeated amphetamine exposure enhances glutamate release in the nucleus accumbens upon subsequent psychostimulant challenge[128, 158]. Furthermore, regional antagonism of NMDA receptors has shown that the NMDA receptors in the VTA are important for the induction of drug-induced sensitization[159]. In addition, simultaneous activation of dopamine and NMDA receptors by stimulant drugs induces extracellular-signal regulated kinase (ERK) activation[160, 161] leading to activation of transcription of genes that are critical for drug-induced plasticity[162].

Presynpatic mGluR2/3 are inhibitory autoreceptors that suppress excess glutamate release from the presynaptic terminal[163] and are, in part, responsible for regulating extracellular

glutamate release from the PFC to the nucleus accumbens. Stimulant-induced reductions in the inhibitory function of mGluR2/3 contribute to the increase in glutamate release during drug seeking behavior[164]. mGluR2/3 agonists suppress behavioral signs of nicotine withdrawal[165] and reduce cocaine reinforcement and drug-seeking behavior[166]. However, while mGluR2/3 agonists attenuate cue-induced reinstatement of cocaine-seeking behavior, mGluR2/3 agonists also have effects on the suppression of seeking natural reinforcers[166].

Stimulant-induced changes in Corticostriatal signaling

Chronic cocaine and amphetamine exposure has also been shown to increase the spine density and the number of branched spines in pyramidal cells of the prefrontal cortex (PFC) [147, 148]. Drug-induced morphological plasticity leads to long-lasting alterations in neurotransmission[167] and enhances the activity of prefrontal glutamatergic projections through G-protein coupled receptors[168]. Both D1-type and D2-type receptors are found in the PFC. However, expression of D1-type receptors on pyramidal neurons in the PFC appear to be substantially greater than D2-type receptors, and both types of dopamine receptors are localized on GABAergic interneurons and presynaptic excitatory glutamate terminals[169-171]. An increase in D_1 receptor hypersensitivity and membrane excitability in PFC neurons has been shown following cocaine exposure[172, 173] through stimulant-induced PKA modulation of D1 receptor function. The enhanced excitatory output of PFC projection neurons contributes to NMDA-dependent AMPA-mediated long-term potentiation in dopamine neurons[157, 174] and an increase in the firing rate of VTA DA neurons[175]. Alterations in the morphology of prefrontal neurons and presynaptic glutamatergic release in the mesocorticolimbic DA system play a critical role in mediating several important components of addictive behaviors. For example, increased release of glutamate in the nucleus accumbens occurs following drug- and stress-primed

reinstatement[176], and treatments that prevent the release of glutamate also prevent drug-seeking behavior in rats[144]. Moreover, direct electrical stimulation of PFC leads to rewarding effects and sensitization to stimulants, whereas lesions to the PFC or impairments in corticomesolimbic glutamate transmission prevent the development of cocaine sensitization[177-179].

Circuit and Network Abnormalities in Addiction

As discussed above, stimulant drugs lead to dopamine nerve terminal degeneration, greater dopamine turnover, lower levels of dopamine receptor and DAT availability[40, 99-101, 110]. In addition, these dysfunctions, including increases of local tonic dopamine concentrations, presynaptic glutamate release and reduction of long-term depression in dopamine neurons[180], lead to impaired striatal and cortical function. However, systems-level assessments of the neural adaptations that result from chronic drug intake in humans have only recently been explored. Recent advances in assessing network dynamics through resting-state functional connectivity (RSFC) have contributed to new insights of drug-related adaptations by identifying abnormalities in the functional organization of brain systems[181]. As repeated drug exposure induces long-lasting synaptic plasticity and sensitization of the mesocorticolimbic system[182], studies have interrogated the RSFC among regions of the meoscorticolimbic system in substance users[183-185, 186]. Alterations in RSFC strength between ventral striatum and various subcortical and cortical regions have been observed in cocaine- [183-185], prescription opioid- [186], and heroin-dependent individuals[187] compared to healthy controls.

An increase in RSFC between subcortical and cortical areas[185, 187] has been shown in some studies, while a decrease in connectivity[183, 186] has been shown in others. For example, abstinent cocaine-users exhibited an increase in RSFC between ventral striatum and ventromedial PFC (vmPFC) [185]; however, active cocaine-users had a general decrease in RSFC

between most regions within the mesocorticolimbic pathway and interconnected brain areas[183]. A single dose of methylphenidate has recently been shown to decrease RSFC between the striatum and VTA in cocaine users. Therefore, differences in results between active and abstinent cocaine users may reflect differences in recent drug use, and the extent to which the mesocorticolimbic system is activated by direct or indirect stimulation of the dopamine system. While understanding of the molecular and cellular drug-induced changes within the mesocorticolimbic has advanced[188], much less is known about the effect of these manifestations on cognition or associated brain function.

Summary

The mesocorticolimbic neural circuitry contributes to a variety of adaptive and goal-directed behaviors, and pathological drug-seeking behavior may arise as a consequence of stimulant-induced changes in this circuit[189]. These include changes in cell signaling through induction of immediate early genes [190], changes in dendritic morphology, and neurotransmitter receptor adaptations. Chronic exposure also leads to changes in protein expression, receptor function and circuit-level interactions of the mesocorticolimbic system that mediate craving, loss of control, and compulsive drug-seeking behavior[191, 192]. The mesocorticolimbic system is thought to contribute to decision-making and reward learning by encoding information of the expected value of rewards through dopaminergic neurotransmission. [193, 194] As dopaminergic and glutamatergic inputs to the nucleus accumbens play a critical role in the activity of this mesocorticolimbic circuitry and underlying motivational processes, the stimulant-induced increase, reduction, and redistribution of dopaminergic and glutamatergic markers may explain the abnormal evaluation of rewards and maladaptive decision-making processes exhibited by addicted subjects.

It is important to understand the impact of neurobiological abnormalities on functions that subserve motivated drug-taking behavior in order to consider them as therapeutic targets for the improvement of treatment of MA dependence. The neurobiology of addiction, however, is not a unitary construct, as addiction is a disorder with unique adaptations in cellular, molecular, and behavioral processes [113, 192]. This dissertation focuses on mesocorticolimbic dysregulation as it relates to maladaptive decision-making that characterizes addiction.

The specific focus of this dissertation investigates decision-making involving risk and reward and the underlying neurobiological substrates that are affected in MA-dependent individuals. Risky decision-making is most frequently associated with choices that involve uncertainty, which is often defined in terms of the variability[195], unknown distribution probabilities[196] and the uncontrollability[197] of an outcome. These definitions differ substantially from the broader meaning of risk used by clinicians and the lay public. In addition to the uncertainty of an outcome, many associate risk with situations that potentially lead to adverse consequences. As risk-taking is a multidimensional construct and can be both adaptive and maladaptive, for the purposes of this dissertation, risky decision-making includes choices that involve uncertain outcomes with a potential for both loss and reward. To the extent that faulty decision-making is a target for addiction therapies, understanding its determinants in the context of different contingencies and associated neural modulators could perhaps, aid in the development of more effective interventions.

This dissertation includes two projects. They were designed to understand the neural processes that underlie human risky decision-making and to apply this knowledge to identify dysfunctions that contribute to maladaptive decision-making in MA dependence. The research was intended to address gaps in the literature and to provide a more coherent examination of

neural substrates of decision-making.

Evidence from rodent studies suggests that dopaminergic neurotransmission contributes to risky decision-making[198,199] and that D2-like receptor agonists enhance reward-expectancy signaling via dopaminergic transmission[200] and reduce risky choices[201]. In humans, however, the interaction of the dopamine system with frontostriatal activation and risky decision-making has not been examined. Therefore, in Study 1 the relationship between risky decision-making and associated neural activation and D2-type dopamine receptor availability was examined.

The dopamine D2-type receptor ligand, [^{18}F]fallypride with PET imaging was used to measure D2-type receptor availability[202], and the BART paired with fMRI was used to examine neural activation during risky decision-making. The research objective was to examine whether striatal D2-type receptor BP_{ND} influences the dynamic interactions between frontal and striatal regions during decision-making and whether striatal BP_{ND} predicts the propensity for risk-taking in humans. Evidence for a relationship between striatal D2-type receptor BP_{ND} and risky decision-making may provide a link between the biological abnormalities in MA dependence to abnormalities in brain function during decision-making.

As striatal D2-type receptors contribute to individual differences in reward sensitivity[203], a deficit in striatal D2-type BP_{ND} in MA-dependent individuals may play a role in impairments in decision-making involving risk and reward. Goal-directed behavior may be guided by differential responses to rewards through dopaminergic signaling pathways linking the VTA, striatum and PFC (e.g., mesocorticolimbic system). It has been proposed that mesocorticolimbic dysfunction may enhance stimulus-reward associations[204, 205], and animal studies have demonstrated that signaling through the mesocorticolimbic system promotes motivated drug-seeking behavior[204, 205]. In addition, structural neuroplasticity[149] and changes in activity[206, 207] in

prefrontal and striatal regions after repeated exposure to stimulants have shown to contribute to cognitive and motivational impairments. However, empirical evidence that links intrinsic activity of the mescorticolimbic system and deficits in frontostriatal brain activation during decision-making in drug-dependent individuals is lacking. The objective of Study 2, therefore, was to examine the resting-state activity of the mesocorticolimbic system using resting-state fMRI as a potential mechanism to explain deficient decision-making in MA-dependent individuals. As resting-state fMRI enables the examination of intrinsic brain activity by measuring temporal correlations of spontaneous brain activity, the identification of alterations in RSFC may help delineate circuit-level dysfunction from that of specific task-based activation. Such information could clarify whether maladaptive choices in MA-dependent individuals reflect dysfunctions in specific brain regions during decision-making, intrinsic network activation, or both.

The studies in this dissertation used task-based and resting-state fMRI and PET imaging to extend behavioral observations and link abnormalities in brain activity to the dopamine system. The studies extend our understanding of the neural and molecular basis of risky decision-making and show that individual differences in a marker for dopamine function modulate risk-taking behavior. Furthermore, as the neural substrates of decision-making are influenced by intrinsic resting-state activity of the mesocorticolimbic system, the studies support a link between abnormal patterns of activation during decision-making and circuit-level abnormalities in MA dependence.

CHAPTER 2
RESEARCH QUESTIONS

The research described in this dissertation was designed to address the following questions:

Study 1

1. *What are the neural correlates of decision-making under conditions of escalating risk and reward?*

Risky decision-making is often a dynamic process but how level of risk and reward and brain processes are integrated to influence this activity is incompletely understood. The answer to this first question in study 1 will provide a better understanding of the trade-offs imposed on the brain systems involved in decision-making.

2. *What is the relationship between dopamine D2-type receptor availability and the neural circuitry underlying decision-making with increasing levels of risk and reward magnitude?*

Despite the evidence from animal studies describing the role of dopamine in risky decision-making [199, 208], few studies have examined the interaction of the dopamine system with risky decision-making in humans. The answer to this question may clarify the precise relationship between brain activation during risky decision-making and its neurochemical correlates.

3. *Do recent outcomes affect subsequent choices and are these choices influenced by dopamine D2-type receptor availability or activity of the neural circuitry underlying decision-making?*

Risky decision-making often fluctuates dynamically as a function of experience. Although the experience of loss is associated with activation in brain regions sensitive to aversive stimuli [209-

[211], studies examining the effect of losses on subsequent risk-taking behavior and associated neural substrates have been notably absent. The answer to question 3 will increase the understanding of the neurobiological processes of risk-taking by providing evidence that risky decision-making varies as a function of individual differences in the striatal dopamine system and the context in which decisions are made.

Study 2

1. *Do healthy controls and MA-dependent individuals differ in the neural correlates of decision-making under conditions of escalating risk and reward?*

There is experimental evidence that stimulant users engage in more risk-taking behaviors than non-users[212, 213]. The propensity of risk-taking has also shown to correlate with years of substance use[16]. The identification of abnormal brain processes that lead to maladaptive decision-making in drug-dependent individuals remains an important topic for the improved understanding of addictive behaviors.

2. *Do healthy controls and MA-dependent individuals differ in the intrinsic activity of the mesocorticolimbic system?*

Amphetamine sensitization has shown to increase neuronal firing of mesolimbic structures[214] in animal models of addiction, however the neuroadaptations within the mesocorticolimbic system following drug exposure[182] in humans is unclear. As activity in the mesocorticolimbic system has been linked to the reinforcing effects of drugs[189], the evaluation of the intrinsic activity of the mesocorticolimbic system in drug-dependent individuals may serve to further refine models of addictive states such as relapse, withdrawal, and craving.

3. *What is the relationship between the intrinsic activity of the mesocorticolimbic system and brain function during risky decision-making?*

Animal studies have shown that structural plasticity[149,215] and activity[206, 207] in prefrontal and striatal regions after repeated stimulant exposure are related to performance deficits, and that signaling through the mesolimbic system promotes drug-seeking behavior[204, 205]. However, empirical evidence that links mescorticolimbic resting-state activity with deficits in frontostriatal brain activation during decision-making in humans has been lacking. An answer to question 3 of study 2 may raise the possibility that abnormalities in intrinsic connectivity may contribute to maladaptive decision-making and associated frontostriatal deficits.

Aims and Hypotheses

To address these questions, the following aims and accompanying hypotheses were established:

Aim 1. Examine the extent to which an increase in levels of risk and reward modulate neural activation during risky decision-making in healthy control participants.

Hypothesis 1: Given that the DLPFC is involved in reasoning and analytical deliberation[216] and activity in the ventral striatum has been associated with tracking reward magnitude[47], healthy controls would exhibit greater modulation of activation in the DLPFC by level of risk when taking risk and greater modulation of activation in the ventral striatum by reward magnitude when taking reward.

Aim 2. To determine whether dopamine D2-*type* receptor availability is associated with risk-taking behavior and the modulation of activation in the DLPFC and striatum by level of risk and reward.

Hypothesis 2a: As D2-*type* receptor agonist administration attenuates risk-taking in rodents[201], modulation of ventral striatal activation by pump number during cash-out events would predict risk-taking in subsequent trials, and that this relationship would reflect differences in striatal BP_{ND}.

Hypothesis 2b: Signaling through corticostriatal pathways is thought to facilitate adaptive decision-making through PFC inhibition of ventral striatal activity[217]. It was, therefore, expected that striatal D2-*type* BP_{ND} would be inversely related to the modulation of PFC activation when participants took risk and also to overall monetary gain.

Aim 3. To determine whether MA-dependent individuals show functional deficits compared to healthy individuals in the neural circuitry associated with risky decision-making.

Hypothesis 3: As MA-dependent individuals exhibit abnormal evaluation of rewards and frontostriatal impairments in tasks of decision-making[22], MA-dependent individuals would show less modulation of activation in the DLPFC but greater modulation of ventral striatal activation when taking risk.

Aim 4. To determine whether MA-dependent individuals show differences in mesocorticolimbic and corticostriatal resting-state functional connectivity compared to healthy individuals.

Hypothesis 4: Given that repeated drug use leads to adaptations in the activity of the prefrontal and striatal regions and in dopaminergic projections from the VTA and limbic structures[189], MA-dependent subjects would show elevated intrinisic activity in the mesocorticolimbic network compared to healthy controls.

Aim 5. To determine whether abnormalities in resting-state functional connectivity contribute to deficits in frontostriatal activation during risky decision-making

Hypothesis 5: The balance between reward-seeking and goal-directed behavior mediated by corticostriatal and mesocorticolimbic connectivity, respectively, facilitates adaptive decision-making[217]. A positive relationship between corticostriatal RSFC and modulation of DLPFC activation in the healthy control group and a negative correlation between mesolimbic RSFC and modulation of DLPFC activation during decision-making in the MA-dependent group was hypothesized.

CHAPTER 3
RISK TAKING BEHAVIOR: DOPAMINE D2-TYPE RECEPTORS, FEEDBACK, AND FRONTOLIMBIC ACTIVATION

Decision-making is a complex executive function that integrates past experiences, present goals, and the perceived probability of outcomes. Evidence from rodent studies suggests that dopaminergic neurotransmission contributes to risky decision-making, as signaling through the mesolimbic dopamine system modulates risk preferences [198], risk-taking behavior [199], and goal-directed actions [218]. In addition, D2-type receptor agonists have shown to attenuate risk-taking in rodents [201]. Human neuroimaging studies have shown that decision-making involves frontal, parietal and subcortical regions [219-221]; however, the interaction of dopamine signaling with risky decision-making and associated activation has not been examined. Therefore, a goal of this study was to assess the extent to which striatal D2-type dopamine receptor availability (BP_{ND}) and frontal and striatal involvement during decision-making can predict risk-taking behavior.

In addition, the experience of losses and rewards has been shown to activate the insula and amygdala [222] and the striaum [48], yet few studies have examined the effect of losses and gains on activation of the circuitry underlying risky decision-making. While experience-dependent fluctuations in neural activation likely influence risky decision-making [223-225], the precise relationships between brain activation during risky decision-making and its neurochemical correlates in the context of recent outcomes are relatively underexplored. Therefore, the change in risk-taking behavior and neural activation following gains or losses was assessed.

To model decision-making and measure associated neural activation, we paired functional magnetic resonance imaging (fMRI) with an fMRI-compatible version of the Balloon

Analogue Risk Task (BART) [226]. During the BART, participants risk losing accumulated earnings for greater potential gains by continuing to pump a virtual balloon. The alternate choice is to cash out the earnings accrued at any point before the balloon explodes. We used a parametric analysis to study how an increase in risk and potential reward (represented by pump number in a trial) modulated brain activation during decision-making. Although BART performance has been associated with engagement in risky behaviors [226], human subjects who presumably have high propensities for risk-taking, including young adult cigarette smokers [227] or alcohol-dependent individuals [228] tolerate less risk on the BART than healthy controls. The BART, therefore, appears to provide an assessment of adaptive and maladaptive risk-taking behavior .

In order to determine the neural mechanism by which recent experience influences risky decision-making, we examined the effect of losses (balloon explosion) and wins (taking a reward) on neural activation and subsequent risk-taking behavior (the number of balloon pumps chosen on the next trial). Since the inclination to avoid loss is substantially greater than the preference to acquire reward [229], we expected recent losses to attenuate subsequent risk-taking, and that this change in behavior would be mediated by the insula and amygdala [222], regions that are sensitive to negative affect.

The study also examined whether responses to reward during risky decision-making are associated with individual differences in a dopaminergic marker and whether they contribute to risky choices. Because activity in dopaminergic neurons increases with the magnitude of anticipated rewards [230], and reward induces dopamine release and activation in the nucleus accumbens [231], we hypothesized that activation in the ventral striatum during cash-out events would be positively correlated with a marker for dopaminergic neurotransmission. A recent

study has shown that allelic variants of variable number tandem repeat (VNTR) polymorphism of the dopamine transporter gene (DAT1) influence risk-taking [232]. Here we determined D2-type dopamine-receptor availability, as binding potential (BP_{ND}), using [^{18}F]fallypride and PET in a subset of the participants who underwent fMRI. As D2-type receptor agonist administration attenuates risk-taking in rodents [201], we expected that modulation of ventral striatal activation by pump number during cashing out would predict risk-taking in subsequent trials, and that this relationship would reflect variation in striatal D2-type receptor BP_{ND}.

Risky decisions are determined, in part, by a combination of ventral striatal and prefrontal cortical activity that integrates motivational states [233] and the maintenance and flexible updating of goal states [216], respectively. As dopaminergic efferents from the VTA and glutamatergic efferents from the PFC often terminate on the same postsynaptic cell in the ventral striatum[234], ventral striatal D2-type receptors may play an integral role in attributing salience to available options. Efferents from the PFC have also shown to contact dopamine neurons of the VTA that project to the nucleus accumbens directly[114]. Furthermore, a striato-thalamo-cortical loop has also been described [235]. Differential responses to rewards may guide goal-directed behavior through these various signaling pathways linking the striatum and PFC. Considering this possibility, adaptive decision-making would require a balance between behavioral control and reward-seeking behavior, and this balance may be influenced by frontal cortical regulation of ventral-limbic response to reward. Consistent with this view is the observation that patients with lesions of the ventral medial PFC have difficulty resisting immediate rewards at the expense of larger, future rewards (i.e., exhibiting greater temporal discounting of rewards) [236]. We therefore expected that when participants made risky decisions, modulation of PFC activation by risk

levels would be negatively correlated with striatal D2-type BP_{ND} and positively correlated with overall monetary gains on the BART.

METHODS

Participants. A total of 60 healthy, right-handed research volunteers (18-51 years of age; 27 female) participated in this study. They were recruited for two separate projects that were approved by the UCLA Office of the Human Research Protection Program. In both studies, participants performed the BART during fMRI using identical procedures. In one study, participants had the option of undergoing PET to assess dopamine D2-like receptor $BP_{ND.}$ Sixty participants performed the BART during fMRI, and a subset of these participants (n=13) had PET scans as well for determination of D2-like receptor BP_{ND}. Exclusion criteria, determined by a physical examination and psychiatric evaluation using the Structured Clinical Interview for DSM-IV, were: systemic, neurological, cardiovascular, or pulmonary disease; head trauma with loss of consciousness; any current Axis I psychiatric diagnoses except nicotine dependence; and current use of prescribed psychotropic medications. Participants who tested positive for cocaine, marijuana, methamphetamine, benzodiazepines, or opiates by urinalysis were excluded, as were those with MRI contraindications.

Balloon Analogue Risk Task. A version of the BART [226], adapted for event-related fMRI, was used (Fig. 3.1). Balloons were either red or blue on active trials and white on control trials. When presented with an active balloon, participants selected between pumping the balloon for a potential increase in earnings ($0.25/pump) or cashing out to retain earnings accumulated during that trial. Pumping increased the size of the balloon and of the accumulated earnings, or it resulted in balloon explosion and forfeiture of unrealized earnings accumulated during the trial. Trials started with the first presentation of a balloon, and included all pumps from that point until

the choice to cash out, which resulted in a 2-s display of the total earned, or in explosion of the balloon, which was followed by a 2-s display of an exploded balloon with the message, "Total=$ 0.00."

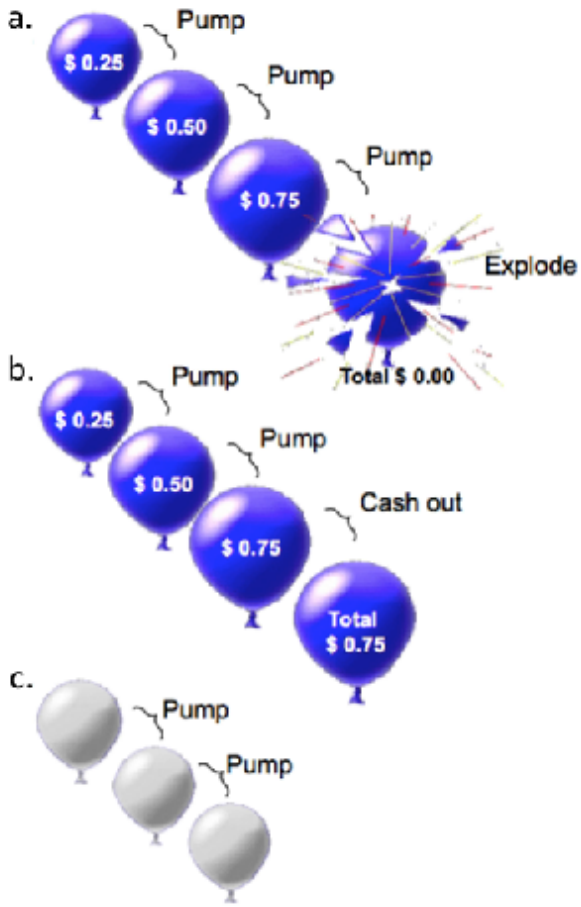

Figure 3.1. Balloon Analogue Risk Task. (a) Pumping the balloon increased potential earnings but carried the risk of the balloon exploding, resulting in a loss of accumulated earnings during the trial. (b) If a participant cashed out before the balloon exploded, he retained the earnings accumulated. (c) In control trials, white balloons were presented. These balloons did not increase in size with pumping, did not explode, and were not associated with reward potential.

Prior to scanning, participants were informed that red and blue balloons were associated with monetary reward and that they would receive their winnings after scanning, but they were not told that the number of pumps that would produce an explosion was pre-determined. For each active balloon trial, that number was determined from a uniform probability distribution, ranging from 1 to 8 and 1 to 12 pumps for red and blue balloons, respectively. Participants were informed that the white balloons did not explode and were not associated with potential reward, and they were instructed to pump each white balloon until the trial ended. The white balloon

trials were used to control for motor- and visual-related activation. The number of white-balloon presentations within the trial varied randomly between 1-12 (M = 6.34, SD = 3.44), according to a uniform distribution. Red, blue and white balloon trials were randomly interspersed throughout the task. The task was administered in two 10-min runs. As the task was self-paced and each balloon remained on the screen until the participant pressed a button, the total number of trials varied with the participant (active trials: M=56.62, SD = 8.47; control trials: M = 11.40, SD = 2.39). Participants were able to cash out at any time prior to a balloon explosion, and the number of pumps within a trial varied with the participant (number of pumps on trials ending with the choice to cash out: M = 2.92, SD = 0.934; number of pumps on all active trials: M = 8.48, SD = 2.29). The inter-stimulus interval for balloon presentations was randomly sampled from a uniform distribution ranging from 1-3 s, and the inter-trial interval was randomly sampled from an exponential distribution (mean: 4 s; range: 1-14 s). Participants received their earnings in cash at the end of the scanning session.

fMRI Acquisition. Imaging was performed at 3 Tesla on a Siemens Magnetom Trio MRI system. A set of 302 functional, T2*-weighted, echoplanar images (EPI) were acquired (slice thickness= 4 mm; 34 slices; repetition time = 2 s; echo time = 30 ms; flip angle = 90°; matrix = 64 x 64; field of view = 200 mm). High-resolution, T2-weighted, matched-bandwidth and magnetization-prepared rapid-acquisition gradient echo (MPRAGE) scans were also acquired. The orientation for matched-bandwidth and EPI scans was oblique axial to maximize brain coverage and to optimize signal from ventromedial prefrontal regions.

PET Scanning. Dopamine D2-type receptor BP_{ND} was assayed using [^{18}F]fallypride, a high-affinity radioligand for dopamine D2-type receptors [237]. Images were acquired using a Siemens ECAT EXACT HR+ scanner [in-plane resolution full-width at half-maximum (FWHM) 4.6 mm,

axial FWHM = 3.5 mm, axial field of view = 15.52 cm] in three-dimensional mode. A 7-min transmission scan was acquired using a rotating $^{68}Ge/^{68}Ga$ rod source for attenuation correction. PET dynamic data acquisition was initiated with a bolus injection of [^{18}F]fallypride (~5 mCi in 30 s). To minimize discomfort and to reduce radiation exposure to the bladder wall, emission data were acquired in two 80-min sessions separated by a break. Data were reconstructed using ECAT v7.3 OSEM (Ordered Subset Expectation Maximization; 3 iterations, 16 subsets) after corrections for decay, attenuation, and scatter.

Analysis of Behavioral Data. A general linear mixed model was used to examine risk-taking behavior while simultaneously modeling trial-by-trial data and taking into account individual subject variables, such as age and sex. As participants received feedback at the end of every trial, it is possible that participants learned the probabilities associated with the explosion of red and blue balloons. Trial number (continuing across the two fMRI runs) and balloon color (red vs. blue balloons) were, therefore, included in the model to assess the effect of learning on pumping behavior. In addition, to assess the effects of recent experience on subsequent behavior, the outcome of the immediately preceding trial was also included in the model with pumps per trial as the dependent variable.

The general linear mixed model allows the inclusion of both trial-level and subject-level covariates and accounts for the non-independence of observations clustered within subjects, and as such, is a reasonable approach for the analysis of the BART where both of these types of covariates may influence results. It also is robust to missing data or to the exclusion of data, such as the outcome of white-balloon trials and pumping behavior on trials following white-balloon trials. The resulting estimates are valid and unbiased by missing or excluded observations, provided that the model accounts for factors associated with the pattern of exclusion [238-240]. That

is the case here since the white control balloons were not associated with monetary outcome and did not explode but were fully modeled in the trial-by-trial effects. Data were analyzed using the Statistical Package for the Social Sciences.

Analysis of fMRI Data. Image analysis was performed using the FMRIB Software Library (FSL; version 4.1.8; www.fmrib.ox.ac.uk/fsl). The image series from each participant was first realigned to compensate for small head movements [241], and then a high-pass temporal filtering (100-sec) was applied. Data were spatially smoothed using a 5-mm FWHM Gaussian kernel, and skull-stripping was performed using the FSL Brain Extraction Tool. Registration was conducted through a three-step procedure, whereby EPI images were first registered to the matched-bandwidth structural image, then to the high-resolution MPRAGE structural image, and finally into standard Montreal Neurological Institute space, using 12-parameter affine transformations. Registration of MPRAGE structural images to standard space was further refined using FNIRT nonlinear registration [242]. Statistical analyses were performed on data in native space using FMRIB's fMRI Expert Analysis Tool (FEAT), and the statistical maps were spatially normalized to standard space prior to higher-level analysis.

Four types of events were included in the general linear model (GLM): pumps on active balloons, cash outs, balloon explosions and pumps on control balloons. Active-balloon and control-balloon pump events were defined as starting with the onset of the balloon presentation and ending with the button press to pump. A cash-out event was defined as the time between the appearance of the balloon and the disappearance of the feedback message regarding the total earned. The balloon explosion event started with the appearance of the exploded balloon and the message "Total Earned = $0.00", and ended when the image and message disappeared. As a trial progressed, risk and potential reward increased with each pump, as did the amount to be received

with the choice to cash out. For each of the four types of events, estimates of mean activation and of parametric modulation of activation [243] by pump number were included in a GLM using FEAT. Parametric regressors tested the linear relationship between pump number and blood oxygen level dependent (BOLD) signal, by using demeaned pump number (pump number minus mean number of pumps within each trial) as a parametric modulator. In this way, greater weight was assigned to later pumps. For example, within a trial, the second pump event, for which twice the reward was at stake, was given twice the weight as the first. The parametric modulator for cash-out and explode events was the number of pumps before the decision to cash out or before the balloon exploded, respectively. The nonparametric regressors were used to estimate the mean response for each event without consideration of the escalation of potential reward/loss within the trial.

Regressors were created by convolving a set of *delta* functions that represented the onset times of the events with a canonical (double-*gamma*) hemodynamic response function (HRF). The participant's response time to pump and the inter-stimulus interval determined the width of the HRF for each event. In order to allow the HRF to approach baseline prior to the cash-out or balloon-explosion event, the width of the HRF for the last pump of each trial was modeled using the participant's response time. Additional regressors that represented the first temporal derivatives of the eight event-related regressors were included to capture variance associated with slight variations in the temporal lag of the hemodynamic response.

Whole-brain statistical analyses, using a fixed effects model, were conducted separately for each imaging run per participant, and again to combine contrast images across the two runs. For between-participant analyses, the FMRIB Local Analysis of Mixed Effects module was used with sex and age as covariates. Statistical images were thresholded at a voxel height of $Z > 2.3$

and a cluster-probability threshold of $p < 0.05$, corrected for whole-brain multiple comparisons using the Theory of Gaussian Random Fields. Parameter estimates (β-values from the whole-brain GLM parametric analysis, corresponding to the modulation of activation by pump number) from a *priori* regions were extracted and used for subsequent correlation analyses with BART performance and striatal D2-type BP_{ND} (see below).

Effects of Outcome of the Preceding Trial. A separate GLM was used to examine the effects of the outcome of the previous trial on the modulation of activation by pump number. For each participant, pump events in a trial were categorized on the basis of the outcome of the previous trial. The GLM included parametric and nonparametric regressors separately for pumps that followed cash outs, balloon explosions, control balloon trials, and the first trial of each run (with no preceding contextual outcome). The contrast of interest was: "Pumps Following a Cash Out versus Pumps Following a Balloon Explosion" (parametric regressors). The analysis was performed using a voxel-height threshold of $Z > 2.3$ and a cluster-probability threshold of $p < 0.05$, corrected for whole-brain multiple comparisons.

Analysis of PET Data. Reconstructed PET data were combined into 16 images, each containing an average of 10-min dynamic frames. PET images were corrected for head motion by aligning the other 15 images to the second image in the series using rigid-body transformation with FSL FLIRT. The second PET image was co-registered to the respective structural MRI using the ART software package and a six-parameter, rigid-body transformation was applied to all 16 PET images in the series [244]. Bilateral caudate, putamen and nucleus accumbens regions were defined on the participant's MPRAGE using FSL FIRST (http://www.fmrib.ox.ac.uk/fsl/first/index.html).

Time-radioactivity data from the caudate, putamen and nucleus accumbens were extracted from the motion-corrected, co-registered images and imported into the PMOD 3.2 for kinetic modeling (PMOD Technologies Ltd., Zurich, Switzerland). Time-radioactivity curves were fit using the simplified reference-tissue model SRTM; [245]; to provide an estimation of k2′, the rate constant for transfer of the tracer from the reference region to the plasma. As the cerebellum is nearly devoid of specific binding sites for the radiotracer, a cerebellar volume of interest (VOI) was used as a reference region [246]. A volume-weighted average of k2′ estimates from high-radioactivity regions (i.e., the caudate and putamen) was computed. The time-radioactivity curves were refit using the SRTM2 model [247] with the computed k2′ value held constant across all VOIs. BP_{ND} was then calculated by subtracting 1.0 from the product of the tracer delivery (R1) and the tracer washout (k2′/k2a).

Analysis of fMRI Parameter Estimates, D2-type Receptor Availability and Behavior. The relationships between fMRI parameter estimates, striatal D2-type dopamine receptor BP_{ND}, risk-taking behavior following wins and losses, and total earnings were assessed. Parameter estimates (β-values from the whole-brain GLM parametric analysis that correspond to the modulation of activation by pump number) during pump events and cash-out events were extracted from VOIs anatomically defined on the basis of *a priori* hypotheses. The dorsolateral PFC (DLPFC) was sampled as a spherical VOI with a 10-mm radius around the *peak* voxel (MNI coordinates: x=30, y=36, z=20) from a cluster previously associated with risk-taking on the BART [221]. Bilateral caudate, putamen and nucleus accumbens regions were anatomically derived from the Harvard-Oxford subcortical atlas and were combined to create a VOI of the whole striatum. To ensure that the correlations with striatal D2-type dopamine receptor BP_{ND} were specific to our hypothesized VOIs, we tested the correlation of D2-type dopamine receptor BP_{ND} with parameter

estimates from the insula and visual cortex, regions that were not hypothesized to have activation correlated with striatal $BP_{ND.}$ VOIs of the insula and visual cortex were anatomically defined from the Harvard-Oxford cortical atlas.

In order to assess pumping behavior that was not limited by a balloon explosion, an adjusted average number of pumps was calculated by dividing the total number of pumps in trials without explosions by the number of such trials. *Risk-taking after reward* was calculated by subtracting the adjusted number of pumps following control-balloon trials from those following cash-out events. *Risk-taking after loss* was calculated as the difference between the adjusted number of pumps following explosion events and following control-balloon trials. Sex and age were entered as covariates for all correlation analyses, and multiple-comparison correction was performed by controlling for the rate of false discoveries (5% α level) (FDR) [248].

Results

Behavioral Performance. On average, participants decided to cash out on 52% of all trials (SD = 10.22%) and pumped active balloons 8.48 times (SD = 2.29) across all trials and 2.92 times (SD = 0.97) on trials ending with a choice to cash out. There were significant main effects of balloon color ($F(1, 1,450) = 38.665$, $p < 0.001$) and previous trial outcome ($F(1, 1,463) = 12.061$, $p = 0.001$); however, there was no significant main effect of trial number ($F(88, 1,452) = 1.194$, $p = 0.112$) on balloon pumps. The results also showed no significant interactions between trial number and balloon color ($F(80, 1,455) = 0.664$, $p = 0.990$) or between trial number and previous trial outcome ($F(76, 1,455) = 1.238$, $p = 0.085$). Post-hoc analyses showed that participants made significantly fewer pumps on red than blue balloons and on trials following balloon explosion events compared to cash-out events (Fig. 3.2).

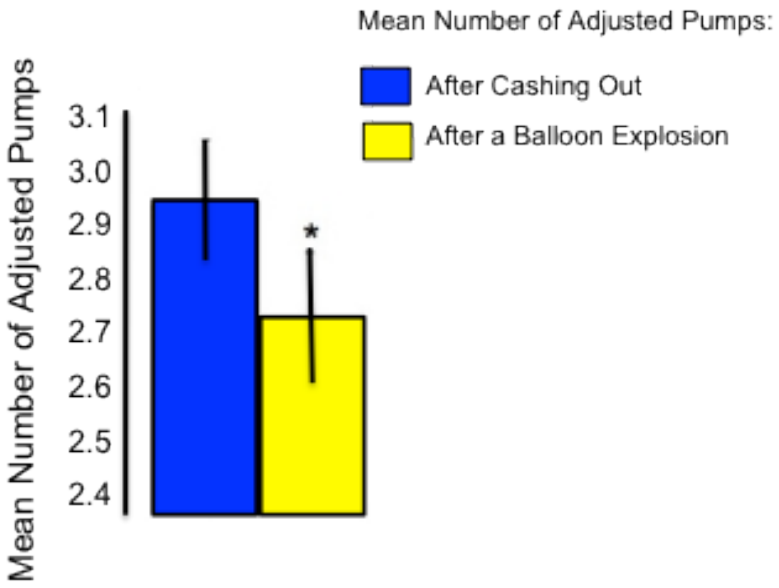

Figure 3.2. Effect of outcome risk-taking behavior. Participants make significantly fewer pumps on active balloon in trials following a balloon explosion compared to trials following the choice to cash-out ($p < .01$).

fMRI Results.

Modulation of Activation by Pump Number. Activation in the right inferior and right middle frontal gyri, right orbitofrontal cortex, right insula, anterior cingulate, thalamus and brainstem during active balloon pumps was modulated by pump number ($p < 0.05$, whole-brain corrected) (Fig. 3.3a, Table 3.1). In cash-out events, activation in nucleus accumbens, right caudate, subcallosal and precuneus cortices, and parahippocampal and post central gyri was modulated by pump number ($p < 0.05$, whole-brain corrected) (Fig. 3.3c, Table 3.1).

Table 3.1: Brain regions that exhibited activation modulated by pump number[a] in the pump and cash-out events

Brain region	Cluster size (voxels)	x [b]	y	z	Z statistic
Contrast: Pumping an active balloon					
Cluster #1[c]	2414				
Occipital cortex (L/R[d])		2	-84	-6	5.52
Cluster #2	1749				
Insula cortex (R)		32	24	-2	5.52
Middle frontal gyrus (R)		38	46	26	4.52
Orbital frontal cortex (R)		30	22	-12	4.51
Inferior frontal gyrus (R)		54	12	4	3.55
Cluster #3	1312				
Anterior cingulate cortex		6	28	28	4.57
Cluster #4	460				
Brainstem		6	-24	-8	3.75
Thalamus		4	-2	0	3.75
Contrast: Cashing out an active balloon					
Cluster #1[c]	1027				
Precuneus cortex (L/R[d])		-14	-58	18	4.05
Cluster #2	980				
Postcentral gyrus (L)		-28	-32	66	4.03
Cluster #3	687				
Nucleus accumbens (L/R)		12	8	-8	3.40
Caudate (R)		10	22	2	3.34
Subcallosal cortex		2	18	-6	3.33

[a] Amplitude of BOLD responses associated with pumps and cash outs on active balloons were modeled as a function of parametrically varied levels of risk and reward (represented by pump number) (see Methods). Z-statistic maps were thresholded using cluster-corrected statistics with a height-threshold of $Z > 2.3$ and cluster-forming threshold of $p < 0.05$.

[b] x, y, z reflect coordinates for peak voxel or for other local maxima in MNI space.

[c] Clusters are numbered and presented in order of decreasing size.

[d] L or R refers to left or right hemisphere.

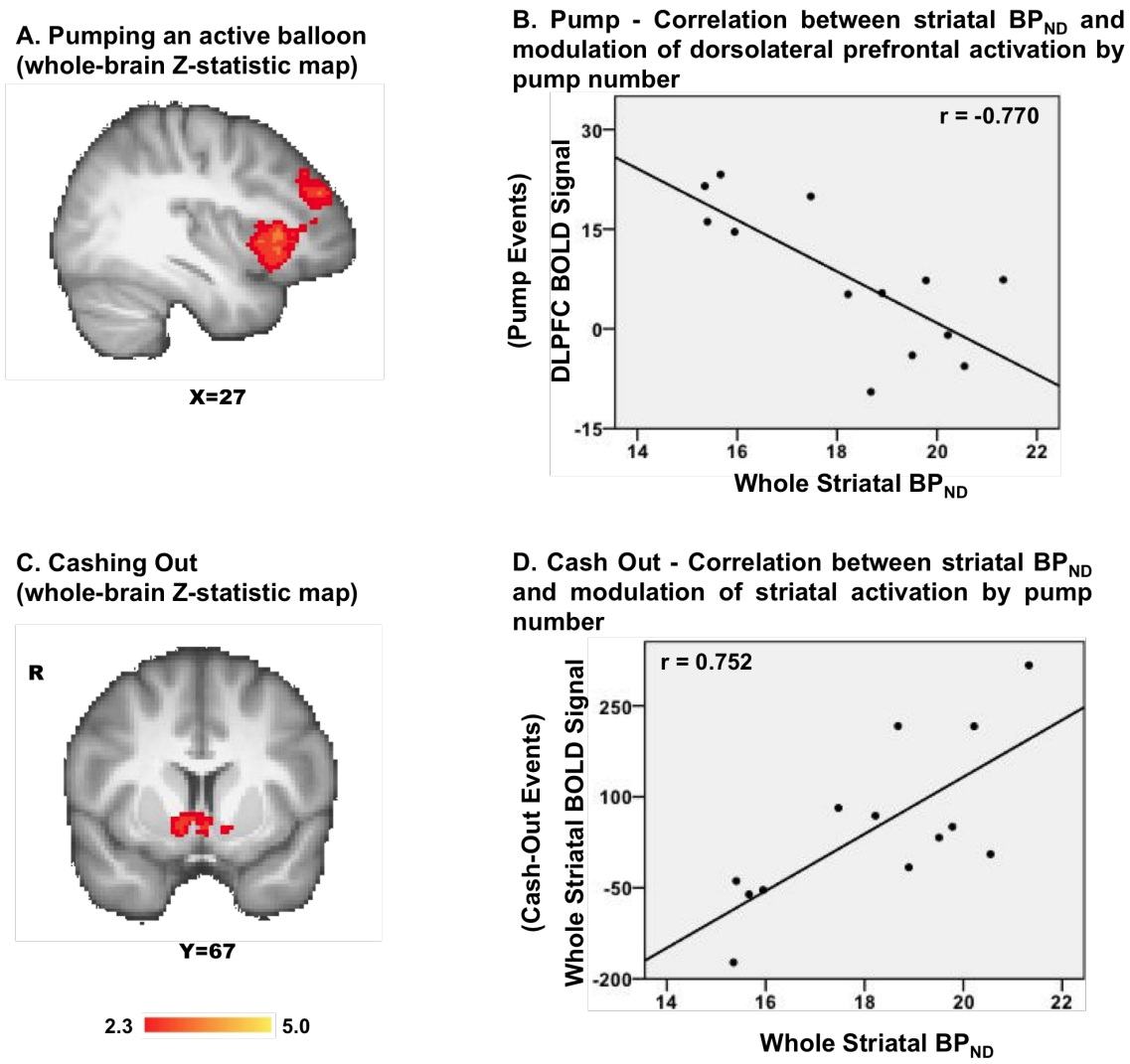

Figure 3.3. Modulation of striatal and prefrontal cortical activation by pump number and the relationship with striatal BP_{ND}. a. Activation was modulated by pump number during active balloon pumps (see Methods for details of parametric modulation analysis) (see Table 1 for list of regions). Colored areas shown here indicate significant modulation in DLPFC and insula. **b.** The fMRI parameter estimates (in β-values) extracted from DLPFC (independently-defined VOI) from pump events were negatively correlated with striatal BP_{ND} (x-axis). **c.** In cash-out events, activation in the ventral striatum was modulated by pump number (see Table 1 for complete list of regions). **d.** The fMRI parameter estimates (in β-values) for the whole striatum (anatomically-defined VOI) from cash-out events (y-axis) were positively correlated with striatal BP_{ND} (x-axis). Color maps represent Z-statistic values (whole-brain cluster-corrected).

Effects of Loss on Subsequent Risk-taking.

Activation in left amygdala, hippocampus, parahippocampal gyrus, posterior cingulate cortex and precuneus showed greater modulation by pump number during active balloon pumps following a balloon explosion than following a cash-out event number ($p < 0.05$, whole-brain corrected) (Fig. 3.4, Table 3.2). No regions showed greater modulation of activation by pump number during pumping after a cash-out event than after a balloon-explosion event.

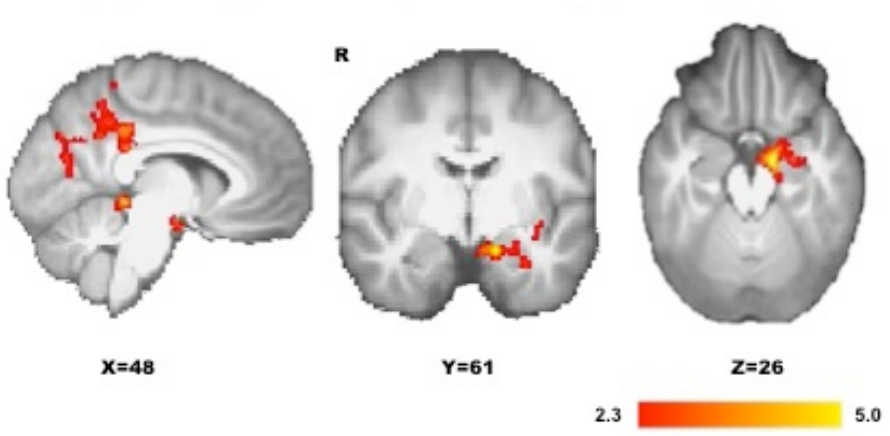

Figure 3.4. Effect of balloon explosions on the modulation of brain activation by pump number while pumping in subsequent trials. Modulation of activation by pump number was greater in the left amygdala, hippocampus, parahippocampal gyrus, posterior cingulate and precuneus cortices for pumps after a balloon explosion compared to pumps after cashing out. Color maps represent Z-statistic values (whole-brain cluster-corrected).

Table 3.2: Brain regions that exhibited greater modulation of activation by pump number[a] in pump events following a balloon explosion than after a cash-out event

Brain region	Cluster size (voxels)	x[b]	y	z	Z statistic
Contrast: Pumping following an explosion > Pumping following a cash out					
Cluster #1 [c]	946				
Posterior cingulate cortex (L[d])		-8	-38	36	3.38
Cluster #2	767				
Hippocampus (L)		-14	-8	-20	3.83
Amygdala (L)		-16	-4	-20	3.78
Parahippocampal gyrus (L)		-16	-28	-14	3.38

[a] Amplitude of BOLD responses associated with pumps on active balloons were modeled as a function of parametrically varied levels of risk and reward (represented by pump number) (see Methods). Z-statistic maps were thresholded using cluster-corrected statistics with a height-threshold of $Z > 2.3$ and cluster-forming threshold of $p < 0.05$.

[b] x, y, z reflect coordinates for peak voxel or for other local maxima in MNI space.

[c] Clusters are numbered and presented in order of decreasing size.

[d] L or R refers to left or right hemisphere.

Relationships between Striatal D2-type BP_{ND}, Frontostriatal Activation, and Risk-taking Behavior.

Striatal D2-type BP_{ND} and Frontostriatal Activation.

The fMRI parameter estimates (β-values from the whole-brain GLM parametric analysis that correspond to the modulation of activation by pump number) extracted from the DLPFC during pump events showed significant negative correlations with D2-type BP_{ND} for the whole striatum (Fig. 3.3b). Post-hoc analyses showed significant negative correlations with D2-type BP_{ND} for

the caudate nucleus ($r = -0.911$, $p < 0.001$), putamen ($r = -0.725$, $p = 0.006$) and nucleus accumbens ($r = -0.495$, $p = 0.05$) (FDR corrected). In contrast, fMRI parameter estimates of the whole striatum for cash-out events showed a significant positive correlation with whole striatal D2-type BP_{ND} (Fig. 3.3d). Post-hoc analyses showed positive correlations with D2-type BP_{ND} for the caudate nucleus ($r = 0.600$, $p = 0.025$), putamen ($r = 0.523$, $p = 0.049$) and nucleus accumbens ($r = 0.502$, $p = 0.05$) (FDR uncorrected). There were no significant correlations between striatal D2-type BP_{ND} and the fMRI parameter estimates of activation in the control regions: insula ($r = 0.099$, $p = 0.772$) and visual cortex ($r = 0.269$, $p = 0.424$), demonstrating that the effects were not generalized.

Striatal D2-type BP_{ND}, Risk-taking after a Reward or after a Loss and Overall Performance.

The number of risky choices that a participant took after a reward (number of pumps after cash-out trials minus after control trials was negatively correlated with D2-type BP_{ND} for the whole striatum (Fig. 3.5A). In post-hoc analyses, this correlation was significant for each striatal sub-region (caudate, putamen and nucleus accumbens ($p < 0.011$, FDR corrected; Fig. 3.5A)). There were no significant correlations between the number of risky choices after a loss (number of pumps after balloon explosions minus the number of pumps after control trials and striatal D2-type BP_{ND} ($r = -0.350$, $p = 0.291$). Overall performance on the BART, measured by total earnings, was negatively correlated with D2-type BP_{ND} for the whole striatum and for each sub-region; caudate nucleus ($r = -0.645$, $p = 0.016$), putamen ($r = -0.555$, $p = 0.038$) and nucleus accumbens ($r = -0.633$, $p = 0.018$) (FDR uncorrected) (Fig. 3.5A).

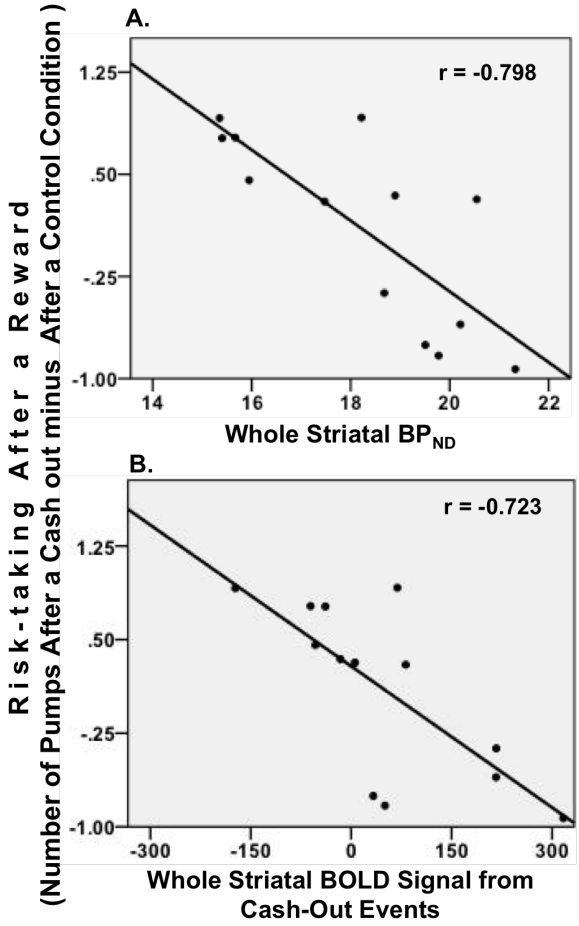

Correlations between BP_{ND} in striatal regions and risk-taking behavior after reward

Striatal Regions	Correlation Coefficient	Significance
Whole Striatum	r = -0.798	p = 0.002*
Caudate Nucleus	r = -0.681	p = 0.011*
Putamen	r = -0.730	p = 0.005*
Nucleus Accumbens	r = -0.845	p = 0.001*

Correlations between striatal BOLD of cash-out events and risk-taking behavior after reward

Striatal Regions	Correlation Coefficient	Significance
Whole Striatum	r = -0.723	p = 0.006*
Caudate Nucleus	r = -0.758	p = 0.003*
Putamen	r = -0.597	p = 0.026*
Nucleus Accumbens	r = -0.415	p = 0.102

Figure 3.5. Relationship between risk-taking after a reward, striatal BP_{ND}, and modulation of striatal fMRI activation. Shown are scatter plots, correlation coefficients (r), and associated significance values (p) from post-hoc Pearson correlations. **A.** Risk-taking after a reward was negatively correlated with striatal BP_{ND}. **B.** Negative relationship between modulation of striatal activation by pump number in cash-out events and risk-taking in subsequent trials. Risk-taking after a reward was the difference between the number of pumps following trials that ended in a cash-out and those following control trials. Results were controlled for age and sex and remained significant (*) after correcting for the number of tests by controlling the False Discovery Rate. There were no significant correlations between the difference in number of pumps after an explosion and the number of pumps after control trials and BP_{ND} in the striatum or striatal parameter estimates.

Frontostriatal Activation, Risk-taking after a Reward and a Loss and Overall Performance.

The number of risky choices after a reward was also negatively correlated with fMRI parameter estimates for cash-out events for the whole striatum (Fig. 3.6b). Post-hoc analyses showed significant negative correlations for the caudate nucleus and putamen ($p < 0.03$, FDR corrected; Fig. 3.6b). In the larger sample (n=60), the number of risky choices after a reward was also negatively correlated with fMRI parameter estimates for cash-out events for the whole striatum and each striatal subregion ($p < 0.05$). There were no significant correlations between the number of risky choices after a loss (number of pumps after balloon explosions minus the number of pumps after control trials) and striatal fMRI parameter estimates for cash-out events ($r = -0.388$, $p = 0.238$). Total earnings, which was negatively correlated with striatal D2-type BP_{ND} was positively correlated with DLPFC fMRI parameter estimates for pump–events (n=13: $r = 0.545$, $p = 0.005$, n=60; $r = 0.200$, $p = 0.06$) (Fig. 3.6b).

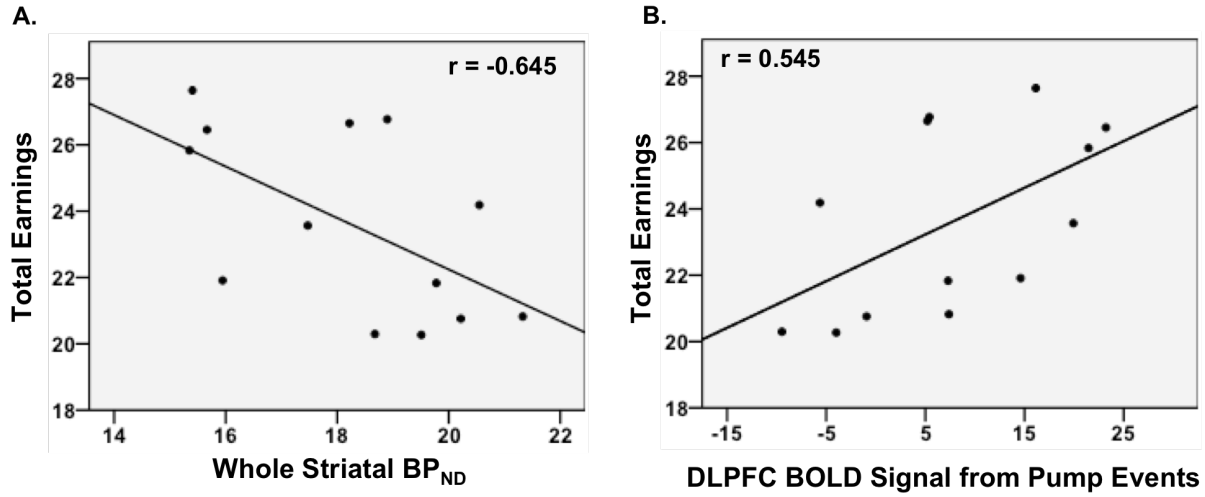

Correlations between BP_{ND} in striatal regions and total earnings

Striatal Regions	Correlation Coefficient	Significance
Whole Striatum	r = -0.645	p = 0.016
Caudate Nucleus	r = -0.555	p = 0.038
Putamen	r = -0.504	p = 0.057
Nucleus Accumbens	r = -0.633	p = 0.018

Figure 3.6. Relationship between BART performance, striatal BP_{ND} and modulation of DLPFC activation by pump number. a. Total earned on the BART was negatively correlated with striatal BP_{ND}. Shown are correlation coefficients (r) and associated significance values (p) from post-hoc Pearson correlations for the relationship between total earnings on the BART and striatal BP_{ND} for each striatal subregion. **b.** Modulation of the DLPFC activation by pump number in pump events showed a positive relationship with amount earned on the BART (p=0.005). Results are controlled for age and sex.

Discussion

The findings reported here show that risky decision-making is a dynamic construct consisting of the outcomes of previous decisions, striatal D2-type BP_{ND} and modulation of frontal cortical and subcortical activation. Presenting direct evidence for the involvement of striatal D2-type receptors in risk-taking behavior, our results extend previous findings of frontostriatal activation in decision-making [219-221] and suggest a potential mechanism by which striatal dopamine may modulate frontal and striatal regions during risky choices.

As participants took fewer risks when the preceding trial resulted in a loss rather than a gain, the results show that risky decision-making varies as a function of previous trial outcomes. This is consistent with reports that prior outcomes biased decision-making [213, 232]. Greater modulation of activation in the amygdala, by pump number, following a loss than after a gain suggests that amygdala signaling attenuates risky behavior following aversive outcomes. This view is in line with observations that loss-aversion behavior is positively correlated with amygdala activation in a risky monetary-choice task [249] and that patients with amygdala lesions are less loss-averse than healthy controls [250]. Our results confirm involvement of the insula during risky decision-making [50] and provide evidence that the risk-prediction signal of the insula [52] is insensitive to recent experience. The hippocampus, which is implicated in encoding recent experiences [251], showed a greater response after a loss than after a win. Given the involvement of the hippocampus in processing associations among different experiences [252] and of the amygdala in promoting cautious behavior in uncertain situations [253], the results suggest a neural mechanism by which recent losses promote risk-aversion by signaling the potential for further negative outcomes to guide subsequent choices.

The results also highlight the importance of rewarding experiences in shaping behavior. Modulation of striatal activation by pump number during the cash-out condition was related to striatal D2-type BP_{ND}, and both predicted risk-taking behavior on the subsequent trial. These results are consistent with prior observations that ventral striatal activation [48] and firing in dopaminergic neurons [230] are related to the magnitude of anticipated reward. It has been suggested that anticipatory responses of the dopamine system promote reinforcement learning [53] and modulate risk preferences [198, 199]. It has also been observed that D2-type receptor agonists enhance reward-expectancy signaling via dopaminergic transmission [200] and reduce risky choices [201]. The results from this study extend these findings by showing that striatal D2-type BP_{ND} is positively related to striatal activation during reward-seeking behavior that involves risk in humans.

Risky decisions are determined, in part, by motivational states that reflect activity in the ventral striatum [233] and by assessment and maintenance of goal states supported by PFC activity [216]. Pharmacological studies in rodents have demonstrated a crucial role of striatal dopamine in the adaptation of these processes by the flexible updating of reinforcement contingencies [254, 255]. The PFC and striatum interact through an elaborate system of interconnections [118, 256] that likely contributes to goal-directed states. In the context of decision-making involving risk and reward, these interactions may be described in a framework (described below) in which reinforcement values are reflected in activity-dependent plasticity that is governed by differences in striatal D2-type receptor BP_{ND}, which can effectively bias decisions in favor of reward-seeking or goal-directed behavior.

Corticostriatal computational models show a modulatory role of the PFC on striatal activity [257, 258]. The PFC can influence striatal activity through various signaling pathways

including mesocortical glutamatergic projections that enhance tonic striatal dopamine release, which in turn increases the effective threshold for striatal firing [259, 260], other corticostriatal projections that enhance non-AMPA mediated glutamatergic synaptic transmission [261-263], and a cortico-subthalamic-striatal hyperdirect pathway that has been implicated in inhibiting premature responses in high-conflict situations [258, 264]. As presynaptic striatal D2-type receptors play a critical role in inhibiting glutamate release in these pathways [265, 266], striatal D2-type receptor availability may thereby determine the extent to which PFC activity and associated glutamate release can activate GABAergic striatal neurons to inhibit activity and maintain goal-directed behavior.

While presynaptic D2-type receptors can limit prefrontal influence over striatal activity [265], postsynaptic striatal D2-type receptor activation can attenuate the spiking of prefrontal neurons (Seamans and Yang, 2004). Postsynaptic striatal D2-type receptor activation can indirectly disinhibit the dorsomedial nucleus of the thalamus through afferents to the ventral pallidum or substantia nigra pars reticulata, which both provide inhibitory inputs to GABAergic inhibitory neurons in the thalamus [117, 118]. As the disinhibition of the dorsomedial nucleus of the thalamus results in the excitation of prefrontal pyramidal neurons that have been implicated in motivational states, striatal D2-type receptor activation has the capacity to modify goal-directed behavior governed by the prefrontal cortex [258, 267].

As presynaptic and postsynaptic striatal D2-type receptors affect glutamatergic and GABAergic signaling in the striatum [255], D2-type receptor availability may contribute to changes in the computational properties of frontostriatal circuits during risky decision-making. Supporting this view is our observation that participants with low D2-type BP_{ND} exhibited less ventral striatal response to reward but greater modulation of DLPFC activation while pumping

and better performance on the BART. As lesions to corticostriatal projections shift decisions related to reward contingencies in rodents [268] and neurocomputational models indicate that PFC activity can directly override striatal representations of reinforcement value [257], the inverse relationship between ventral striatal activation when taking reward and DLPFC activation when taking risk may reflect corticostriatal regulation of reward-driven responses through D2- receptor mediated effects on glutamate release.

Individuals with high D2-type BP_{ND} exhibited both greater reward-driven activation in the ventral striatum and more immediate reward-seeking behavior following reward than counterparts with low D2-type BP_{ND}. The results suggest that individuals with high striatal D2-type receptor BP_{ND} are more sensitive to reward and have less effective cortical inhibition of reward-driven responses that lead to a preference for immediate smaller gains over potentially larger delayed ones. Striatal D2-type receptors may thereby determine the capacity to respond to striatal dopamine release in response to a signal for imminent reward, and the signal in turn would update reinforcement values represented in the prefrontal cortex. The results presented here, however, are inconsistent with the observation that stimulant-dependent individuals, who exhibit low striatal BP_{ND} [269], exhibit temporal discounting of rewards [22]. One possible explanation is that there is a nonlinear relationship between dopaminergic function and temporal discounting of rewards, as suggested by the observation that low doses of amphetamine significantly increased the preference for rats to work harder or to wait longer for larger rewards, while high doses had the opposite effect [270]. Our findings may reflect the descending limb of an inverted U-shaped function that describes the relationship between dopamine function and adaptive risky decision-making, although small sample size and a limited range in binding potential prevent definitive interpretation. In view of the preceding discussion, it is plausible that

individual differences in striatal D2-type receptors that contribute to individual differences in reward sensitivity [203] may guide goal-directed behavior and associated modulation of frontal and striatal activation by facilitating or inhibiting glutamate and dopamine release in various signaling pathways linking the striatum and PFC.

This study has some limitations. Combination of the temporal resolution of fMRI with the BART was not sufficient to allow clear dissociation between the decision to cash out and receipt of reward. In addition, as potential earnings as well as the risk of forfeiting earnings increased in tandem with each pump, it was not possible to discern whether level of risk or reward modulated the activation. As striatal activation is associated with the response to aversive [271] as well as rewarding [48] stimuli, the modulation of activation of the ventral striatum during cash-out events may reflect anticipation of an aversive outcome (balloon explosion) and not just expectation of reward. Therefore, caution should be taken when attempting to assign function to brain activations via reverse inference [272].

Despite these limitations, our results not only corroborate but also extend previous findings of activation in frontostriatal regions during decision-making by highlighting the molecular basis of such activation. They strengthen support for the role of dopamine in risky decision-making by showing that D2-type receptor availability is associated with risky choices as well as the risk sensitivity of a relevant frontostriatal network during decision-making. This study provides evidence that the neural substrates of decision-making vary as a function of individual differences in the striatal dopamine system and the context in which decisions are made.

CHAPTER 4
MESOCORTICOLIMBIC RESTING-STATE ACTIVITY AND RELATIONSHIP TO PREFRONTAL ACTIVATION DURING DECISION-MAKING

Introduction

Study 1 provides evidence for the influence of dopamine D2-type receptors in risky choices and in the modulation of activation in the DLPFC and striatum by level of risk and reward during decision-making. Maladaptive decision-making involving risk, impairments in frontostriatal activation and dopamine dysfunctions are characteristics of addictions, study 2, therefore was designed to explain the interactions between the activity of the mesocorticolimbic dopamine system and frontostriatal activation as it relates to risky decision-making in a sample of MA-dependent participants. A natural extension of Study 1 would be to determine how differences in striatal D2-type receptor BP_{ND} between the groups relate to frontostriatal activation during decision-making; however, the small sample of MA-dependent participants with both fMRI and PET scans prevented such examination. We examined whether D2-type dopamine BP_{ND} was related to resting-state functional connectivity (RSFC) of the midbrain. A preliminary analysis testing the correlation of striatal BP_{ND} to midbrain RSFC was conducted in 10 healthy controls. The results showed that striatal BP_{ND} was negatively correlated with the intrinsic connectivity between the midbrain and striatum, amygdala and medial PFC (Fig 4.1).

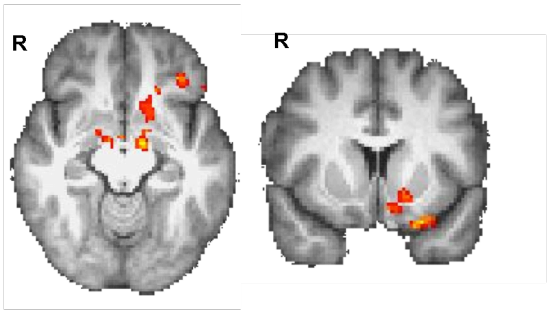

Figure 4.1. Relationship between striatal dopamine D2-type BP_{ND} and midbrain RSFC. Connectivity maps show a negative correlation between striatal BP_{ND} and RSFC between the midbrain and nucleus accumbens, putamen, amygdala, and orbital frontal cortex ($p < 0.05$, whole-brain cluster corrected). Results were controlled for age, sex, smoking status, and marijuana use.

The first objective of Study 2, therefore, was to determine whether healthy controls and MA-dependent subjects differed in the intrinsic brain activity of the mesocorticolimbic dopaminergic pathway, a network comprising the ventral tegmental area, striatum, and limbic and prefrontal cortices. The second objective in this study was to evaluate whether the differences in RSFC affect task-related brain activation during risky decision-making.

Risky decision-making is a feature of various neuropsychiatric disorders, including addictions, and risk-taking has been positively associated with the duration of drug abuse [16] and the severity of dependence [273-275]. In laboratory tests of decision-making, drug-dependent individuals exhibit hypersensitivity to reward and hyposensitivity to losses [18], characteristics that may contribute to greater propensity for risk-taking in drug-dependent individuals compared to matched controls [18-20, 276].

During decision-making, a balance between striatal and prefrontal activity, maintained, in part, by striatal dopamine receptors [277] and connections of the corticostriatal and mesolimbic systems facilitates adaptive choices [217] . It has been proposed that abnormal activity among mesocorticolimbic neurons may enhance stimulus-reward associations [204, 205] while inhibition of reward-seeking behavior depends upon activity in corticostriatal projections [278]. Consistent with this view, animal studies have demonstrated that signaling through the mesocorticolimbic system promotes motivated drug-seeking behavior [204, 205], and that plasticity of structure [149, 215] and activity [206, 207] in prefrontal and striatal regions after repeated exposure to stimulants leads to cognitive impairments and aberrant motivated behavior.

Human neuroimaging studies have also identified abnormalities in frontal and striatal activation [22, 46, 51, 279, 280] and intrinsic connectivity of brain regions [183, 187, 281-284] in drug-dependent subjects, but empirical evidence linking resting-state functional connectivity (RSFC) in the mescorticolimbic system with deficits in frontostriatal brain activation during decision-making in drug-dependent individuals has been lacking. The identification of RSFC alterations may delineate circuit-level dysfunction from that of specific task-based activation. Such information could clarify whether maladaptive choices reflect dysfunctions in specific brain regions during decision-making, intrinsic network activation, or both. The goals of this study, therefore, were to compare methamphetamine-dependent (MA) and healthy control subjects with respect to RSFC of the mesocorticolimbic and corticostriatal systems, and in the extent to which intrinsic RSFC of these networks influences frontostriatal activation during risky decision-making.

Functional magnetic resonance imaging (fMRI) was performed when participants were performing the Balloon Analogue Risk Task (BART) [226]. As described in the previous chapter, the BART is a test of risky decision-making, and it presents sequential choices ─ pumping a virtual balloon to increase potential gains while risking loss if the balloon explodes, or cashing out to retain earnings accrued. Again a parametric analysis was conducted to evaluate how the levels of risk and of potential reward (both represented by pump number) modulates brain activation during decision-making (i.e., modulation of activation by pump number). Performance on the BART has been correlated with self-reported impulsivity, sensation-seeking, and engagement in risky behaviors [226, 285] and has been associated with activation in the dorsolateral prefrontal cortex (DLPFC) and striatum [221, 286, 287]. In order to determine whether specific task-based activation on the BART is related to intrinsic activity at the circuit-level, fMRI was also

performed when participants were at rest. Resting-state fMRI was used to measure coherence between components of mesocorticolimbic and corticostriatal systems and their effect on modulation of activation during risky decision-making.

Given that fluctuations in both prefrontal and nucleus accumbens dopamine signaling have been related to changes in risk and reward probabilities [288], neurochemical changes in both prefrontal and striatal regions seen with chronic MA administration [289, 290] may contribute to altered patterns of frontostriatal activation during risky decision-making. Stimulant users exhibit an exaggerated response to reward in the ventral striatum [291] but less decision-making related activation in the DLPFC [51, 279], it was therefore, hypothesized that, compared with healthy controls, MA-dependent participants would exhibit less modulation of activation in DLPFC by pump number but greater modulation in ventral striatum during risky decision-making.

Resting-state fMRI was used to measure temporal correlations between intrinsic brain activity in the mesocorticolimbic and corticostriatal networks at rest. Because stimulant exposure leads to altered activity in regions of the mesocorticolimbic system [127, 278], differences in mesocorticolimbic RSFC were expected between the groups. Furthermore, as dysregulated mesocorticolimbic neurotransmission is thought to underlie decision-making deficits seen in drug addiction [127], it was hypothesized that individual differences in mesocorticolimbic RSFC would be related to frontostriatal activation during decision-making.

METHODS

Participants

Fifty-three volunteers were recruited via newspaper and Internet advertisements. They provided written informed consent, as approved by the UCLA Office for Protection of Research Subjects. A physical examination was performed and a medical history and samples for standard

blood chemistry and hematology profiles were collected. The Structured Clinical Inventory for DSM-IV-TR (SCID) established psychiatric diagnoses. Any current Axis I diagnosis other than nicotine dependence for controls, and nicotine dependence and MA dependence for the MA-dependent group was exclusionary.

Twenty-six non-treatment seeking MA-dependent volunteers (13 of each sex, 20 smokers, 35.68 ± 1.64 years old), who met the diagnosis of MA dependence and a positive test for MA were recruited. One individual was excluded due to excessive head motion during scanning (see below), leaving 25 for final analysis. MA use was reported as 3.57 ±1.04 grams/week, and in the month before enrollment, use of MA, alcohol, and marijuana was reported occurring on 23.60 ± 1.29, 4.68 ± 1.64, 1.68 ± 0.70 days, respectively (Table 1). Eleven MA-dependent participants were inpatients at the UCLA Medical Center. They abstained from MA for 4-7 days before scanning, and negative urine tests confirmed abstinence from cocaine, methamphetamine, benzodiazepines, opiates, and cannabinoids. Fourteen MA-dependent individuals completed the study as outpatients, and abstained from MA for 5.78 ± 1.84 days before scanning. Urine testing confirmed abstinence.

The control group included 27 participants (11 women/16 men, 16 smokers, 33.88 ± 2.30 years old). Controls reported no drug use except for light alcohol or marijuana use; they reported alcohol and marijuana use on 4.36 ± 1.15 and 0.08 ± 0.08 days in the month before enrollment (Table 1). Urine was tested at intake and on testing days.

Table 1. Characteristics of Research Participants

	Healthy Control (n=27)[a]	MA-dependent (n=25)[b]
Age (years)[c]	33.88 ± 2.30	35.68 ± 1.64
Sex (# male)	16	12
Education (years)	13.62 ± 0.38	13.00 ± 0.38
Alcohol Use		
Days used in the last 30 d	4.36 ± 1.15	4.68 ± 1.64
Marijuana Use*		
Days used in the last 30 d	0.08 ± 0.08	1.68 ± 0.70
Tobacco Use (# smokers)	16	20
Days used in the last 30 d	17.57 ± 2.87	21.16 ± 2.54
Methamphetamine Use		
Days used in the last 30 d		23.60 ± 1.29
Grams per week		3.57 ± 1.04
Years of heavy use		8.59 ± 1.37

[a]n=18 and [b]n=15 for resting-state functional connectivity analysis

[c]Data shown are means ± SEM

B**alloon Analogue Risk Task**

As the same version of the BART [226] (Fig. 4.2) that was described in the previous chapter was used here, see page 33 for a detailed description of the task and design.

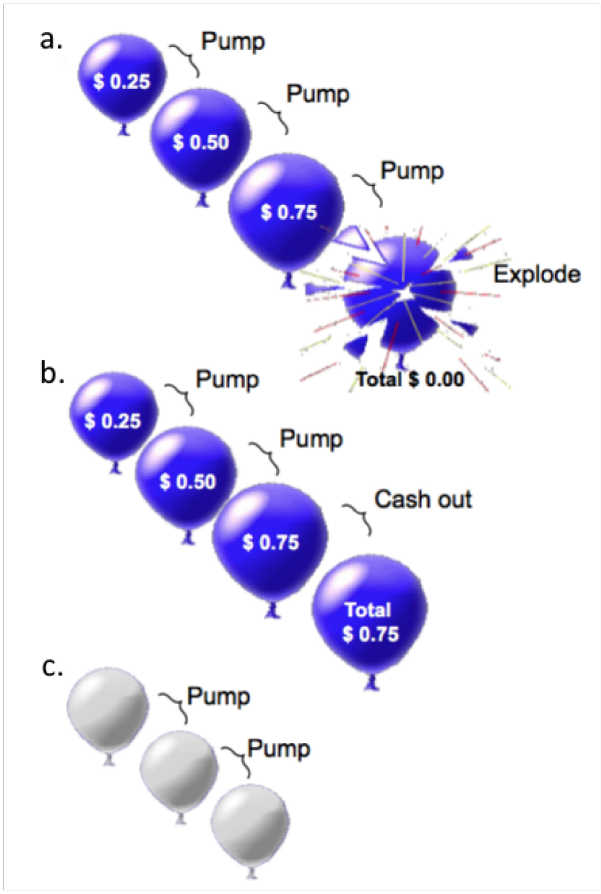

Figure 4.2. Balloon Analogue Risk Task. (a) Pumping the balloon increased potential earnings but carried the risk of the balloon exploding, resulting in a loss of accumulated earnings during the trial. (b) If a participant cashed out before the balloon exploded, he retained the earnings accumulated. (c) In control trials, white balloons were presented. These balloons did not increase in size with pumping, did not explode, and were not associated with reward potential.

fMRI Acquisition

Scans were collected from 25 MA-dependent and 27 control participants while they performed the BART. A subset of participants, 18 healthy and 15 MA-dependent individuals, also underwent resting-state fMRI scans, during which they stared at a black screen for 5-min. Imaging was performed on a 3-Tesla Siemens Magnetom Trio MRI system, and 302 functional task-based and 152 resting-state T2*-weighted, echoplanar images (EPI) were acquired (slice thickness = 4 mm; 34 slices; repetition time (TR) = 2s; echo time (TE)= 30ms; flip angle = 90°; matrix = 64 x 64; fov = 200 mm). High-resolution, T2-weighted, matched-bandwidth and magnetization-prepared rapid-acquisition gradient echo (MPRAGE) scans were also acquired. The orientation for matched-bandwidth and EPI scans was oblique axial to maximize brain coverage and to optimize signal from ventromedial prefrontal regions.

Analysis of Behavioral Data

The general linear mixed model (GLMM) that used to examine trial-by-trial risk-taking behavior in Chapter 3 was used. A detailed description of the GLMM is presented on page 36 but briefly,

the model included trial number (continuing across the two fMRI runs), balloon color, and the outcome of the immediately preceding trial (cash-out or explode), with pumps per trial as the dependent variable.

Regions of interest (ROIs)

The right DLPFC was sampled with a 10-mm spherical ROI around the *peak* voxel (MNI coordinates: x = 30, y = 36, z = 20) from a cluster associated with BART performance in previous studies [221, 277]. A bilateral anatomical nucleus accumbens ROI was derived from the Harvard-Oxford subcortical atlas. A 9-mm radius spherical midbrain ROI was created using the coordinates (MNI: x = 0, y = -15, z = -9) that were reported in a study examining midbrain RSFC in cocaine users [292].

Analysis of fMRI BART Data

Image analysis was performed using FSL 5.0.2.1 (www.fmrib.ox.ac.uk/fsl). Each participant's images were realigned to compensate for motion [241], and high-pass temporal filtering was applied (Gaussian-weighted least-squares straight-line fitting, sigma = 33s). One MA-dependent participant was excluded due to excessive head motion (> 2 mm translational displacement, > 1.5 degrees rotation). Data were skull-stripped and spatially smoothed (5-mm FWHM Gaussian kernel). Registration was conducted in three steps, whereby EPI images were first registered to the matched-bandwidth image, then to the high-resolution MPRAGE image, and finally into standard Montreal Neurological Institute space, using 12-parameter affine transformations. Registration of MPRAGE images to standard space was further refined using FNIRT nonlinear registration [242]. Statistical analyses were performed using FMRIB's FEAT, and statistical maps were spatially normalized to standard space prior to higher-level analysis.

As a trial progressed, the risk of balloon explosion increased with each pump (pump

number), as did the amount earned with cashing out. The general linear model (GLM) included regressors to obtain estimates of parametric modulation [243] of activation by pump number and of mean activation for each event type (i.e., pumps on active balloons, control balloons, cash outs, and explosions). Escalation of risk was not considered for regressors that estimated mean activation for each event. Parametric regressors tested the linear relationship between pump number and activation by assigning greater weight to events that carried greater potential risk and reward (i.e., modulation of activation by pump number). For example, within a trial, the second pump event, for which twice the reward was at stake, was given twice the weight as the first.

Regressors were created by convolving a set of *delta* functions, representing onset times of each event with a canonical (double-*gamma*) hemodynamic response function (HRF). The first temporal derivatives of the eight task-related regressors were included to capture variance associated with the temporal lag of the hemodynamic response as well as six motion parameters estimated during motion correction.

Fixed-effect analyses were conducted separately for each imaging run per participant, and again to combine contrast images across the two runs. For between-group analyses, the mixed effects module, FLAME1 was used with sex, age, smoking status (smoker, non-smoker), and marijuana use (days used in the last month) as covariates. The analysis was restricted to the right DLPFC and striatal ROIs. To test for differences in activation during risky decision-making and for the increase in activation with risk and reward levels, the contrasts of interest were nonparametric pump events versus nonparametric control-balloon events and parametric pump events, respectively. Statistical images were thresholded at voxel-heights of $Z > 2.3$ and a

cluster-probability threshold of $p < 0.05$, corrected for multiple comparisons using the theory of Gaussian Random Fields.

Analysis of fMRI Resting-state Data (DLPFC and midbrain seeds)

Resting-state images were pre-processed in the same manner as above. The following nuisance regressors were included in the GLM: average signal of cerebrospinal fluid, six motion parameters estimated during motion correction, and two metrics of motion-related artifact, specifically frame-wise displacement and a combination of the temporal derivative of the time series and root mean squared variance over all voxels [293]. The mean time series across all voxels within the DLPFC and midbrain seeds from pre-processed images were used as covariates in separate whole-brain, voxel-wise correlation analyses.

The relationship between RSFC and the modulation of activation during decision-making was examined at the group level. DLPFC parameter estimates (β-values) corresponding to the modulation of activation by pump number from *a priori*-defined DLPFC ROIs were regressed against whole-brain voxel-wise maps of DLPFC and midbrain RSFC. Sex, age, smoker status, and frequency of marijuana use were modeled as nuisance covariates.

RESULTS

Behavioral Performance

There was a significant main effect between red and blue balloons ($F(1, 1{,}828.28) = 16.684$, $p < 0.001$) on pumping, but no significant main effect of group ($F(1, 62.413) = 0.043$, $p = 0.836$) or any two-way group interactions. There were no significant group differences in the average number of pumps prior to cashing out ($t = 1.342$, $p = 0.180$): control group ($M=2.84$, $SD= 1.518$), MA group ($M = 2.74$, $SD = 1.544$). A two-tailed t-test showed significant differences in

overall performance (t(49) = 2.357, p= 0.022) with the controls earning more money (M = 33.33 USD, SD = 3.83) than MA-dependent participants (M = 30.15 USD, SD = 5.65).

fMRI BART Analysis

ROI analyses indicated that, while pumping, controls exhibited greater modulation of activation by pump number in the right DLPFC than MA-dependent subjects, while MA-dependent participants displayed greater modulation of activation in the ventral striatum than controls (Fig. 4.3). Whole-brain analysis revealed that controls had greater modulation of activation than MA users in a right DLPFC cluster that included and extended beyond the a *priori*-defined DLPFC ROI (peak coordinates: X = 42, Y = 40, Z = 30; Cluster extent: 610 voxels; Z-statistic: 3.4, p < 0.001). No significant group differences for other regions in whole-brain analysis were found or for mean activation in whole-brain or ROI analyses.

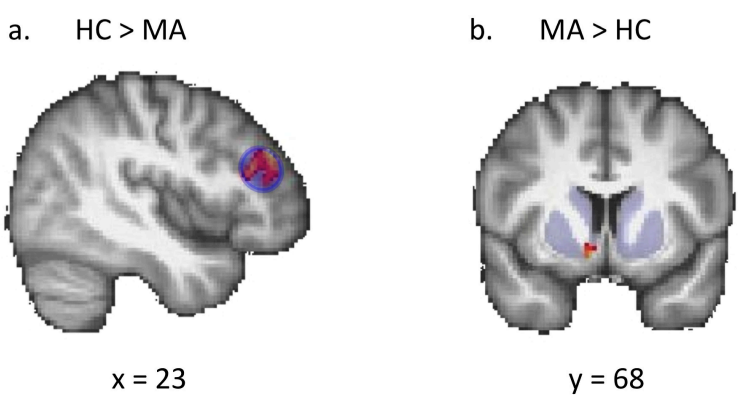

Figure 4.3. Modulation of striatal and prefrontal cortical activation by pump number during risky decision-making (ROI analysis) a. Healthy controls exhibited greater modulation of activation by pump number in the right DLPFC during active balloon pumps compared to the MA-dependent group. b. Compared to healthy controls, MA-dependent individuals displayed greater modulation of ventral striatal activation by pump number during active balloon pumps. Statistical maps representing Z-statistic values are shown, masked by regions of interest in which statistical comparisons were confined (p < 0.05, cluster corrected). Results were controlled for age, sex, smoking status, and marijuana use.

fMRI Resting-State Analysis

The RSFC analysis using the midbrain seed showed that MA-dependent subjects exhibited greater RSFC between the midbrain and putamen, amygdala, hippocampus and insula ($p < 0.05$, whole-brain, cluster corrected) than controls (Table 4.4, Fig. 4.4). There were no regions where controls exhibited greater midbrain RSFC than MA-dependent subjects or any group differences in DLPFC RSFC.

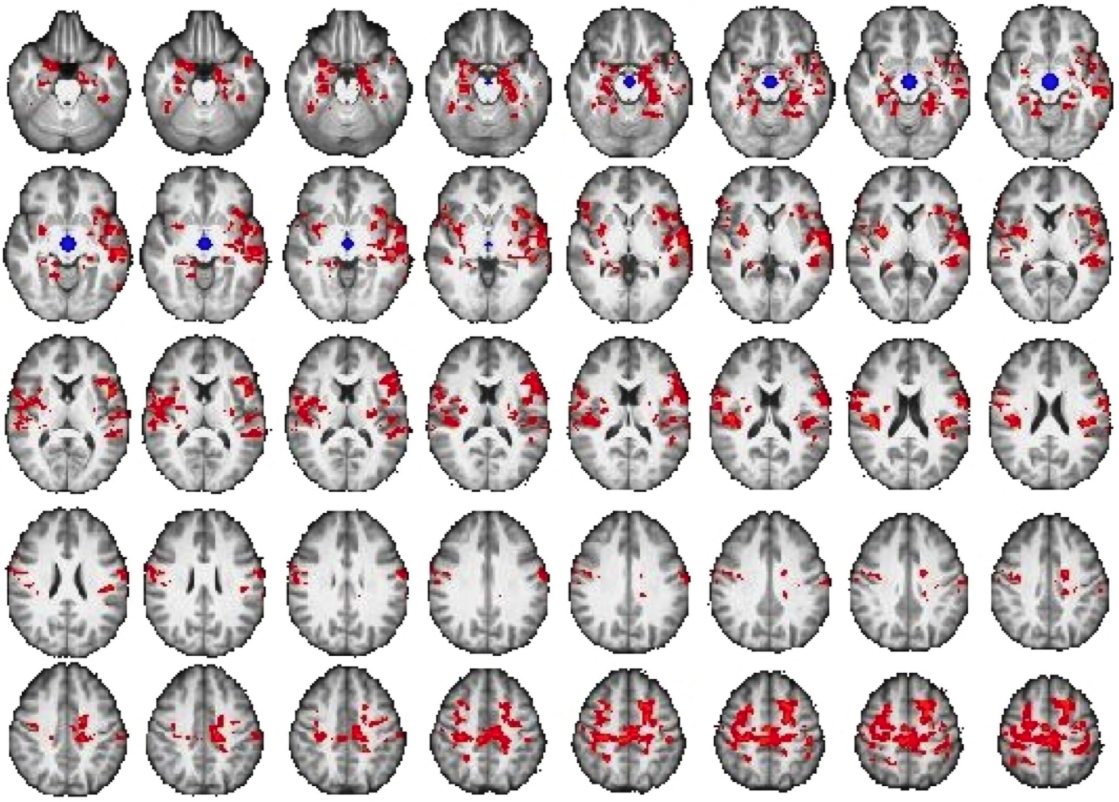

Figure 4.4. Comparison of mesocorticolimbic resting-state connectivity in methamphetamine-dependent and healthy control group. Connectivity maps show greater connectivity between midbrain seed (shown in blue) and putamen, amygdala, hippocampus, insula, and prefrontal cortex in MA-dependent compared to healthy individuals ($p < 0.05$, whole-brain cluster corrected) Results controlled for age, sex, smoking status and marijuana use.

Table 4.2. Brain regions that exhibited greater RSFC with the midbrain in methamphetamine-dependent than control subjects

Brain region	Cluster size (voxels)	x[a]	y	z	Z statistic
MA-dependent group > Healthy Control group					
Cluster #1[b]	2698				
Precentral gyrus (L/R)[c]		-6	-34	60	4.28
Superior frontal gyrus (L)		-22	10	52	4.23
Cluster #2	1776				
Inferior frontal gyrus (L)		-50	10	8	4.07
Superior temporal gyrus (L)		-62	-14	2	3.92
Middle temporal gyrus (L)		-56	-26	-8	3.79
Insula cortex (L)		-34	22	-2	2.32
Cluster #3	698				
Putamen (R)		32	-2	4	4.88
Parietal operculum		46	-20	18	4.75
Insula (R)		36	-2	8	2.52
Cluster #4	165				
Amygdala (L/R)		16	-2	-20	3.56
Hippocampus (L/R)		-18	-12	-18	2.39
Parahippocampal gyrus		20	4	-26	2.37
Cluster #5	122				
Insula (posterior) (L)		-36	-18	-4	3.62
Putamen (L)		-32	-16	-4	2.51

Z-statistic maps were thresholded using cluster-corrected statistics with a height-threshold of $Z > 2.3$ and cluster-forming threshold of $p < 0.05$. [a] x, y, z reflect coordinates for peak voxel or for other local maxima in MNI space. [b] Clusters are numbered and presented in order of decreasing size. [c] L or R refers to left or right hemisphere.

Relationships between Task-based Activation and Midbrain RSFC

The MA-dependent group showed a negative correlation between DLPFC modulation of activation during BART performance and midbrain RSFC with orbital frontal cortex, putamen, ventral striatum, amygdala, insula and cerebellum ($p < 0.05$, whole-brain, cluster corrected) (Table 4.3, Fig. 4.5). There were no correlations with midbrain RSFC in the control group or group by activation interactions.

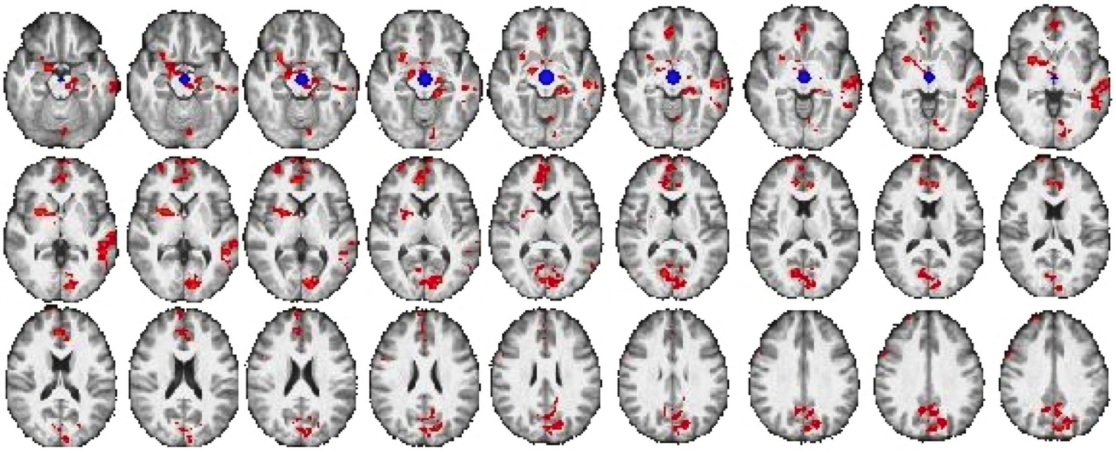

Figure 4.5. Relationship between resting-state connectivity of the midbrain and modulation of activation in DLPFC during risky decision-making in methamphetamine-dependent group. Connectivity maps show a negative correlation between modulation of activation in right DLPFC during balloon pumps and the connectivity between midbrain seed (shown in blue) and nucleus accumbens, putamen, amygdala, hippocampus, orbital frontal cortex, ACC, and superior frontal gyrus in the MA-dependent group ($p < 0.05$, whole-brain cluster corrected) (see Table 3 for list of regions). Results controlled for age, sex, smoking status and marijuana use.

Table 4.3. Brain regions of methamphetamine-dependent subjects, which showed negative correlations between midbrain RSFC and the modulation of activation by pump number[a] in DLPFC during risky decision-making

Brain region	Cluster size (voxels)	Coordinates			Z statistic
		x[b]	Y	z	
MA-dependent group: Negative correlation					
Cluster #1[c]	1768				
Superior frontal gyrus (R)[d]		4	38	52	2.97
Cluster #2	1663				
Occipital cortex		-6	-90	10	2.34
Cluster #3	1001				
Anterior cingulate cortex		4	46	6	3.77
Frontal medial cortex		0	50	-2	2.32
Cluster #4	770				
Parahippocampal gyrus		-16	-34	-12	3.88
Amygdala (L/R)		16	-4	-18	3.29
Putamen (R)		26	6	2	3.07
Nucleus Accumbens (L/R)		-6	6	-10	3.03
Hippocampus		-18	-18	-16	3.01
Cluster #5	726				
Superior temporal gyrus (L)		-62	-22	4	3.01
Middle temporal gyrus (L)		-64	-22	-22	2.92

[a] Amplitude of BOLD responses associated with pumps were modeled as a function of parametrically varied levels of risk and reward (represented by pump number). Z-statistic maps were thresholded using cluster-corrected statistics with a height-threshold of $Z > 2.3$ and cluster-forming threshold of $p < 0.05$. [b] x, y, z reflect coordinates for peak voxel or for other local maxima in MNI space. [c] Clusters are numbered and presented in order of decreasing size. [d] L or R refers to left or right hemisphere.

Relationships between Task-based Activation and DLPFC RSFC

ANCOVA showed an interaction of group with DLPFC modulation of activation during risk-taking on RSFC between DLPFC and the mesocorticolimbic system ($p < 0.05$, whole-brain, cluster corrected) (Table 4.4, Fig. 4.6A). Post-hoc analysis showed that in controls, DLPFC modulation of activation during risk-taking was positively correlated with DLPFC RSFC with ventral striatum, caudate, putamen, hippocampus and orbital frontal cortex ($p < 0.05$, whole-brain cluster corrected) (Table 4.4, Fig. 4.6B). In contrast, MA users exhibited a negative correlation between DLPFC modulation of activation during risk-taking and DLFPC RSFC with anterior cingulate ($p < 0.05$, whole-brain cluster corrected).

A.

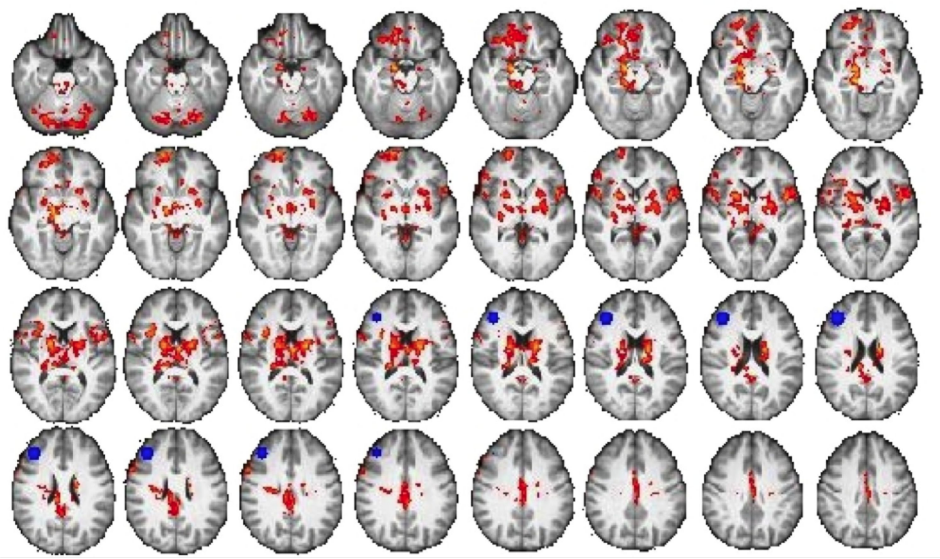

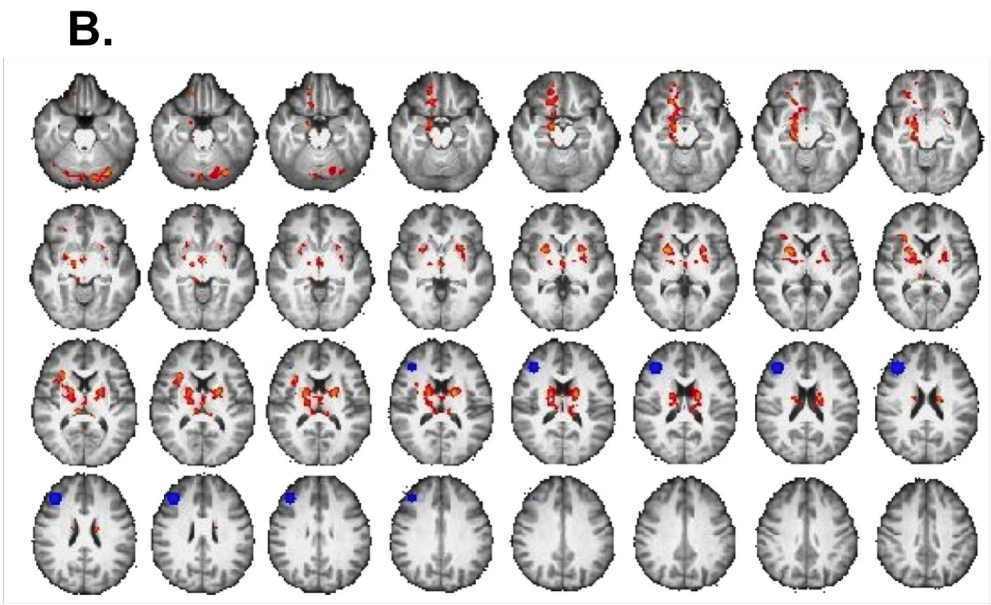

Figure 4.6. Relationship between resting-state connectivity of DLPFC and modulation of activation in DLPFC during risky decision-making. A. Brain regions where the relationship between resting-state connectivity with the DLPFC seed (shown in blue) and modulation of activation in right DLPFC by pump number varied by group. Connectivity maps show a group interaction between modulation of activation in right DLPFC during balloon pumps and RSFC of DLPFC with nucleus accumbens, putamen, amygdala, hippocampus, thalamus, orbital frontal cortex and cerebellum ($p < 0.05$, whole-brain cluster corrected) (see Table 4 for list of regions). **B.** Post-hoc analysis within the healthy control group showed a positive correlation between modulation of activation in right DLPFC during balloon pumps and RSFC of right DLFPC (show in blue) with caudate, putamen, nucleus accumbens, and orbital frontal cortex ($p < 0.05$, whole-brain cluster corrected) (see Table 4 for list of regions).

Table 4.4. Brain regions in which relationship between RSFC with DLPFC and modulation of activation in DLPFC by pump number[a] varied by group, with positive relationships in controls*

Brain region	Cluster size (voxels)	Coordinates			Z statistic
		x[b]	Y	z	
Regions exhibiting an interaction by group					
Cluster #1[c]	2549				
Amygdala (R)[d]*		16	-8	-12	4.63
Hippocampus (L/R)		16	-8	-20	4.38
Thalamus (L/R)		-4	-8	10	4.01
Putamen (L/R)*		20	6	4	4.06
Caudate (L/R) *		-16	-8	20	4.00
Insula cortex (R) *		34	12	10	3.32
Subcallosal Cortex (R)		12	20	-14	2.75
Nucleus Accumbens (R) *		12	12	-12	2.40
Cluster #2	1548				
Cerebellum (L/R)		-32	-68	-28	4.38
Cluster #3	610				
Superior frontal gyrus (R)		20	66	00	3.92
Frontal medial cortex		10	-54	-10	3.54
Orbital frontal cortex (R) *		18	26	-14	3.33
Cluster #4	286				
Inferior frontal gyrus (L/R)		-46	6	2	3.91
Cluster #5	125				
Paracingulate gyrus		4	12	50	4.52

[a] Amplitude of BOLD responses associated with pumps were modeled as a function of parametrically varied levels of risk and reward (represented by pump number). Z-statistic maps were thresholded using cluster-corrected statistics with a height-threshold of $Z > 2.3$ and cluster-forming threshold of $p < 0.05$. [b] x, y, z reflect coordinates for peak voxel or for other local maxima in MNI space. [c] Clusters are numbered and presented in order of decreasing size. [d] L or R refers to left or right hemisphere.

DISCUSSION

Our findings suggest that neuroadaptations in the mesocorticolimbic circuitry underlie abnormalities in frontostriatal activation during decision-making. Observed biochemical and structural differences in the frontal cortex and striatum associated with MA dependence [58, 60, 61, 64, 294-296 56, 99, 100, 110, 297, 298] may contribute to cognitive deficits. In this regard, stimulant-dependent individuals have deficits in decision-making [18, 19], cognitive control [24, 29, 299-301], and temporal discounting of rewards [22, 28].

Consistent with this view, MA-dependent subjects in this study performed worse than controls on the BART, as measured by total earnings and had fewer pumps. This finding may seem counterintuitive as risk-taking is often considered problematic. The results, however, are consistent with research indicating that greater pumping on the BART represents adaptive decision-making [227], with less pumping possibly reflecting a myopic preference for small-immediate rewards over larger-later rewards [227].

The observation that MA-dependent users exhibited greater modulation of activation by risk in the ventral striatum but less in the DLPFC than controls suggests that MA abusers have an impulsive, reward-driven decision-making process. The results are consistent with observations that deactivation of the rodent analog of the DLPFC results in suboptimal and maladaptive risky behavior [302], and that modulation of DLPFC activation by risk is associated with greater earnings but is negatively related to striatal D2-type dopamine receptor availability in humans performing the BART [277]. Activation of DLPFC has also been related to choices leading to large-future rewards despite incurring small immediate losses while ventral striatal activation was related to obtaining short-term reward [303]. Group differences in modulation of activation by risk level,

therefore, may reflect differences in reward-prediction latencies, with MA users focusing on short-term stakes while controls focusing on perceived long-term outcomes.

The relationship between corticostriatal RSFC and modulation of DLPFC activation in controls but not MA-dependent subjects during risky decision-making supports the notion that corticostriatal abnormalities contribute to top-down impairments observed in addiction [278]. Corticostriatal computational models show a modulatory role of prefrontal cortex (PFC) on striatal activity [257, 258] and indicate that PFC activity can override striatal representations of reinforcement value [257]. However, repeated stimulant exposure can alter the firing rates of prefrontal cortical neurons. In this regard, reductions in extracellular PFC glutamate [164] and depression at corticostriatal synaptic terminals [304] have been shown following chronic stimulant administration. Taken together, the heightened ventral striatal but blunted PFC response of MA-dependent users may, in part, be explained by dysregulated corticostriatal connectivity.

As repeated drug exposure induces long-lasting synaptic plasticity and sensitization of the mesocorticolimbic system [182], many studies have examined RSFC between regions of the mesocorticolimbic system in substance users [183-185 186 187, 283]. Here, abstinent MA-dependent participants exhibited greater mesocorticolimbic RSFC than controls, and this finding is consistent with results showing greater RSFC between nucleus accumbens and ventral medial PFC in abstinent cocaine users compared to controls [185]. A conflicting finding of less RSFC between ventral tegmental area, amygdala and medial PFC in cocaine users, most of whom presented evidence of cocaine use on the scan day [18318317717724](Gu et al., 2010)(Gu et al., 2010), most likely reflects acute effects of cocaine.

From a theoretical standpoint, mesolimbic hyperexcitability may reflect stimulant-induced sensitization as posited by the Incentive Sensitization Theory of Addiction [145, 146]. Amphetamine

sensitization in rats increases neuronal firing of mesolimbic structures [214], and in humans, amphetamine-induced sensitization of dopamine release can persist for 1 year [305]. Although the Incentive Sensitization Theory postulates a heightened sensitivity of the mesolimbic system in response to further drug use or associated cues [145], elevated mesocorticolimbic RSFC in MA users may reflect sensitization even in the absence of reward-related stimuli. Drug-induced sensitization has been studied primarily in terms of facilitating drug self-administration, conditioned place preference and the motivation for drugs [306-308]; however, our study suggests that mesolimbic sensitization has more global effects on psychological processes and behaviors. The results imply that intrinsic hyperactivity in the putative connections among regions involved in reward processing diminish activation in regions of executive functioning and lead to maladaptive decision-making.

LIMITATIONS

The temporal resolution of fMRI combined with the BART did not allow complete isolation of decision-making processes, such evaluation, selection and anticipation. In this regard, striatal activation has been associated both with the anticipation of reward [48] and aversive stimuli [271]. Modulation of ventral striatal activation by pump number in the MA group, therefore, may reflect anticipation of aversive outcomes (balloon explosion) rather than of reward. In addition, RSFC does not assess directional influence of brain regions; therefore, it is unclear whether RSFC between DLPFC and striatum reflects top-down control or spontaneous coherence of activation. Finally, risk-taking could not be dissociated from learning risk probabilities, and tasks that decompose risk-taking into distinct cognitive constructs is needed [309].

Conclusion

As a number of neuroadaptations occur within the mesocorticolimbic system following drug exposure [182], it is critical to understand the behavioral consequences of such drug-induced plasticity. In addition to providing information about mesocorticolimbic RSFC in MA dependence, the findings presented here raise the possibility that abnormalities in intrinsic connectivity may contribute to maladaptive decision-making and associated frontostriatal deficits associated with addiction.

CHAPTER 5
SUMMARY AND CONCLUSIONS

Many people abuse addictive substances despite their negative, long-term consequences. Addictive behaviors are likely to arise from multiple factors [310], and abnormalities in the dopamine system and in signaling between the prefrontal cortex and striatum often accompany them [278, 311, 312]. As dopamine signaling and frontostriatal activation play a critical role in executive functioning, maladaptive risky decision-making exhibited by stimulant users may reflect the effects of stimulants on the dopamine system and associated signaling pathways.

Acute stimulant exposure increases intracellular and extrasynaptic levels of dopamine [312], and the persistent use of stimulants may contribute to low levels of D2-type receptor availability exhibited by MA-dependent individuals [100]. As D2-type receptor availability serves as a marker for dopamine function, the dysfunction in dopamine signaling may contribute to the maintenance of addiction. This view is in line with results linking low D2-type receptor availability with relapse [310, 313, 314]. In addition, chronic stimulant use may alter dopamine signaling related to positive reward-prediction errors. As learning about future expectations and reward predictions is thought to drive synaptic modifications and enhance reward-seeking behavior[315], dysfunctions in dopamine signaling may thereby strengthen the propensity to abuse substances [310, 314] In this regard, it has been proposed that drug-related cues become salient motivational stimuli, and that such incentive sensitization might be mediated by the action of dopamine in the ventral striatum and by signaling within the mesocorticolimbic system [316].

These neurobiological phenomena associated with addiction may contribute substantially to maladaptive decision-making, specifically in the context of potential risk and reward. Risky decision-making and faulty evaluation of reward may facilitate drug use by assigning greater weight to reward than to the potential for negative long-term consequences. Studies have shown

that stimulant users take more risk and implement worse decision-making strategies than healthy control subjects in laboratory tasks of decision-making [16, 18, 19, 317]. MA-dependent individuals also exhibit steeper temporal discounting of reward[28] compared to controls, and show deficits in superior and middle prefrontal cortical and striatal activation when performing the Delay Discounting Task paired with fMRI[22]. In addition, animal studies measuring dopamine efflux using microdialysis have shown a role of the PFC and striatum in integrating signals about reward, delay and uncertainty[288] and aberrant signaling of the mesocorticolimbic system induced with NMDA and dopamine receptor antagonists has produced effects on reward-driven behavior[270].

The mesocorticolimbic system serves to connect regions activated by rewarding stimuli and those involved in executive functioning. Therefore, a disruption in the mesocortical circuit may lead to the abnormal evaluation of a stimulus and the assignment of value and contribute to the maladaptive decision-making exhibited by MA abusers [41, 212 22, 46]. Activity of the mesocorticolimbic system depends on dopaminergic signaling [217], and therefore, dopamine receptor binding is a necessary link between the evaluation of potential future rewards and the execution of a decision [193, 318, 319].

A postmortem study showed low levels of striatal dopamine and dopamine transporters[110] in MA abusers, and in vivo studies using PET showed MA abusers exhibit low levels of D2 receptor availability[99, 100]. Abnormalities in these components of the dopamine system likely disrupt dopamine signaling in the mesocorticolimbic system[320], and such disruption, in turn, produces deficits in the evaluation of rewards and thereby, in decision-making. The studies described here provide evidence of dysfunction in cortical and striatal regions of MA-dependent individuals during risky decision-making and in intrinsic activity of the mesocorticolimbic

system at rest, and also show the relationship between these neurobiological processes. They also provide evidence for the involvement of dopamine D2-type receptors in risky decision-making and associated modulation of frontostriatal activation in healthy controls. Furthermore, the preliminary results in healthy controls show a negative relationship between D2-type receptor availability and the resting-state connectivity of the mesocorticolimbic system. Taken together, the findings presented here suggest that neurobiological differences in dopamine D2-type receptor availability and mesocorticolimbic resting-state functional connectivity between healthy and MA-dependent subjects may underlie maladaptive risky decision-making observed in MA dependence.

Given what is known about the neural circuitry connecting the PFC to the striatum and the experimental evidence obtained in this study, it is reasonable to conclude that dopamine signaling in the mesocorticolimbic system, as inferred from dopamine D2-type receptor availability and mesocorticolimbic resting-state activity, are important in determining the modulation of frontostriatal activation as a function of context. These experiments, however, did not distinguish the contributions of the three subpopulations of striatal dopamine D2-type receptors, which include postsynaptic receptors, autoreceptors on terminals of midbrain afferents, and presynaptic receptors on corticostriatal terminals. Postsynaptic D2-type receptors are localized on GABAergic interneurons in the striatum, while presynaptic D2-type receptors are found on corticostriatal glutamate terminals and on terminals of afferents from the midbrain.

Presynaptic and postsynaptic dopamine receptors facilitate two functionally independent firing patterns of dopamine neurons[259] – termed "phasic" and "tonic: firing[259]. Repeated firing of dopamine neurons induces a high amplitude transient increase in dopamine release within or near the synapse. Such phasic dopamine release in the striatum functions as a signal for the presence

of relevant stimuli and, in part, is regulated by presynaptic dopamine autoreceptors[321]. High-affinity dopamine transporters along the dopaminergic terminals terminate transmitter action by reuptake of extracellular dopamine , thereby restoring dopamine homeostasis[66]. Activation of autoreceptors on somatodendrites slows the firing rate of dopaminergic neurons while activation of nerve terminal autoreceptors inhibit the synthesis and release of dopamine[321, 322]. In contrast, tonic firing of midbrain neurons is mediated by presynaptic D2 receptors on the corticostriatal glutamate-containing projections from the prefrontal to the ventral striatum [323-326]. The tonic firing of dopamine neurons induces the release of dopamine, which is maintained at stable concentrations (nanomolar range) of extrasynaptic dopamine in the striatum [259, 327].

D2-type receptors play an important role in maintaining the balance of phasic and tonic dopamine release in the striatum. In response to low levels of tonic dopamine concentrations, postsynaptic D2-type receptors are upregulated to restore baseline levels of dopamine receptor stimulation [328]. However, D2 receptors also have an inhibitory role in striatal glutamatergic transmission, and activation of presynaptic D2 receptors on corticostriatal terminals attenuates glutamate-mediated excitation in the striatum [263, 267]. Activation of postsynaptic D2-type receptors by high-amplitude phasic dopamine signaling can potentiate nucleus accumbens activity, thereby inhibiting PFC glutamatergic neurotransmission and effectively shifting the balance of information in favor of limbic inputs through striato-thalamo-cortical and striato-meso-cortical loops.

In contrast, tonic dopamine release, which is enhanced by PFC activity and presynaptic D2 receptors in corticostriatal terminals, is thought to attenuate phasic dopamine release in the ventral striatum[259, 327, 329]. An increase in tonic dopamine release may thereby explain the mechanism by which descending corticostriatal pathways can influence the balance in favor of

PFC predominance in behavioral control [278]. Given the specificity of presynaptic autoreceptors and postsynaptic D2-type receptors in the regulation of striatal dopamine release, we suggest that mediation of the antagonistic relationship of tonic and phasic dopamine release by D2-type receptor availability influences PFC and the ventral striatum during risky decision-making.

In Study 1, individuals with higher striatal D2-type dopamine receptor BP_{ND} exhibited greater nucleus accumbens responsivity to reward compared to individuals with lower receptor BP_{ND}. This finding may reflect presynaptic corticostriatal D2-type receptor mediated attenuation of glutamate transmission leading to greater striatal influence over PFC through striato-thalamo-cortical and striato-meso-cortical signaling. In addition, participants with low striatal BP_{ND} earned more money and exhibited greater modulation of activation in the DLPFC by risk level during decision-making than participants with higher striatal BP_{ND}. These results are consistent with the view that low levels of postsynaptic D2-type receptors may attenuate ventral striatal response to reward and low levels of presynaptic D2-type receptors on corticostriatal afferents would increase prefrontal glutamate. Together, low presynaptic and postsynaptic receptor availability would lead to greater PFC regulation over striatal responses to reward.

These results, concerning healthy control subjects, are inconsistent with the observation that stimulant-dependent individuals, who exhibit low striatal BP_{ND} [269], have less activation in the PFC during decision-making compared to controls. The heightened activity of the mesolimbic system at rest and of the ventral striatum during decision-making in the MA-dependent group may be associated with an imbalance of tonic and phasic dopamine release. Striatal dopamine D2-type receptor BP_{ND} in the healthy control sample was negatively associated with the modulation of activation in the PFC, and the preliminary results showed that BP_{ND} was negatively correlated with midbrain RSFC. As downregulation of dopamine receptors

is associated with increased or elevated levels of tonic dopamine concentrations in the striatum, resting-state activity may serve as a proxy for PFC-mediated tonic activity in the VTA and striatum.

Although these interpretations provide a theoretical model to account for glutamatergic adaptations, heightened mesocorticolimbic activity, and downregulation of D2 receptors associated with MA dependence, a major limitation of the study is the lack of spatial resolution with PET. Measurements of D2-type receptor availability in these experiments do not delineate between distinct subpopulations of D2-type dopamine receptors in the striatum, and interactions of dopamine with these different types of receptors have different effects.–Activation of presynaptic D2 autoreceptors generally causes a decrease in dopamine release that results in decreased locomotor activity whereas activation postsynaptic receptors stimulates locomotion[234]. Because D2 autoreceptors have higher affinities for dopamine compared to postsynaptic receptors, a dopamine agonist can induce a biphasic effect leading to decreased activity at low doses and behavioral activation at high doses[234].

In addition, the precise role of presynaptic and postsynaptic dopamine D2 receptors in striatal dopamine signaling is not completely clear. For example, a study of knock-out mice lacking D2 autoreceptors in the substantia nigra pars compacta and the VTA showed that the regulation of dopamine synthesis and release is not solely regulated by presynaptic D2 autoreceptors, but that postsynaptic D2 receptors also contribute to the regulation of dopamine release[330]. The study also found that activation of postsynaptic D2 receptors by quinpirole reduced motor activity and inhibited dopamine synthesis, supporting the view of a postsynaptic D2 receptor-mediated control of dopamine signaling. These results suggest that D2 postsynaptic receptors contribute to the maintenance of appropriate dopamine levels. In addition, results from pharmacological

studies and studies in D3 knock-out mice suggest that D3 autoreceptors may also contribute to the presynaptic regulation of tonically released dopamine[331, 332]. Future studies would be required to clarify the influence of presynaptic and postsynaptic dopamine receptors in dopamine-mediated behaviors. Understanding the precise nature of dopamine signaling through D2 receptor subtypes will greatly facilitate our understanding of the function of dopamine in both normal and pathological behaviors.

Future Direction

High levels of tonic dopamine induced, in part through irregular tonic activity of the prefrontal cortex are thought to induce homeostatic downregulation of D2-types receptors[259]. A proposal that has yet to be tested is that stimulant exposure leads to an imbalance of tonic striatal and mibrain dopamine release, and that this imbalance may contribute to the maintenance of addiction[329]. Future studies could be conducted in animals to delineate the relationship between persistently low dopamine concentrations in the striatum and stimulant-induced adaptations of prefrontal glutamatergic activity.

As the current literature provides extensive evidence of low D2-type receptor availability in individuals with addictive disorders[100, 313], augmentation of dopamine D2-type receptors might be of therapeutic value. D2-type receptor availability has not only been associated with inhibitory dyscontrol and impulsivity [100], but also been linked to the success of behavioral treatments for stimulant dependence [101]. In addition, relatives of addicted individuals who do not abuse drugs exhibit higher levels of dopamine receptor binding than individuals with no familial history of addiction[333]. These observations suggest that higher densities of dopamine D2-type receptors in the striatum could protect against relapse or the development of addiction. The neurobiological pathology of the dopamine system, as discussed in earlier chapters may

contribute to the unsuccessful attempts of medications aimed to augment the dopamine signaling, and perhaps a more effective therapeutic approach would be to improve dopamine receptor function and return dopamine receptor availability to levels present in normal healthy individuals. An increase in D2-type receptor availability or function may enhance the efficacy of pharmacological treatments aimed at targeting the dopamine signaling and may ameliorate neurobehavioral deficiencies seen with MA dependence.

In addition, as the studies from this dissertation show that resting-state connectivity of the mesocorticolimbic system is negatively related to prefrontal activation during decision-making, another therapeutic approach would be to use real-time fMRI to provide biological feedback to downregulate mescorticolimbic activity. Biofeedback of real-time fMRI data is a new technique in which the temporal pattern of activity in a specific region or distributed patterns of brain activity are presented to subjects in real time[334, 335]. Neurofeedback experiments use participant-regulated brain activity as feedback to examine the effects of voluntarily controlled brain activity on task performance such as reaction time or emotional regulation[334, 335,336]. Although a relatively new technique, a measure of coupling between two or more areas can be used as a feedback parameter and possibly trained for modification[336]. In this way, biofeedback with fMRI may provide a method for addicts to downregulate the connectivity between regions of the mesocorticolimbic system.

APPENDIX
BASICS OF fMRI AND PET IMAGING

There are a variety of methods used in neuroscience to study neural activity. Functional magnetic resonance imaging (fMRI), despite poor temporal resolution, is a common method to study decision-making as it is a noninvasive approach that provides good spatial resolution. Neuronal activity is measured indirectly with fMRI, which relies on the assumption that neuronal activity and blood flow are linked. The power of fMRI imaging is greatly improved when they are combined with other imaging methods and in particular, positron emission tomography (PET), which can provide in vivo assessments of the molecular function. The combination of such imaging modalities link functional brain activation to neurotransmitter systems. This chapter will briefly discuss the principles behind fMRI and PET imaging and standard analysis methods.

BASICS OF fMRI

MRI Physics

Images produced by Magnetic Resonance Imaging (MRI) are based on spatial variations in the phase and frequency of the radio frequency (RF) energy being absorbed and emitted by the imaged object. Each proton in the body has its own magnetic field and can receive and emit RF energy. However, the signal from protons is small as the orientation and spin of a proton and that of its neighboring neurons are random. When a constant magnetic field B_0 is applied, the spins of the protons will align either with or against the magnetic field (Fig. A1). A brief magnetic pulse orthogonal to B_0 (90 degree excitatory RF or RF pulse) tips the aligned spins to the transverse field (Fig. A1). Protons absorb the RF energy and to flips to a higher energy state (i.e., nuclear magnetic resonance). Following application of the RF pulse, the protons gradually relax into their natural lower energy state and emit the excess energy in the form of RF waves. The rateof relaxation indicates the surrounding environment of the protons.

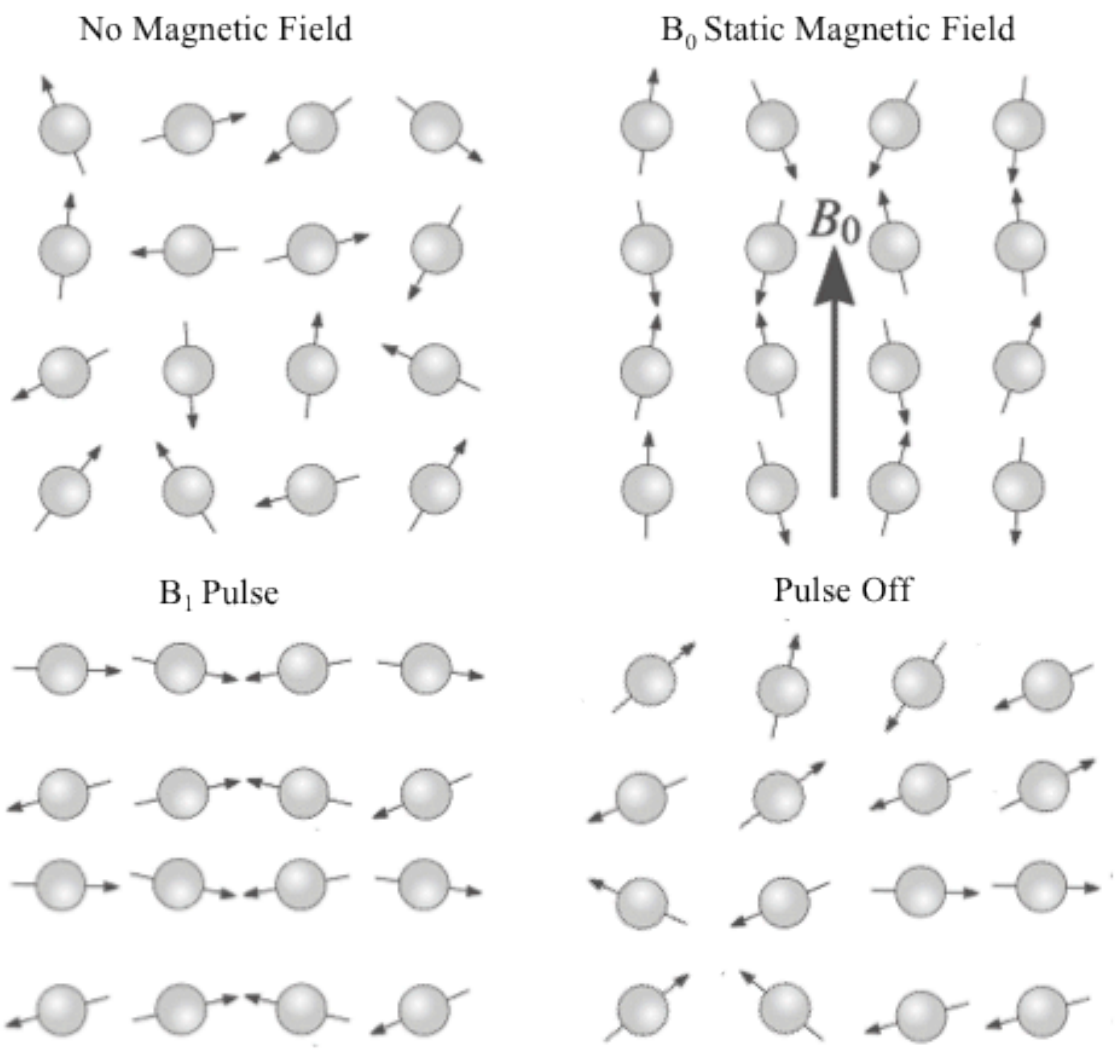

Figure A1. Proton Spins. Top left panel represents proton spins in the absence of a magnetic field. Top right panel depicts protons that are aligned in parallel or opposite to the external magnetic field. Bottom left shows the protons aligned to the transverse field following an RF pulse. Bottom right shows relaxation of proton spins following the RF pulse.

The times that it takes for the protons to relax are known as T1 (longitudinal) and T2 (transverse). T1 relaxation times are highly dependent on tissue type, whereas T2 is caused by spin-spin interactions and is independent of the nature of the tissue. T1-weighted MR images are obtained by measuring the decay times or the different rates of energy release in different tissues of the brain. As the protons realign with the magnetic field (T1 relaxation), they precess around

B_0 according to: $\omega_0 = \gamma B_0$, where ω_0 is the precessing frequency (also called Larmor frequency) and γ is the gyromagnetic ratio. T1-weighted MR imaging are high-resolution anatomical images where white matter with their long T1 appear white and gray matter with short T1's appear gray.

In T2-weighted images white matter appears grey and grey matter appears white and the change in intensity is a function of brain activity. T2 relaxation is the time that it takes for the protons to spin out of phase with each other in the transverse plane and is dependent on the inhomogeneity in the local magnetic field caused by blood flow. As firing neurons consume oxygen in hemoglobin of red blood cells, the increase in blood flow and blood oxygenation is measured with Functional Magnetic Resonance imaging (fMRI). Oxygenated hemoglobin is diamagnetic and has the same magnetic properties as the rest of the tissue, whereas deoxygenated hemoglobin is paramagnetic. Deoxygenated hemoglobin causes a change in the magnetic susceptibility of the blood flow, thereby creating inhomogeneity in the local magnetic field, which in turn decreases the time constant T2. Blood Oxygenation Level Dependent (BOLD) signal is obtained by T2 and is therefore an indirect measure of neuronal function. The BOLD response has a characteristic shape (called hemodynamic response function or HRF): after an initial dip it peaks approximately 6 seconds after a stimulus onset, and then decays back to baseline after a small undershoot (Fig. A2). This temporal resolution is one limitation of measuring neuronal activity with the BOLD signal, as neuronal spiking is on the order of milliseconds.

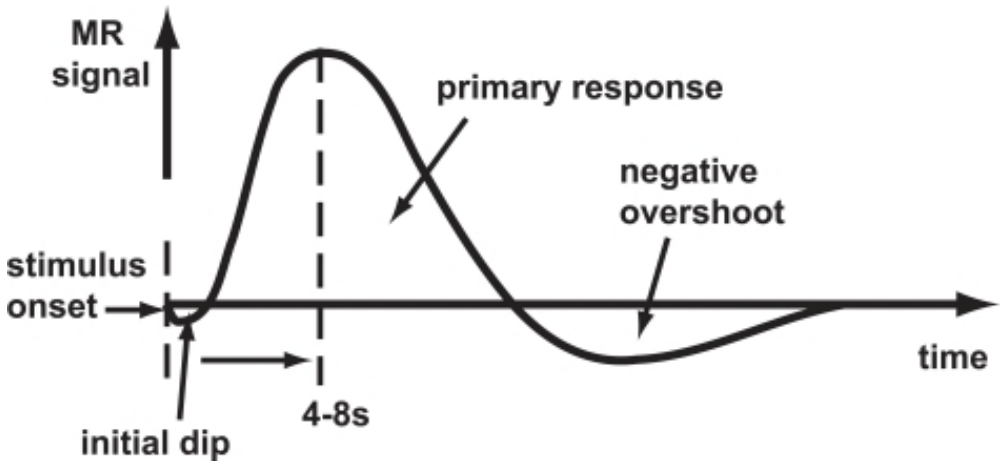

Figure A2. Hemodynamic Response Function (HRF).

fMRI Data Acquisition

In order to create 3-dimensional images of the brain, three mutually orthogonal magnetic gradients are applied in addition to the uniform magnetic field B_0 (Fig. A3).

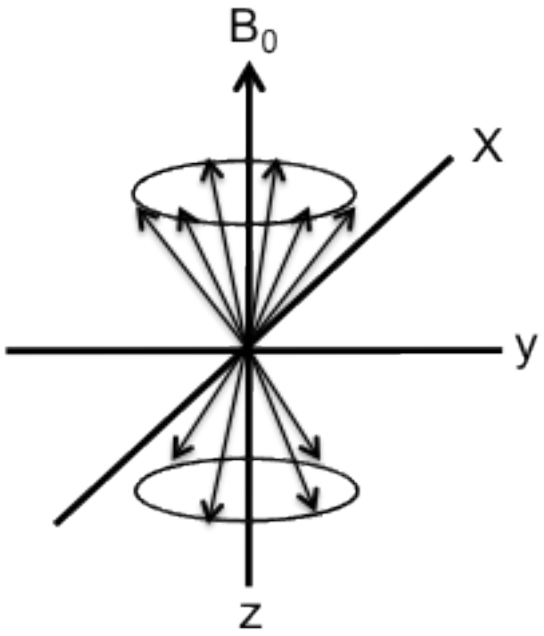

Figure A3. Magnetic Gradients.

In the z-dimension this is achieved through a method called slice selection. Individual slices are selected by turning on a gradient during the excitatory RF pulse that tips the spins into the

transverse plane. This process is repeated consecutively for all slices. Frequency encoding is achieved by turning on a magnetic gradient that changes the precessing frequency of the spins depending on their location along the x-axis. Another gradient is applied that causes the spins to be out of phase with respect to each other in a predictable manner along the y-axis. Both the frequency and phase encoding are then recovered through Fourier transform to recover the signal from a single voxel. The fMRI times series are the set of 3-D images that are taken at a specified time repetition (TR) (usually 1-3 seconds). However, each slice images is not taken sequentially as noise can be introduced from adjacent slice. Instead slice acquisition is interleaved and each slice is repeatedly acquired at the specified TR.

fMRI Data Preprocessing

All fMRI data preprocessing in this dissertation was done using the FMRIB Software Library (FSL) v5.0 http://www.fmrib.ox.ac.uk.

Realignment/Motion correction

One of major sources of noise in fMRI data is subject head movement. All images are realigned sequentially with respect to the previous image, and together all of the images are aligned with respect to the first image using a linear rigid body transformation where 3 rotation and 3 translation parameters are applied.

Brain Extraction

Brain extraction is applied to create a brain mask that contains valid brain voxels by removing skull, dura and neck.

Spatial Smoothing

As activity of neighboring voxels are correlated, spatial smoothing increases signal to noise by filtering each image with a three-dimensional Gaussian smoothing kernel (Fig. A4). Spatial

smoothing reduces noise without reducing valid activation as long as the underlying activation area is larger than the extent of the smoothing. Thus if you are looking for very small activation areas then the smoothing kernel should be 5mm or less; however, if the expected activation is in large brain regions, the smoothing kernel can be increased. The smoothing carried out on data for this dissertation was with a FWHM=5 mm (Full Width at Half Maximum) Gaussian smoothing kernel.

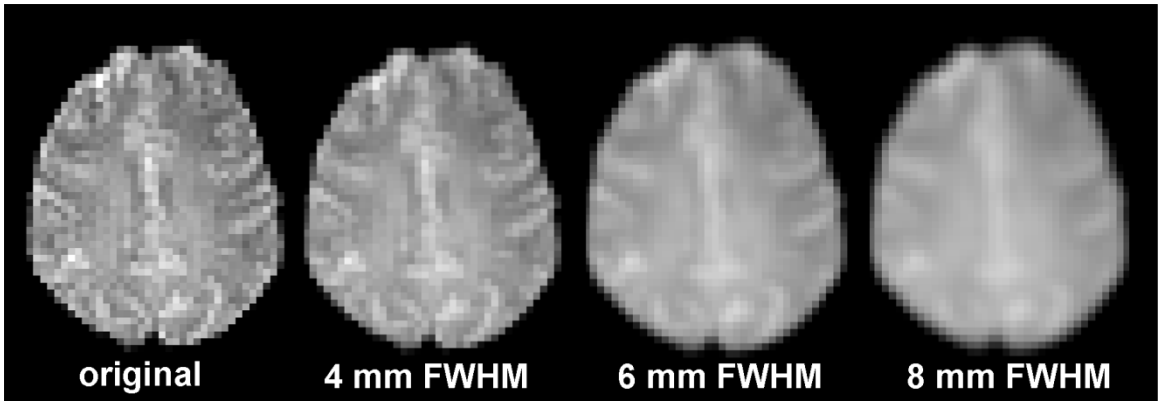

Figure A4: Spatial smoothing. Functional imaging data before and after spatial smoothing with 4 mm, 6 mm, and 8mm FWHM Gaussian kernels

Temporal Filtering

Signal and noise are present at different frequencies and by attenuating the noise using filters, the signal to noise ratio can be enhanced. Highpass filtering removes low frequency artifacts that are typically caused by scanner drift. By using a local fit of a Gaussian-weighted straight line, highpass filtering will "straighten out" or flatten any gradual linear or quadratic drifts (Fig. A5).

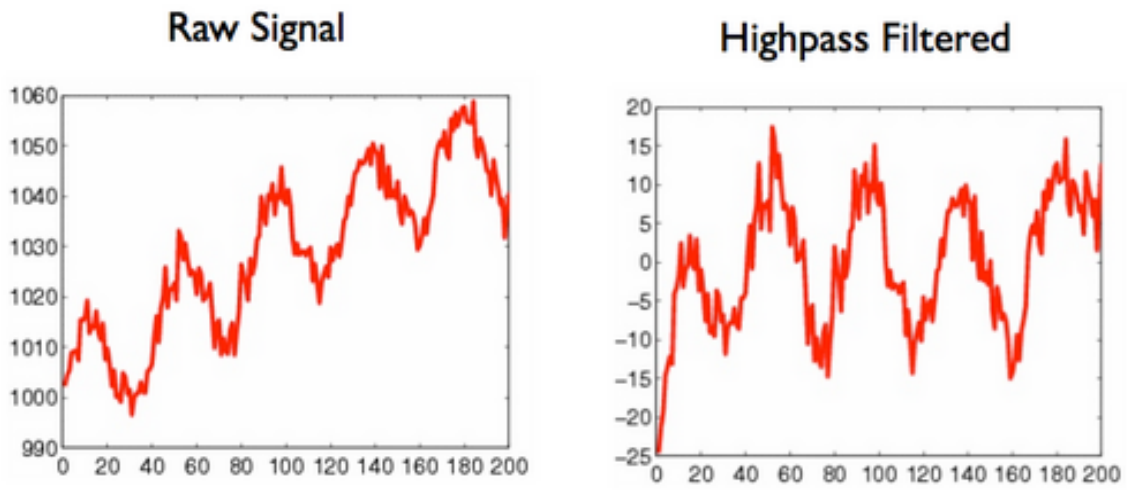

Figure A5. Temporal filtering. Scanner drift is depicted in the raw data (left), data is flattenened after highpass straight line filtering (right).

Temporal filtering, as opposed to spatial filtering is most common in fMRI data analysis because frequencies that repeat over a timescale that exceeds the experimental temporal parameters are removed. Lowpass temporal filtering reduces high frequencies that are oscillating too rapidly to correspond to the signal of interest. Lowpass spatial filtering is accomplished by Gaussian smoothing, as mentioned above but temporal lowpass filtering reduces the strength of the signal of interest and remains a topic of controversy.

Registration

In order to collect fMRI data rapidly, spatial resolution is compromised. In order to map brain activation to brain areas, the registration of brain data in this dissertation was conducted in four steps. Functional images were first realigned to a full-brain medium-quality image with the same MR sequence as the functional data using 3 translation parameters (x, y and z directions). The data were then registered to a high-resolution T1 image using the 3 translation parameters and 3 rotation parameters (pitch, roll and yaw). In order to account for brain variability across

individuals and to generalize regions of activation, the data were then registered to a standard MNI-template from the Montreal Neurological Institute (Evans, Collins et al. 1993) using a 12-parameter affine transformation (3 translation, 3 rotation, 3 shears and 3 zoom parameters) (Fig. A6).

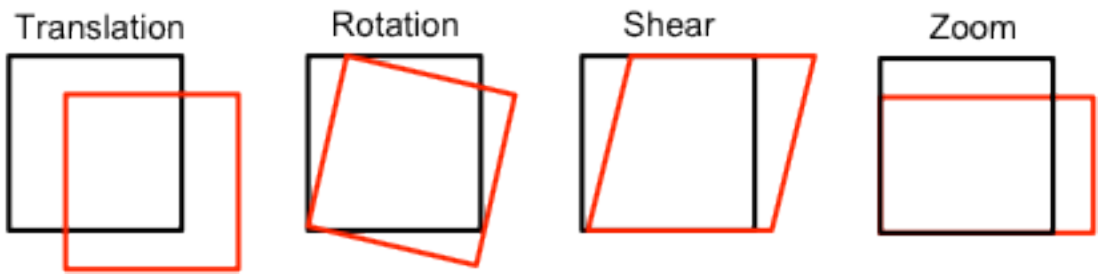

Figure A6. 12-parameter affine transformation: 3 translation, 3 rotation, 3 shears and 3 zoom parameters

The 12 parameters are sufficient to model overall differences in position and size between different brains, however, if more local differences such as enlarged ventricles or reduced gray matter volume is suspected, non-linear transformations may provide a more accurate registration. The registration of data in this dissertation was further refined using a nonlinear warp resolution of 10 mm. The warp fields are represented as linear combinations of discrete cosine basis functions and are modeled using the sum of squared differences between the template and source images (Fig. A7).

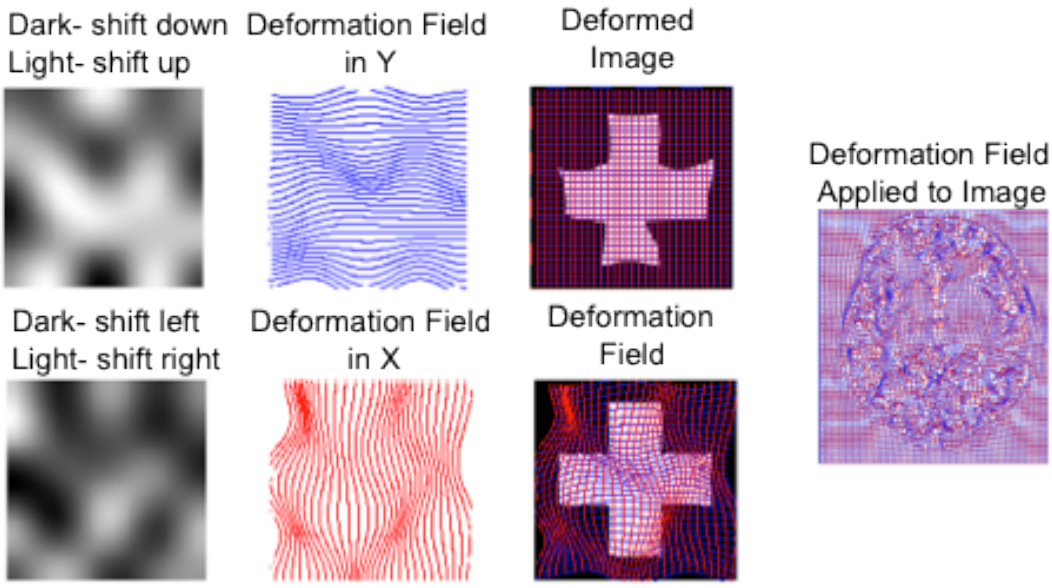

Figure A7. Non-linear warping

fMRI Data Analysis

The functional data in this dissertation has been analyzed using a General Linear Model (GLM). The GLM obtains statistics about the fit of a series of observations (the fMRI data) that can be described by a linear combination of explanatory variables (the stimuli and/or subject responses). This requires *a priori* hypothesis about the time and shape of the brain response. In order for these regressors to explain the brain data it must be convolved with the hemodynamic response function (HRF) (Fig. A8).

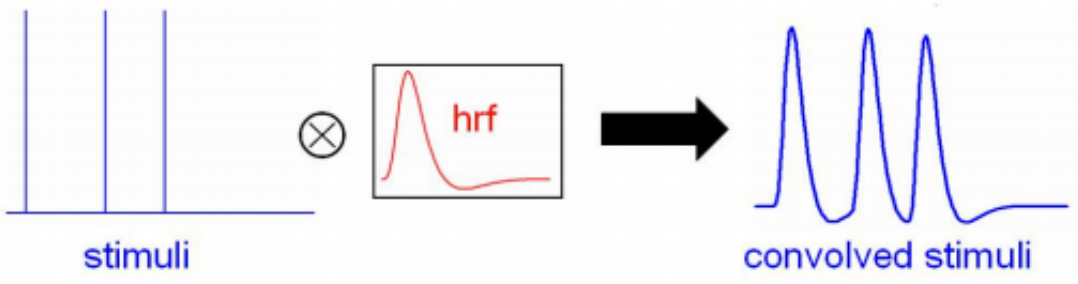

Figure A8. Convolution with a hemodynamic response function (HRF). The stick functions on the left panel represent stimulus onset times, which are convolved with an HRF to model the BOLD response (right panel).

For a given voxel, a time-series is created: $y = (y_1, y_2, y_3,\ldots, y_n)$, where y_1 represents the intensity of that voxel at a given time. A linear fit of the data and stimulus events (explanatory variables/regressors) that might describe the data are modeled. Two stimulus events for example would be modeled as: $x_1 = (x_{11}, x_{12}, x_{13},\ldots, x_{1n})$ and $x_2 = (x_{21}, x_{22}, x_{23},\ldots, x_{2n})$. Then the independent variable y as a linear combination of x_1 and x_2 plus a constant term and an error term are calculated:

$$y_1 = \beta_0 + \beta_1 x_{11} + \beta_2 x_{21} + \varepsilon_1$$
$$y_2 = \beta_0 + \beta_1 x_{12} + \beta_2 x_{22} + \varepsilon_2$$
$$y_n = \beta_0 + \beta_1 x_{1n} + \beta_2 x_{2n} + \varepsilon_n$$

t-tests are then performed on all voxels of the brain to give a statistical parametric map, which is color-coded and overlaid on the high-resolution anatomical scan. For within-subject analyses, a fixed-effect model is used to ignore the variance within a subject and to increase the sensitivity of observing significant observations. In order to generalize the findings and account for variances across subjects, a mixed effect model is incorporated at the group level.

The analyses conducted in this dissertation also used a method to de-weight outliers by an automatic outlier detection process, where for each voxel, each subject's data is considered with respect to the other subjects in order to detect regarding any outliers. Outliers are then automatically de-weighted at the group level statistics.

Although the GLM is the most commonly used method to analyze fMRI data, it has some limitations, the most important one being the assumption of linearity. When performing a GLM analysis, one assumes that the BOLD response is linear; however different functions can be applied to the model by specifying the amplitude and shape of the HRF associated with each regressor.

BASICS OF POSITRON EMISSION TOMOGRAPHY

PET Physics

Molecular imaging with positron emission tomography (PET) and radiolabeled compounds has enabled the in vivo assessment of the distribution and availability of receptors, enzymes and other cellular processes pertaining to the dopamine system in normal and pathological states.

PET imaging uses radiolabeled compound, otherwise known as a radiotracer or radioligand and is based on the principles of positron decay and coincidence detection of two gamma rays by radiation detectors[337]. The unstable proton-rich radioisotope undergoes positron or positive beta decay, whereby it emits one proton into one neutron, one positron, and one neutrino[337]. The positron then travels a distance of about 1.0 – 2.0 mm, where it annihilates with a negative electron[337]. Two photons are emitted, each with energy equal to 511 keV, in the exact opposite directions (Fig. A9). The photon energy of 511 keV is equal to the electron rest mass, e=mc2[337]. The positron decay, shown below, where β+ is the positron.

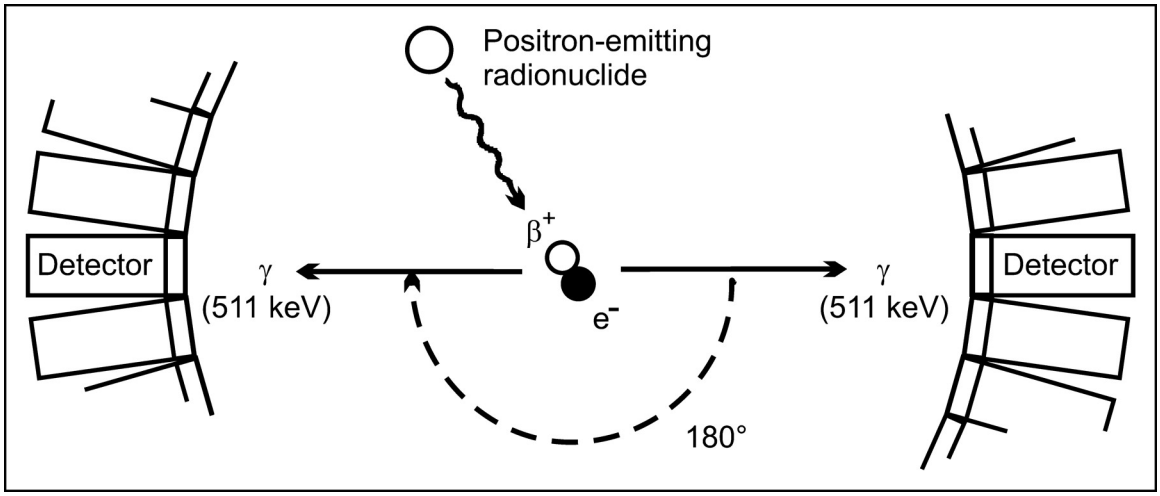

Figure A9. Positron decay and coincidence detection of two gamma rays by radiation detectors

A PET scanner contains multiple rings of detector crystals. Detectors are connected to photomultiplier tubes, which amplify the detection signal and locate the photon line of origin[338]. A PET image is produced by detecting the two annihilation photons. Two opposed detectors record the line of coincidence of the photon pair making it possible to localize the source of the annihilation event along the straight line of projection. Scintillation occurs once the detectors interact with the photons, and photomultiplier tubes then convert the light photons to a measurable electrical pulse[337].

PET has inferior spatial resolution as compared to computed tomography (CT) and magnetic resonance imaging (MRI). CT can produce images with submillimeter resolution, where as MRI can produce images with a resolution of about 1.0 mm. PET scans are produced with a maximum resolution of about 4.0 - 5.0 mm[338]. Likewise, the temporal resolution of PET is much slower than MRI, as the kinetics of PET tracers occur over a slow time course (of minutes), and therefore cannot track fast changes in chemical concentration or neuronal activity.

Photon scatter

One or both of the emitted photons can be scattered and the scattered events can be detected coincidently at another detector not along its true line of response. This results in a false calculation for the origin of the tracer activity[339] (Fig. A10, B). Scattered events cause blurred images and poor image contrast by introducing a source of error in positron localization. Large energy windows will detect more scattered photons and result in a greater percentage of misalignments thereby decreasing spatial resolution[337]. Lead or tungsten collimating septa between the rings can prevent detection of scattered photons at high incident angles. The scanner that was used to collect PET data contained in this dissertation used a tungsten septa.

Photon attenuation

Photon attenuation is another factor that contributes to the inferior spatial resolution of PET, where one or both of the annihilated photons undergoes total absorption in tissue[339] (Fig. A10, C). Attenuation can decrease the energy of the emitted photons or reduce the total number of photons that reach the detectors. Attenuation reduces the statistical quality of the image by decreasing the signal to noise ratio (SNR). By collecting an initial CT scan to determine the attenuation factors for tissues along a line of response, attenuation can be reduced to increase the SNR[339].

Random events

Random events can produce false coincidence detection when two unrelated photons are incorrectly detected in coincidence[339] (Fig. A10, D). Random events increase uncorrelated background counts to the PET image and the detection of random events can be limited by using detectors that have small timing windows.

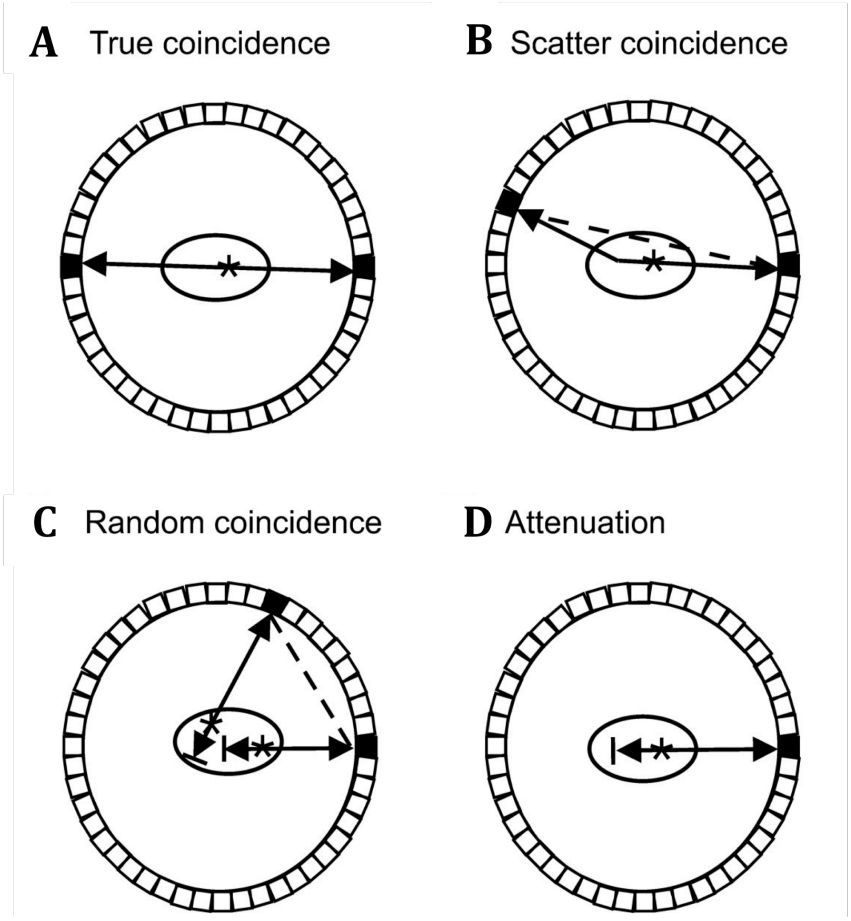

Figure A10. A) True coincidence. Two annihilation photons, emitted from same annihilation event, travel in opposite directions and are detected by opposing detectors. **(B) Scatter coincidence.** One photon from annihilation travels without interaction, and other annihilation photon is deflected because of scattering in body**. (C) Random coincidence.** Two annihilation photons emitted from 2 separate decay events are detected by chance within coincidence time window. **(D) Attenuation.** One (or both) annihilation photons is (are) not detected as result of scattering or absorption within body.

Dead time

Dead time refers to period after a photon is detected and the detector is unable to process another coincident event[337]. The dead time is less than a second but can still decrease the SNR by decreasing the number of coincident detections.

Partial volume effect

A major factor that deteriorates PET image quality is the partial volume effect. Partial volume effects refer to the loss of signal from structures that are smaller than two times the FWHM of the tomography. Contamination from adjacent brain tissue or regions can also cause partial volume effects[340, 341] (Fig. A11). Partial volume effects contribute to blurred images by the miscalculation of radiotracer concentration. The effects of partial volumes on the reconstructed image can be partially corrected with several algorithms or can be minimized by accurate delineation of the regions of interest (ROI)[341].

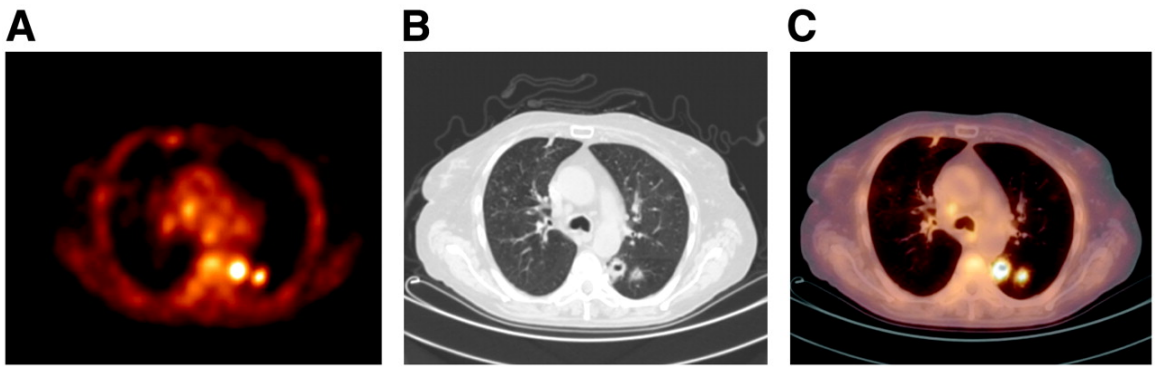

Figure A11. PET image shows more than the real metabolically active part of the tumor because of partial volume effects[342]. **A)** PET image. **B)** Corresponding CT image. **C)** PET/CT image. Discrepancy between tumor contours as seen on CT and PET images is clearly visible.

The PET scanner used to collect emission data for this dissertation was a Siemens ECAT EXACT HR+ scanner with an in-plane resolution full-width at half-maximum (FWHM) 4.6 mm, axial FWHM= 3.5 mm, axial field of view= 15.52 cm in three-dimensional mode. The scanner consists of 32 rings, each with 576 BGO detectors (4.05 x 4.39 x 30 mm). The rings were separated by tungsten septa, which have a length of 66.5 mm and a thickness of 0.8 mm. A 7-min transmission scan was acquired using a rotating $^{68}Ge/^{68}Ga$ rod source for attenuation correction. PET dynamic data acquisition was initiated with a bolus injection of ^{18}F-fallypride (~5 mCi in 30 s). Data were corrected for factors such as attenuation, scatter and random coincidences before

being reconstructed using ECAT v7.3 OSEM (Ordered Subset Expectation Maximization; 3 iterations, 16 subsets).

PET DATA ANALYSIS

Compartmental Model

Once the PET scans are acquired and after the proper corrections for attenuation, dead-time, physical decay of radioactivity and scattered photons are applied, the data represent the tracer concentration (Bq/ml) at a certain time. In order to interpret the observed PET data over time, the data are modeled under the assumption that the tracer passes through physiologically different "compartments". The first compartment is the tracer in the arterial blood. From arterial blood, the radioligand passes into the second compartment, known as the free compartment. The third compartment is the region of interest for specific ligand binding. The fourth compartment is a nonspecific-binding compartment that exchanges with the free compartment. Each compartment is thought to be homogeneous, and that the radioligand passes from one compartment to the next and is instantaneously mixed within the compartment. Modeling a single tissue compartment is the simplest compartmental model (Fig. A12, A); however, it can only efficiently describe the kinetics of certain radioligands, such as $^{150}H_2O$ to measure blood flow. For other radioligands, a two tissue compartmental model (Fig. A12, B) is sufficient to interpret radioligand kinetics, as rapid equilibrium between the nonspecific-binding and free compartments can be assumed.

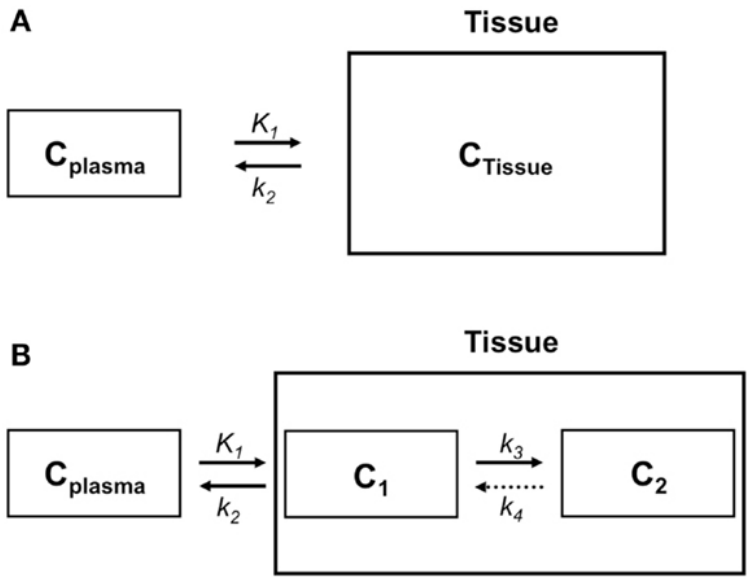

Figure A12. Compartment models. A. Single tissue compartment model. The tracer concentration in tissue (C_{Tissue}) depends on plasma concentration (C_{Plasma}). K_1 refers to the rate constant for the transfer of the ligand from the plasma to the tissue, while k_2 refers to the rate constant for clearance of the ligand from tissue to plasma. **B.** Two tissue compartmental model. C_{Tissue} reflects tracer concentrations in compartments 1 and 2, representing free (C_1) and bound or metabolized tracer (C_2). k_3 and k_4 are kinetic rate constants describing exchange between the two tissue compartments.

Simplified Reference Tissue Model

Simplified reference tissue model can be used when two compartmental models are sufficient to describe the tracer kinetics in tissue (lammertsma and hume 1996). Reference tissue models enable the quantification of receptor kinetics without measuring the arterial input function, thus avoiding arterial cannulation and metabolite measurements. These models rely on the presence of a reference tissue, a region without specific ligand binding. In the reference tissue model, the time course of radioligand uptake in the tissue of interest is expressed in terms of its uptake in the reference tissue, assuming that the level of nonspecific binding is the same in both tissues (Fig. A13). The Simplified Reference Tissue Model (SRTM) produces functional images of receptor binding parameters using an input function derived from a reference region and

assuming a model with one tissue compartment. Three parameters are estimated with SRTM: binding potential (BP_{ND}), relative delivery (R1), and the reference region clearance constant k'2.

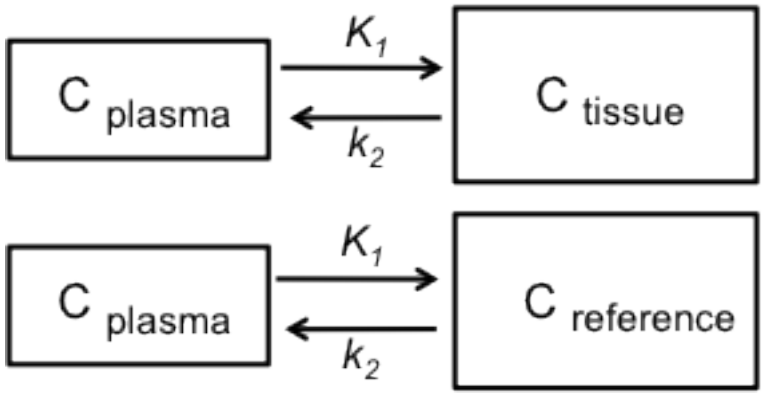

Figure A13. Simplified Reference Tissue Model. The simplified reference tissue model uses a reference region input and collapses the two tissue compartments of the target region into a single apparent compartment (C_T). K_1 refers to the rate constant for the transfer of the ligand from the plasma to the tissue, while k_2 refers to the rate constant for clearance of the ligand from tissue to plasma.

D2-type Dopamine Receptor Radioligands

[^{18}F] fallypride and [^{11}C] raclopride

[^{18}F] fallypride and [^{11}C] raclopride are among the PET D2-type antagonist radioligands that have been used to study the striatal dopamine system. [^{11}C] raclopride enable fast in vivo kinetics but moderate in vivo affinity and is suitable to measure dopamine concentrations on the principle of competition between the endogenous dopamine and the radioligand for binding to the dopamine receptor. An increase in synaptic dopamine concentration will displace or decrease D2 radioligand binding, thereby providing an indirect method to measure synaptic levels of dopamine.

Imaging of synaptic dopamine release according to the binding competition principle can be described within a theoretical framework called the occupancy model[202]. The occupancy

model predicts that changes in D2-type radioligand binding (e.g. with [^{11}C] raclopride) are a direct result of changes in the occupancy or availability of D2-type receptors by dopamine. Pharmacological challenges that increase synaptic dopamine lower the availability of D2-type receptors for radioligand binding, as dopamine will displace bound radioligands and reduce D2-type receptor measurements. Elevation of dopamine concentration initiated by stimulants such as amphetamine or methylphenidate has shown to induce a decrease in D2-type radiotracer binding[313]. The opposite is true for pharmacological challenges that reduce dopamine levels, where depletion of dopamine by agents such as AMPT shows an increase in D2-type radiotracer binding[202].

The low affinity of [^{11}C] raclopride to dopamine receptors produces low signal to noise ratios, and therefore, [^{11}C] raclopride can be used to only reliably quantify receptor availability in regions with high receptor density, such as the striatum[343]. In addition, time constraints imposed by the rapid decay rate of ^{11}C prevent adequate receptor measurements, as the wash-out period exceeds the maximum imaging time with ^{11}C raclopride[343].

[^{18}F] Fallypride

In this dissertation, [^{18}F] fallypride (Fig. A14), a dopamine D2-type receptor ligand with optimal lipophilicity to cross the blood-brain barrier was used to measure D2-type receptor availability[202].

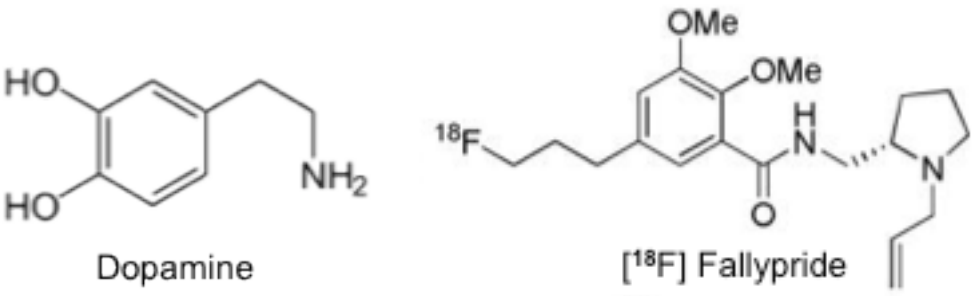

Figure A14. Molecular structure of dopamine (left) and [**18**F] Fallypride (right)

[^{18}F] fallypride has higher affinity and signal-to-noise ratios in vivo compared to [^{11}C] raclopride, and can provide reliable quantitative measures in extrastriatal brain regions where receptor density is an order of magnitude lower than in striatum[343]. As [^{18}F] fallypride clears from the striatum much more slowly than [^{11}C] raclopride, scanning sessions can therefore be extended for a longer duration than for ^{11}C labeled radioligands[344]. Although [^{18}F] fallypride can provide reliable quantification of dopamine receptor binding in the striatum and extrastriatal brain regions, it is not selective to the D2 receptor, as it also binds to D3 receptors.

REFERENCES

1. Meredith CW, MD, Jaffe C, MD, Ang-Lee K, MD, Saxon AJ, MD. Implications of Chronic Methamphetamine Use: A Literature Review. *Havard Review of Psychiatry.* May 1, 2005 2005;13(3):141-154.

2. Pasic J, Russo J, Ries R, Roy-Byrne P. Methamphetamine users in the psychiatric emergency services: a case-control study. *American Journal of Drug Alcohol Abuse.* 2007;33(5):675-686.

3. Shoptaw S, Weiss R, Munjas B, et al. Homonegativity, substance use, sexual risk behaviors, and HIV status in poor and ethnic men who have sex with men in Los Angeles. *Journal of Urban Health.* 2009;86:77-92.

4. Administration SAaMHS. Treatment Episode Data Set (TEDS): 1999-2009. State Admissions to Substance Abuse Treatment Services, DASIS Series S-58. *HHS Publication No. (SMA) 11-4663.* 2011;Rockville, MD. .

5. Administration SAaMHS. Treatment Episode Data Set (TEDS): 2000-2010. State Admissions to Substance Abuse Treatment Services, DASIS Series: S-63. *HHS Publication No. (SMA) 12-4729. .* 2012;Rockville, MD.

6. Vik PW. Methamphetamine use by incarcerated women: comorbid mood and anxiety problems. *Womens Health Issues.* Jul-Aug 2007;17(4):256-263.

7. Glasner-Edwards S, Mooney LJ, Marinelli-Casey P, et al. Identifying methamphetamine users at risk for major depressive disorder: findings from the methamphetamine treatment project at three-year follow-up. *Am J Addict.* Mar-Apr 2008;17(2):99-102.

8. London ED, Simon SL, Berman SM, et al. Mood disturbances and regional cerebral metabolic abnormalities in recently abstinent methamphetamine abusers. *Archives of General Psychiatry.* 2004;61:73-84.

9. Newton TF, Kalechstein AD, Duran S, Vansluis N, Ling W. Methamphetamine abstinence syndrome: Preliminary findings. *American Journal on Addictions.* 2004;13:248-255.

10. Semple SJ, Zians J, Strathdee SA, Patterson TL. Psychosocial and behavioral correlates of depressed mood among female methamphetamine users. *J Psychoactive Drugs.* Nov 2007;Suppl 4:353-366.

11. Zweben JE, Cohen JB, Christian D, et al. Psychiatric symptoms in methamphetamine users. *Am J Addict.* Mar-Apr 2004;13(2):181-190.

12. Hall W, Hando J, Darke S, Ross J. Psychological morbidity and route of administration among amphetamine users in Sydney, Australia. *Addiction.* Jan 1996;91(1):81-87.

13. Cohen JB, Dickow A, Horner K, et al. Abuse and violence history of men and women in treatment for methamphetamine dependence. *Am J Addict.* Oct-Dec 2003;12(5):377-385.

14. Sekine Y, Ouchi Y, Takei N, et al. Brain Serotonin Transporter Density and Aggression in Abstinent Methamphetamine Abusers. *Arch Gen Psychiatry.* 2006;63(1):90-100.

15. Kreek MJ, Nielsen DA, Butelman ER, LaForge KS. Genetic influences on impulsivity, risk taking, stress responsivity and vulnerability to drug abuse and addiction. *Nature Neuroscience.* 2005;8(11):1450-1457.

16. Rogers RD, Everitt BJ, Baldacchino A, et al. Dissociable deficits in the decision-making cognition of chronic amphetamine abusers, opiate abusers, patients with focal damage to prefrontal cortex, and tryptophan-depleted normal volunteers: evidence for monoaminergic mechanisms. *Neuropsychopharmacology.* Apr 1999;20(4):322-339.

17. Gossop M, Darke S, Griffiths P, et al. The Severity of Dependence Scale (SDS): psychometric properties of the SDS in English and Australian samples of heroin, cocaine and amphetamine users. *Addiction.* May 1995;90(5):607-614.

18. Bechara A. Decision making, impulse control and loss of willpower to resist drugs: a neurocognitive perspective. *Nature Neuroscience.* November 2005 2005;8(11):1458-1463.

19. Grant S, Contoreggi C, London ED. Drug abusers show impaired performance in a laboratory test of decision making. *Neuropsychologia.* 2000;38(8):1180-1187.

20. Rogers RD, Robbins TW. Investigating the neurocognitive deficits associated with chronic drug misuse. *Curr Opin Neurobiol.* Apr 2001;11(2):250-257.

21. Kirby KN, N.N. Marakovic. Modelling myopic decisions: evidence for hyperbolic delay-discounting within subjects and amounts. *Organizational Behavior and Human Decision Processes.* 1995;64:22-30.

22. Monterosso JR, Ainslie G, Xu J, Cordova X, Domier CP, London ED. Frontoparietal Cortical Activity of Methamphetamine-Dependent and Comparison Subjects Performing a Delay Discounting Task. *Human Brain Mapping.* August 30, 2006 2007;28:383-393.

23. Nordahl TE, Salo R, Leamon M. Neuropsychological effects of chronic methamphetamine use on neurotransmitters and cognition: a review. *J Neuropsychiatry Clin Neurosci.* Summer 2003;15(3):317-325.

24. Dean AC, Groman SM, Morales AM, London ED. An evaluation of the evidence that methamphetamine abuse causes cognitive decline in humans. *Neuropsychopharmacology.* Jan 2012;38(2):259-274.

25. Simon SL, Domier CP, Sim T, Richardson K, Rawson RA, Ling W. Cognitive performance of current methamphetamine and cocaine abusers. *J Addict Dis.* 2002;21(1):61-74.

26. Ghahremani DG, Tabibnia G, Monterosso J, Hellemann G, Poldrack RA, London ED. Effect of modafinil on learning and task-related brain activity in methamphetamine-dependent and healthy individuals. *Neuropsychopharmacology.* Apr 2011;36(5):950-959.

27. Monterosso JR, Ainslie G, Xu J, Cordova X, Domier CP, London ED. Frontoparietal cortical activity of methamphetamine-dependent and comparison subjects performing a delay discounting task. *Hum Brain Mapp.* Aug 30 2006;28(5):383-393.

28. Hoffman WF, Moore M, Templin R, McFarland B, Hitzemann RJ, Mitchell SH. Neuropsychological function and delay discounting in methamphetamine-dependent individuals. *Psychopharmacology (Berl).* Oct 2006;188(2):162-170.

29. Monterosso JR, Aron AR, Cordova X, Xu J, London ED. Deficits in response inhibition associated with chronic methamphetamine abuse. *Drug Alcohol Depend.* Aug 1 2005;79(2):273-277.

30. Salo R, Nordahl TE, Moore C, et al. A dissociation in attentional control: evidence from methamphetamine dependence. *Biol Psychiatry.* Feb 1 2005;57(3):310-313.

31. London ED, Berman SM, Voytek B, et al. Cerebral metabolic dysfunction and impaired vigilance in recently abstinent methamphetamine abusers. *Biol Psychiatry.* Nov 15 2005;58(10):770-778.

32. Kalechstein AD, Newton TF, Green M. Methamphetamine dependence is associated with neurocognitive impairment in the initial phases of abstinence. *J Neuropsychiatry Clin Neurosci.* Spring 2003;15(2):215-220.

33. Simon SL, Domier C, Carnell J, Brethen P, Rawson R, Ling W. Cognitive impairment in individuals currently using methamphetamine. *Am J Addict.* Summer 2000;9(3):222-231.

34. Chang L, Ernst T, Speck O, et al. Perfusion MRI and computerized cognitive test abnormalities in abstinent methamphetamine users. *Psychiatry Res.* Jun 15 2002;114(2):65-79.

35. Smout MF, Longo M, Harrison S, Minniti R, Wickes W, White JM. Psychosocial treatment for methamphetamine use disorders: a preliminary randomized controlled trial of cognitive behavior therapy and Acceptance and Commitment Therapy. *Subst Abus.* Apr 2010;31(2):98-107.

36. Rawson RA, Marinelli-Casey P, Anglin MD, et al. A multi-site comparison of psychosocial approaches for the treatment of methamphetamine dependence. *Addiction.* Jun 2004;99(6):708-717.

37. Carroll KM, Onken LS. Behavioral therapies for drug abuse. *Am J Psychiatry.* Aug 2005;162(8):1452-1460.

38. Rawson RA, McCann MJ, Flammino F, et al. A comparison of contingency management and cognitive-behavioral approaches for stimulant-dependent individuals. *Addiction.* Feb 2006;101(2):267-274.

39. Ernst T, Chang L, Oropilla G, Gustavson A, Speck O. Cerebral perfusion abnormalities in abstinent cocaine abusers: a perfusion MRI and SPECT study. *Psychiatry Res.* Aug 28 2000;99(2):63-74.

40. McCann UD, Wong DF, Kyokoi F, Villemagne V, Dannals RF, Ricaurte GA. Reduced Striatal Dopamine Transporter Density in Abstinent Methamphetamine and Methcathinone Users: Evidence from Positron Emission Tomgraphy Studies with [^{11}C]WIN-35,428. *The Journal of Neuroscience.* October 15, 1998 1998;18(20):8417-8422.

41. Gowin JL, Mackey S, Paulus MP. Altered risk-related processing in substance users: imbalance of pain and gain. *Drug Alcohol Depend.* Sep 1 2013;132(1-2):13-21.

42. Tanabe J, Thompson L, Claus E, Dalwani M, Hutchison K, Banich MT. Prefrontal Cortex Activity is Reduced in Gambling and Nongambling Substance Users During Decision-Making. *Human Brain Mapping.* 2007;28:1276-1286.

43. Bolla KI, Eldreth DA, London ED, et al. Orbitofrontal cortex dysfunction in abstinent cocaine abusers performing a decision-making task. *NeuroImage.* Jul 2003;19(3):1085-1094.

44. van Hell HH, Vink M, Ossewaarde L, Jager G, Kahn RS, Ramsey NF. Chronic effects of cannabis use on the human reward system: an fMRI study. *Eur Neuropsychopharmacol.* Mar 2010;20(3):153-163.

45. Paulus MP, Tapert SF, Schuckit MA. Neural activation patterns of methamphetamine-dependent subjects during decision making predict relapse. *Arch Gen Psychiatry.* Jul 2005;62(7):761-768.

46. Hoffman WF, Schwartz DL, Huckans MS, et al. Cortical activation during delay discounting in abstinent methamphetamine dependent individuals. *Psychopharmacology.* August 7, 2008 2008;201:183-193.

47. Knutson B, Fong GW, Adams CM, Varner JL, Hommer D. Dissociation of reward anticipation and outcome with event-related fMRI. *Neuroreport.* Dec 4 2001;12(17):3683-3687.

48. Knutson B, Adams CM, Fong GW, Hommer D. Anticipation of increasing monetary reward selectively recruits nucleus accumbens. *J Neurosci.* Aug 15 2001;21(16):RC159.

49. Paulus MP, Feinstein JS, Leland D, Simmons AN. Superior temporal gyrus and insula provide response and outcome-dependent information during assessment and action selection in a decision-making situation. *NeuroImage.* Apr 1 2005;25(2):607-615.

50. Paulus MP, Rogalsky C, Simmons A, Feinstein JS, Stein MB. Increased activation in the right insula during risk-taking decision making is related to harm avoidance and neuroticism. *NeuroImage.* Aug 2003;19(4):1439-1448.

51. Paulus MP, Hozack N, Frank L, Brown GG, Schuckit MA. Decision Making by Methamphetamine-Dependent Subjects Is Associated with Error-Rate-Independent Decrease in Prefrontal and Parietal Activation. *Biological Psychiatry.* 2003;53:65-74.

52. Preuschoff K, Quartz SR, Bossaerts P. Human insula activation reflects risk prediction errors as well as risk. *J Neurosci.* Mar 12 2008;28(11):2745-2752.

53. Schultz W. Predictive reward signal of dopamine neurons. *J Neurophysiol.* Jul 1998;80(1):1-27.

54. Volkow ND, Chang L, Wang GJ, et al. Higher cortical and lower subcortical metabolism in detoxified methamphetamine abusers. *Am J Psychiatry.* Mar 2001;158(3):383-389.

55. London ED, PhD, Simon SL, PhD, Berman SMP, et al. Mood Disturbances and Regional Cerebral Metabolic Abnormalities in Recently Abstinent Methamphetamine Abusers. *Archives of General Psychiatry.* January 2004 2004;61:73-84.

56. Berman SM, Voytek B, Mandelkern MA, et al. Changes in cerebral glucose metabolism during early abstinence from chronic methamphetamine abuse. *Mol Psychiatry.* Sep 2008;13(9):897-908.

57. Fischman AJ, Thornton AF, Frosch MP, Swearinger B, Gonzalez RG, Alpert NM. FDG hypermetabolism associated with inflammatory necrotic changes following radiation of meningioma. *J Nucl Med.* Jul 1997;38(7):1027-1029.

58. Thompson PM, Hayashi KM, Simon SL, et al. Structural abnormalities in the brains of human subjects who use methamphetamine. *J Neurosci.* Jun 30 2004;24(26):6028-6036.

59. Kim SJ, Lyoo IK, Hwang J, et al. Prefrontal grey-matter changes in short-term and long-term abstinent methamphetamine abusers. *Int J Neuropsychopharmacol.* Jun 28 2005:1-8.

60. Jernigan TL, Gamst AC, Archibald SL, et al. Effects of methamphetamine dependence and HIV infection on cerebral morphology. *Am J Psychiatry.* Aug 2005;162(8):1461-1472.

61. Chang L, Cloak C, Patterson K, Grob C, Miller EN, Ernst T. Enlarged striatum in abstinent methamphetamine abusers: a possible compensatory response. *Biol Psychiatry.* May 1 2005;57(9):967-974.

62. Berman SMP, O'Neill J, Fears S, Bartzokis G, London ED, PhD. Abuse of Amphetamines and Structural Abnormalities in the Brain. *Annals of New York Academy of Sciences.* 2008;1141:195-220.

63. Brody AL, Mandelkern MA, Jarvik ME, et al. Differences between smokers and nonsmokers in regional gray matter volumes and densities. *Biol Psychiatry.* Jan 1 2004;55(1):77-84.

64. Morales AM, Lee B, Hellemann G, O'Neill J, London ED. Gray-matter volume in methamphetamine dependence: cigarette smoking and changes with abstinence from methamphetamine. *Drug Alcohol Depend.* Oct 1 2012;125(3):230-238.

65. Karila L, Weinstein A, Aubin HJ, Benyamina A, Reynaud M, Batki SL. Pharmacological approaches to methamphetamine dependence: a focused review. *Br J Clin Pharmacol.* Jun 2010;69(6):578-592.

66. Rudnick G, Clark J. From synapse to vesicle: the reuptake and storage of biogenic amine neurotransmitters. *Biochim Biophys Acta.* Oct 4 1993;1144(3):249-263.

67. Pereira FC, Lourenco ES, Borges F, et al. Single or multiple injections of methamphetamine increased dopamine turnover but did not decrease tyrosine hydroxylase levels or cleave caspase-3 in caudate-putamen. *Synapse.* Sep 1 2006;60(3):185-193.

68. Vergo S, Johansen JL, Leist M, Lotharius J. Vesicular monoamine transporter 2 regulates the sensitivity of rat dopaminergic neurons to disturbed cytosolic dopamine levels. *Brain Res.* Dec 14 2007;1185:18-32.

69. Volz TJ, Hanson GR, Fleckenstein AE. The role of the plasmalemmal dopamine and vesicular monoamine transporters in methamphetamine-induced dopaminergic deficits. *J Neurochem.* May 2007;101(4):883-888.

70. White FJ, Kalivas PW. Neuroadaptations involved in amphetamine and cocaine addiction. *Drug Alcohol Depend.* Jun-Jul 1998;51(1-2):141-153.

71. Pierce RC, Kumaresan V. The mesolimbic dopamine system: the final common pathway for the reinforcing effect of drugs of abuse? *Neurosci Biobehav Rev.* 2006;30(2):215-238.

72. Ritz MC, Kuhar MJ. Relationship between self-administration of amphetamine and monoamine receptors in brain: comparison with cocaine. *J Pharmacol Exp Ther.* Mar 1989;248(3):1010-1017.

73. Ritz MC, Lamb RJ, Goldberg SR, Kuhar MJ. Cocaine receptors on dopamine transporters are related to self-administration of cocaine. *Science.* Sep 4 1987;237(4819):1219-1223.

74. Roberts DC, Corcoran ME, Fibiger HC. On the role of ascending catecholaminergic systems in intravenous self-administration of cocaine. *Pharmacol Biochem Behav.* Jun 1977;6(6):615-620.

75. Lyness WH, Friedle NM, Moore KE. Destruction of dopaminergic nerve terminals in nucleus accumbens: effect on d-amphetamine self-administration. *Pharmacol Biochem Behav.* Nov 1979;11(5):553-556.

76. Roberts DC, Koob GF, Klonoff P, Fibiger HC. Extinction and recovery of cocaine self-administration following 6-hydroxydopamine lesions of the nucleus accumbens. *Pharmacol Biochem Behav.* May 1980;12(5):781-787.

77. Pettit HO, Ettenberg A, Bloom FE, Koob GF. Destruction of dopamine in the nucleus accumbens selectively attenuates cocaine but not heroin self-administration in rats. *Psychopharmacology (Berl).* 1984;84(2):167-173.

78. Caine SB, Koob GF. Effects of dopamine D-1 and D-2 antagonists on cocaine self-administration under different schedules of reinforcement in the rat. *J Pharmacol Exp Ther.* Jul 1994;270(1):209-218.

79. Caine SB, Koob GF. Effects of mesolimbic dopamine depletion on responding maintained by cocaine and food. *J Exp Anal Behav.* Mar 1994;61(2):213-221.

80. Koob GF, Caine B, Markou A, Pulvirenti L, Weiss F. Role for the mesocortical dopamine system in the motivating effects of cocaine. *NIDA Res Monogr.* 1994;145:1-18.

81. Wise RA, Newton P, Leeb K, Burnette B, Pocock D, Justice JB, Jr. Fluctuations in nucleus accumbens dopamine concentration during intravenous cocaine self-administration in rats. *Psychopharmacology (Berl).* Jul 1995;120(1):10-20.

82. Ranaldi R, Pocock D, Zereik R, Wise RA. Dopamine fluctuations in the nucleus accumbens during maintenance, extinction, and reinstatement of intravenous D-amphetamine self-administration. *J Neurosci.* May 15 1999;19(10):4102-4109.

83. Civelli O, Bunzow JR, Grandy DK. Molecular diversity of the dopamine receptors. *Annu Rev Pharmacol Toxicol.* 1993;33:281-307.

84. Seeman P, Van Tol HH. Dopamine receptor pharmacology. *Curr Opin Neurol Neurosurg.* Aug 1993;6(4):602-608.

85. Missale C, Nash SR, Robinson SW, Jaber M, Caron MG. Dopamine receptors: from structure to function. *Physiol Rev.* Jan 1998;78(1):189-225.

86. Mello NK, Negus SS. Preclinical evaluation of pharmacotherapies for treatment of cocaine and opioid abuse using drug self-administration procedures. *Neuropsychopharmacology.* Jun 1996;14(6):375-424.

87. Platt DM, Rowlett JK, Spealman RD. Behavioral effects of cocaine and dopaminergic strategies for preclinical medication development. *Psychopharmacology (Berl).* Oct 2002;163(3-4):265-282.

88. Self DW, Stein L. The D1 agonists SKF 82958 and SKF 77434 are self-administered by rats. *Brain Res.* Jun 12 1992;582(2):349-352.

89. Weed MR, Woolverton WL. The reinforcing effects of dopamine D1 receptor agonists in rhesus monkeys. *J Pharmacol Exp Ther.* Dec 1995;275(3):1367-1374.

90. Grech DM, Spealman RD, Bergman J. Self-administration of D1 receptor agonists by squirrel monkeys. *Psychopharmacology (Berl).* May 1996;125(2):97-104.

91. Weed MR, Paul IA, Dwoskin LP, Moore SE, Woolverton WL. The relationship between reinforcing effects and in vitro effects of D1 agonists in monkeys. *J Pharmacol Exp Ther.* Oct 1997;283(1):29-38.

92. Self DW, Belluzzi JD, Kossuth S, Stein L. Self-administration of the D1 agonist SKF 82958 is mediated by D1, not D2, receptors. *Psychopharmacology (Berl).* Feb 1996;123(4):303-306.

93. Wise RA, Murray A, Bozarth MA. Bromocriptine self-administration and bromocriptine-reinstatement of cocaine-trained and heroin-trained lever pressing in rats. *Psychopharmacology (Berl).* 1990;100(3):355-360.

94. Caine SB, Negus SS, Mello NK, Bergman J. Effects of dopamine D(1-like) and D(2-like) agonists in rats that self-administer cocaine. *J Pharmacol Exp Ther.* Oct 1999;291(1):353-360.

95. Woolverton WL. Effects of a D1 and a D2 dopamine antagonist on the self-administration of cocaine and piribedil by rhesus monkeys. *Pharmacol Biochem Behav.* Mar 1986;24(3):531-535.

96. Sinnott RS, Mach RH, Nader MA. Dopamine D2/D3 receptors modulate cocaine's reinforcing and discriminative stimulus effects in rhesus monkeys. *Drug Alcohol Depend.* Apr 1 1999;54(2):97-110.

97. Amit Z, Smith BR. Remoxipride, a specific D2 dopamine antagonist: an examination of its self-administration liability and its effects on d-amphetamine self-administration. *Pharmacol Biochem Behav.* Jan 1992;41(1):259-261.

98. Fletcher PJ. A comparison of the effects of risperidone, raclopride, and ritanserin on intravenous self-administration of d-amphetamine. *Pharmacol Biochem Behav.* May 1998;60(1):55-60.

99. Volkow ND, MD, Chang L, MD, Wang G-J, MD, et al. Low Level of Brain Dopamine D_2 Receptors in Methamphetamine Abusers: Association With Metabolism in the Orbitofrontal Cortex. *American Journal of Psychiatry.* December 2001 2001;158(12):2015-2021.

100. Lee B, London ED, Poldrack RA, et al. Striatal dopamine d2/d3 receptor availability is reduced in methamphetamine dependence and is linked to impulsivity. *J Neurosci.* Nov 25 2009;29(47):14734-14740.

101. Wang GJ, Smith L, Volkow ND, et al. Decreased dopamine activity predicts relapse in methamphetamine abusers. *Mol Psychiatry.* Sep 2011;17(9):918-925.

102. Xu M, Koeltzow TE, Santiago GT, et al. Dopamine D3 receptor mutant mice exhibit increased behavioral sensitivity to concurrent stimulation of D1 and D2 receptors. *Neuron.* Oct 1997;19(4):837-848.

103. Khroyan TV, Baker DA, Fuchs RA, Manders N, Neisewander JL. Differential effects of 7-OH-DPAT on amphetamine-induced stereotypy and conditioned place preference. *Psychopharmacology (Berl).* Oct 1998;139(4):332-341.

104. Pritchard LM, Newman AH, McNamara RK, et al. The dopamine D3 receptor antagonist NGB 2904 increases spontaneous and amphetamine-stimulated locomotion. *Pharmacol Biochem Behav.* Apr 2007;86(4):718-726.

105. Volkow ND, Chang L, Wang GJ, et al. Association of dopamine transporter reduction with psychomotor impairment in methamphetamine abusers. *Am J Psychiatry.* Mar 2001;158(3):377-382.

106. Sekine Y, Iyo M, Ouchi Y, et al. Methamphetamine-related psychiatric symptoms and reduced brain dopamine transporters studied with PET. *Am J Psychiatry.* Aug 2001;158(8):1206-1214.

107. Sekine Y, Minabe Y, Ouchi Y, et al. Association of dopamine transporter loss in the orbitofrontal and dorsolateral prefrontal cortices with methamphetamine-related psychiatric symptoms. *Am J Psychiatry.* Sep 2003;160(9):1699-1701.

108. Volkow ND, Chang L, Wang GJ, et al. Loss of dopamine transporters in methamphetamine abusers recovers with protracted abstinence. *J Neurosci.* Dec 1 2001;21(23):9414-9418.

109. Barr AM, Panenka WJ, MacEwan GW, et al. The need for speed: an update on methamphetamine addiction. *J Psychiatry Neurosci.* Sep 2006;31(5):301-313.

110. Wilson JM, Kalasinsky KS, Levey AI, et al. Striatal dopamine nerve terminal markers in human, chronic methamphetamine users. *Nat Med.* Jun 1996;2(6):699-703.

111. Johanson CE, Frey KA, Lundahl LH, et al. Cognitive function and nigrostriatal markers in abstinent methamphetamine abusers. *Psychopharmacology (Berl).* Apr 2006;185(3):327-338.

112. Boileau I, Rusjan P, Houle S, et al. Increased vesicular monoamine transporter binding during early abstinence in human methamphetamine users: Is VMAT2 a stable dopamine neuron biomarker? *J Neurosci.* Sep 24 2008;28(39):9850-9856.

113. Nestler EJ. Is there a common molecular pathway for addiction? *Nat Neurosci.* Nov 2005;8(11):1445-1449.

114. Bunney BS, Chiodo LA, Grace AA. Midbrain dopamine system electrophysiological functioning: a review and new hypothesis. *Synapse.* Oct 1991;9(2):79-94.

115. Nissbrandt H, Sundstrom E, Jonsson G, Hjorth S, Carlsson A. Synthesis and release of dopamine in rat brain: comparison between substantia nigra pars compacts, pars reticulata, and striatum. *J Neurochem.* Apr 1989;52(4):1170-1182.

116. Elsworth JD, Deutch AY, Redmond DE, Jr., Sladek JR, Jr., Roth RH. MPTP-induced parkinsonism: relative changes in dopamine concentration in subregions of substantia nigra, ventral tegmental area and retrorubral field of symptomatic and asymptomatic vervet monkeys. *Brain Res.* Apr 16 1990;513(2):320-324.

117. Montaron MF, Deniau JM, Menetrey A, Glowinski J, Thierry AM. Prefrontal cortex inputs of the nucleus accumbens-nigro-thalamic circuit. *Neuroscience.* Mar 1996;71(2):371-382.

118. Sesack SR, Grace AA. Cortico-Basal Ganglia reward network: microcircuitry. *Neuropsychopharmacology.* Jan 2010;35(1):27-47.

119. Fearnley JM, Lees AJ. Ageing and Parkinson's disease: substantia nigra regional selectivity. *Brain.* Oct 1991;114 (Pt 5):2283-2301.

120. Graybiel AM, Aosaki T, Flaherty AW, Kimura M. The basal ganglia and adaptive motor control. *Science.* Sep 23 1994;265(5180):1826-1831.

121. Cami J, Farre M. Drug addiction. *N Engl J Med.* Sep 4 2003;349(10):975-986.

122. Wise RA. Catecholamine theories of reward: a critical review. *Brain Res.* Aug 25 1978;152(2):215-247.

123. Johnson SW, Seutin V, North RA. Burst firing in dopamine neurons induced by N-methyl-D-aspartate: role of electrogenic sodium pump. *Science.* Oct 23 1992;258(5082):665-667.

124. Kalivas PW. Neurotransmitter regulation of dopamine neurons in the ventral tegmental area. *Brain Res Brain Res Rev.* Jan-Apr 1993;18(1):75-113.

125. Kalivas PW, Alesdatter JE. Involvement of N-methyl-D-aspartate receptor stimulation in the ventral tegmental area and amygdala in behavioral sensitization to cocaine. *J Pharmacol Exp Ther.* Oct 1993;267(1):486-495.

126. Wise RA. Dopamine, learning and motivation. *Nat Rev Neurosci.* Jun 2004;5(6):483-494.

127. Goldstein RZ, Volkow ND. Drug addiction and its underlying neurobiological basis: neuroimaging evidence for the involvement of the frontal cortex. *Am J Psychiatry.* Oct 2002;159(10):1642-1652.

128. Pierce RC, Kalivas PW. Repeated cocaine modifies the mechanism by which amphetamine releases dopamine. *J Neurosci.* May 1 1997;17(9):3254-3261.

129. Montminy MR, Bilezikjian LM. Binding of a nuclear protein to the cyclic-AMP response element of the somatostatin gene. *Nature.* Jul 9-15 1987;328(6126):175-178.

130. Nestler EJ, Aghajanian GK. Molecular and cellular basis of addiction. *Science.* Oct 3 1997;278(5335):58-63.

131. Freedman NJ, Lefkowitz RJ. Desensitization of G protein-coupled receptors. *Recent Prog Horm Res.* 1996;51:319-351; discussion 352-313.

132. Pei G, Kieffer BL, Lefkowitz RJ, Freedman NJ. Agonist-dependent phosphorylation of the mouse delta-opioid receptor: involvement of G protein-coupled receptor kinases but not protein kinase C. *Mol Pharmacol.* Aug 1995;48(2):173-177.

133. Werling LL, McMahon PN, Cox BM. Selective changes in mu opioid receptor properties induced by chronic morphine exposure. *Proc Natl Acad Sci U S A.* Aug 1989;86(16):6393-6397.

134. Dohlman HG, Thorner J. RGS proteins and signaling by heterotrimeric G proteins. *J Biol Chem.* Feb 14 1997;272(7):3871-3874.

135. Thomas EA, Danielson PE, Sutcliffe JG. RGS9: a regulator of G-protein signalling with specific expression in rat and mouse striatum. *J Neurosci Res.* Apr 1 1998;52(1):118-124.

136. Rahman Z, Schwarz J, Gold SJ, et al. RGS9 modulates dopamine signaling in the basal ganglia. *Neuron.* Jun 19 2003;38(6):941-952.

137. Bourtchuladze R, Frenguelli B, Blendy J, Cioffi D, Schutz G, Silva AJ. Deficient long-term memory in mice with a targeted mutation of the cAMP-responsive element-binding protein. *Cell.* Oct 7 1994;79(1):59-68.

138. Sheng M, McFadden G, Greenberg ME. Membrane depolarization and calcium induce c-fos transcription via phosphorylation of transcription factor CREB. *Neuron.* Apr 1990;4(4):571-582.

139. Kivinummi T, Kaste K, Rantamaki T, Castren E, Ahtee L. Alterations in BDNF and phospho-CREB levels following chronic oral nicotine treatment and its withdrawal in dopaminergic brain areas of mice. *Neurosci Lett.* Mar 17 2011;491(2):108-112.

140. Piech-Dumas KM, Tank AW. CREB mediates the cAMP-responsiveness of the tyrosine hydroxylase gene: use of an antisense RNA strategy to produce CREB-deficient PC12 cell lines. *Brain Res Mol Brain Res.* Jul 5 1999;70(2):219-230.

141. Ghee M, Baker H, Miller JC, Ziff EB. AP-1, CREB and CBP transcription factors differentially regulate the tyrosine hydroxylase gene. *Brain Res Mol Brain Res.* Mar 30 1998;55(1):101-114.

142. McClung CA, Nestler EJ. Regulation of gene expression and cocaine reward by CREB and DeltaFosB. *Nat Neurosci.* Nov 2003;6(11):1208-1215.

143. Kalivas PW, McFarland K, Bowers S, Szumlinski K, Xi ZX, Baker D. Glutamate transmission and addiction to cocaine. *Ann N Y Acad Sci.* Nov 2003;1003:169-175.

144. McFarland K, Lapish CC, Kalivas PW. Prefrontal glutamate release into the core of the nucleus accumbens mediates cocaine-induced reinstatement of drug-seeking behavior. *J Neurosci.* Apr 15 2003;23(8):3531-3537.

145. Robinson TE, Berridge KC. The neural basis of drug craving: an incentive-sensitization theory of addiction. *Brain Res Brain Res Rev.* Sep-Dec 1993;18(3):247-291.

146. Robinson TE, Berridge KC. Review. The incentive sensitization theory of addiction: some current issues. *Philos Trans R Soc Lond B Biol Sci.* Oct 12 2008;363(1507):3137-3146.

147. Robinson TE, Gorny G, Mitton E, Kolb B. Cocaine self-administration alters the morphology of dendrites and dendritic spines in the nucleus accumbens and neocortex. *Synapse.* Mar 1 2001;39(3):257-266.

148. Robinson TE, Kolb B. Persistent structural modifications in nucleus accumbens and prefrontal cortex neurons produced by previous experience with amphetamine. *J Neurosci.* Nov 1 1997;17(21):8491-8497.

149. Robinson TE, Kolb B. Structural plasticity associated with exposure to drugs of abuse. *Neuropharmacology.* 2004;47 Suppl 1:33-46.

150. Carlezon WA, Jr., Nestler EJ. Elevated levels of GluR1 in the midbrain: a trigger for sensitization to drugs of abuse? *Trends Neurosci.* Dec 2002;25(12):610-615.

151. White FJ, Hu XT, Zhang XF, Wolf ME. Repeated administration of cocaine or amphetamine alters neuronal responses to glutamate in the mesoaccumbens dopamine system. *J Pharmacol Exp Ther.* Apr 1995;273(1):445-454.

152. Lu W, Chen H, Xue CJ, Wolf ME. Repeated amphetamine administration alters the expression of mRNA for AMPA receptor subunits in rat nucleus accumbens and prefrontal cortex. *Synapse.* Jul 1997;26(3):269-280.

153. Park WK, Bari AA, Jey AR, et al. Cocaine administered into the medial prefrontal cortex reinstates cocaine-seeking behavior by increasing AMPA receptor-mediated glutamate transmission in the nucleus accumbens. *J Neurosci.* Apr 1 2002;22(7):2916-2925.

154. Cornish JL, Kalivas PW. Glutamate transmission in the nucleus accumbens mediates relapse in cocaine addiction. *J Neurosci.* Aug 1 2000;20(15):RC89.

155. Pascoli V, Besnard A, Herve D, et al. Cyclic adenosine monophosphate-independent tyrosine phosphorylation of NR2B mediates cocaine-induced extracellular signal-regulated kinase activation. *Biol Psychiatry.* Feb 1 2010;69(3):218-227.

156. Cepeda C, Levine MS. Where do you think you are going? The NMDA-D1 receptor trap. *Sci STKE.* May 2 2006;2006(333):pe20.

157. Ungless MA, Whistler JL, Malenka RC, Bonci A. Single cocaine exposure in vivo induces long-term potentiation in dopamine neurons. *Nature.* May 31 2001;411(6837):583-587.

158. Pierce RC, Kalivas PW. A circuitry model of the expression of behavioral sensitization to amphetamine-like psychostimulants. *Brain Res Brain Res Rev.* Oct 1997;25(2):192-216.

159. Vezina P, Queen AL. Induction of locomotor sensitization by amphetamine requires the activation of NMDA receptors in the rat ventral tegmental area. *Psychopharmacology (Berl).* Aug 2000;151(2-3):184-191.

160. Valjent E, Herve D, Girault JA. [Drugs of abuse, protein phosphatases, and ERK pathway]. *Med Sci (Paris).* May 2005;21(5):453-454.

161. Valjent E, Pascoli V, Svenningsson P, et al. Regulation of a protein phosphatase cascade allows convergent dopamine and glutamate signals to activate ERK in the striatum. *Proc Natl Acad Sci U S A.* Jan 11 2005;102(2):491-496.

162. Girault JA, Valjent E, Caboche J, Herve D. ERK2: a logical AND gate critical for drug-induced plasticity? *Curr Opin Pharmacol.* Feb 2007;7(1):77-85.

163. Schoepp DD. Unveiling the functions of presynaptic metabotropic glutamate receptors in the central nervous system. *J Pharmacol Exp Ther.* Oct 2001;299(1):12-20.

164. Baker DA, McFarland K, Lake RW, et al. Neuroadaptations in cystine-glutamate exchange underlie cocaine relapse. *Nat Neurosci.* Jul 2003;6(7):743-749.

165. Helton DR, Tizzano JP, Monn JA, Schoepp DD, Kallman MJ. LY354740: a metabotropic glutamate receptor agonist which ameliorates symptoms of nicotine withdrawal in rats. *Neuropharmacology.* Nov-Dec 1997;36(11-12):1511-1516.

166. Baptista MA, Martin-Fardon R, Weiss F. Preferential effects of the metabotropic glutamate 2/3 receptor agonist LY379268 on conditioned reinstatement versus primary

reinforcement: comparison between cocaine and a potent conventional reinforcer. *J Neurosci.* May 19 2004;24(20):4723-4727.

167. Kelley AE, Schiltz CA. Accessories to addiction: G protein regulators play a key role in cocaine seeking and neuroplasticity. *Neuron.* Apr 22 2004;42(2):181-183.

168. Bowers MS, McFarland K, Lake RW, et al. Activator of G protein signaling 3: a gatekeeper of cocaine sensitization and drug seeking. *Neuron.* Apr 22 2004;42(2):269-281.

169. Sesack SR, Pickel VM. Ultrastructural relationships between terminals immunoreactive for enkephalin, GABA, or both transmitters in the rat ventral tegmental area. *Brain Res.* Feb 20 1995;672(1-2):261-275.

170. Muly EC, 3rd, Szigeti K, Goldman-Rakic PS. D1 receptor in interneurons of macaque prefrontal cortex: distribution and subcellular localization. *J Neurosci.* Dec 15 1998;18(24):10553-10565.

171. Wedzony K, Czepiel K, Fijal K. Immunohistochemical evidence for localization of NMDAR1 receptor subunit on dopaminergic neurons of the rat substantia nigra, pars compacta. *Pol J Pharmacol.* Nov-Dec 2001;53(6):675-679.

172. Henry DJ, White FJ. Repeated cocaine administration causes persistent enhancement of D1 dopamine receptor sensitivity within the rat nucleus accumbens. *J Pharmacol Exp Ther.* Sep 1991;258(3):882-890.

173. White FJ, Wolf ME. Psychomotor stimulants. *The Biological Bases of Drug Tolerance and Dependence.* 1991:153-197.

174. Saal D, Dong Y, Bonci A, Malenka RC. Drugs of abuse and stress trigger a common synaptic adaptation in dopamine neurons. *Neuron.* Feb 20 2003;37(4):577-582.

175. Lu W, Marinelli M, Xu D, Worley PF, Wolf ME. Amphetamine and cocaine do not increase Narp expression in rat ventral tegmental area, nucleus accumbens or prefrontal cortex, but Narp may contribute to individual differences in responding to a novel environment. *Eur J Neurosci.* Jun 2002;15(12):2027-2036.

176. McFarland K, Davidge SB, Lapish CC, Kalivas PW. Limbic and motor circuitry underlying footshock-induced reinstatement of cocaine-seeking behavior. *J Neurosci.* Feb 18 2004;24(7):1551-1560.

177. Li Y, Vartanian AJ, White FJ, Xue CJ, Wolf ME. Effects of the AMPA receptor antagonist NBQX on the development and expression of behavioral sensitization to cocaine and amphetamine. *Psychopharmacology (Berl).* Dec 1997;134(3):266-276.

178. Li Y, Hu XT, Berney TG, et al. Both glutamate receptor antagonists and prefrontal cortex lesions prevent induction of cocaine sensitization and associated neuroadaptations. *Synapse.* Dec 1999;34(3):169-180.

179. Tzschentke TM. Pharmacology and behavioral pharmacology of the mesocortical dopamine system. *Prog Neurobiol.* Feb 2001;63(3):241-320.

180. Jones LB, Stanwood GD, Reinoso BS, et al. In utero cocaine-induced dysfunction of dopamine D1 receptor signaling and abnormal differentiation of cerebral cortical neurons. *J Neurosci.* Jun 15 2000;20(12):4606-4614.

181. Greicius M. Resting-state functional connectivity in neuropsychiatric disorders. *Curr Opin Neurol.* Aug 2008;21(4):424-430.

182. Chen BT, Hopf FW, Bonci A. Synaptic plasticity in the mesolimbic system: therapeutic implications for substance abuse. *Ann N Y Acad Sci.* Feb 2010;1187:129-139.

183. Gu H, Salmeron BJ, Ross TJ, et al. Mesocorticolimbic circuits are impaired in chronic cocaine users as demonstrated by resting-state functional connectivity. *NeuroImage.* Nov 1 2010;53(2):593-601.

184. Tomasi D, Volkow ND, Wang R, et al. Disrupted functional connectivity with dopaminergic midbrain in cocaine abusers. *PLoS One.* 2010;5(5):e10815.

185. Wilcox CE, Teshiba TM, Merideth F, Ling J, Mayer AR. Enhanced cue reactivity and fronto-striatal functional connectivity in cocaine use disorders. *Drug Alcohol Depend.* May 1 2011;115(1-2):137-144.

186. Upadhyay J, Maleki N, Potter J, et al. Alterations in brain structure and functional connectivity in prescription opioid-dependent patients. *Brain.* Jul 2010;133(Pt 7):2098-2114.

187. Ma N, Liu Y, Li N, et al. Addiction related alteration in resting-state brain connectivity. *NeuroImage.* Jan 1 2010;49(1):738-744.

188. Moron JA, Green TA. Exploring the molecular basis of addiction: drug-induced neuroadaptations. *Neuropsychopharmacology.* Jan 2010;35(1):337-338.

189. Koob GF, Volkow ND. Neurocircuitry of Addiction. *Neuropsychopharmacology.* 2010;35:217-238.

190. Nestler EJ. Molecular basis of long-term plasticity underlying addiction. *Nat Rev Neurosci.* Feb 2001;2(2):119-128.

191. Koob GF. Dynamics of neuronal circuits in addiction: reward, antireward, and emotional memory. *Pharmacopsychiatry.* May 2009;42 Suppl 1:S32-41.

192. Kalivas PW, Volkow ND. The neural basis of addiction: a pathology of motivation and choice. *Am J Psychiatry.* Aug 2005;162(8):1403-1413.

193. Redgrave P, Prescott TJ, Gurney K. The basal ganglia: a vertebrate solution to the selection problem? *Neuroscience.* 1999;89(4):1009-1023.

194. Salamone JD, Correa M. Motivational views of reinforcement: implications for understanding the behavioral functions of nucleus accumbens dopamine. *Behav Brain Res.* Dec 2 2002;137(1-2):3-25.

195. Libby R, Fishburn PC. Behavioral Models of Risk Taking in Business Decisions: A survey and evaluation. *Journal of Accounting Research.* 1977;15:272-292.

196. March JG, Shapira Z. Managerial Perspectives on Risk and Risk Taking. *Management Science.* 1978;33(11):1404-1418.

197. Vlek C, Stallen P. Rational and Personal Aspects of Risk *Acta Psychologica* 1980;45:273-300.

198. Sugam JA, Day JJ, Wightman RM, Carelli RM. Phasic nucleus accumbens dopamine encodes risk-based decision-making behavior. *Biol Psychiatry.* Feb 1 2012;71(3):199-205.

199. St Onge JR, Floresco SB. Dopaminergic modulation of risk-based decision making. *Neuropsychopharmacology.* Feb 2009;34(3):681-697.

200. Winstanley CA, Cocker PJ, Rogers RD. Dopamine modulates reward expectancy during performance of a slot machine task in rats: evidence for a 'near-miss' effect. *Neuropsychopharmacology.* Apr 2011;36(5):913-925.

201. Simon NW, Montgomery KS, Beas BS, et al. Dopaminergic modulation of risky decision-making. *J Neurosci.* Nov 30 2011;31(48):17460-17470.

202. Laruelle M. Imaging synaptic neurotransmission with in vivo binding competition techniques: a critical review. *J Cereb Blood Flow Metab.* Mar 2000;20(3):423-451.

203. Cohen MX, Young J, Baek JM, Kessler C, Ranganath C. Individual differences in extraversion and dopamine genetics predict neural reward responses. *Brain Res Cogn Brain Res.* Dec 2005;25(3):851-861.

204. Wise RA. Brain reward circuitry: insights from unsensed incentives. *Neuron.* Oct 10 2002;36(2):229-240.

205. Koob GF. Drugs of abuse: anatomy, pharmacology and function of reward pathways. *Trends Pharmacol Sci.* May 1992;13(5):177-184.

206. Nogueira L, Kalivas PW, Lavin A. Long-term neuroadaptations produced by withdrawal from repeated cocaine treatment: role of dopaminergic receptors in modulating cortical excitability. *J Neurosci.* Nov 22 2006;26(47):12308-12313.

207. Trantham H, Szumlinski KK, McFarland K, Kalivas PW, Lavin A. Repeated cocaine administration alters the electrophysiological properties of prefrontal cortical neurons. *Neuroscience.* 2002;113(4):749-753.

208. Simon NW, Gilbert RJ, Mayse JD, Bizon JL, Setlow B. Balancing risk and reward: a rat model of risky decision making. *Neuropsychopharmacology.* Sep 2009;34(10):2208-2217.

209. Yacubian J, Glascher J, Schroeder K, Sommer T, Braus DF, Buchel C. Dissociable systems for gain- and loss-related value predictions and errors of prediction in the human brain. *J Neurosci.* Sep 13 2006;26(37):9530-9537.

210. De Martino B, Kumaran D, Seymour B, Dolan RJ. Frames, biases, and rational decision-making in the human brain. *Science.* Aug 4 2006;313(5787):684-687.

211. Paulus MP, Stein MB. An insular view of anxiety. *Biol Psychiatry.* Aug 15 2006;60(4):383-387.

212. Lane SD, Cherek DR. Analysis of risk taking in adults with a history of high risk behavior. *Drug Alcohol Depend.* Aug 1 2000;60(2):179-187.

213. Leland DS, Paulus MP. Increased risk-taking decision-making but not altered response to punishment in stimulant-using young adults. *Drug Alcohol Depend.* Apr 4 2005;78(1):83-90.

214. Tindell AJ, Berridge KC, Zhang J, Pecina S, Aldridge JW. Ventral pallidal neurons code incentive motivation: amplification by mesolimbic sensitization and amphetamine. *Eur J Neurosci.* Nov 2005;22(10):2617-2634.

215. Groman SM, Morales AM, Lee B, London ED, Jentsch JD. Methamphetamine-induced increases in putamen gray matter associate with inhibitory control. *Psychopharmacology (Berl).* Jun 10 2013.

216. Ridderinkhof KR, Ullsperger M, Crone EA, Nieuwenhuis S. The role of the medial frontal cortex in cognitive control. *Science.* Oct 15 2004;306(5695):443-447.

217. Ivlieva NY. Mesocorticolimbic dopaminergic system in adaptive behavior. *Neuroscience and Behavioral Physiology.* September 2011 2011;41(7):715-729.

218. Floresco SB, Magyar O. Mesocortical dopamine modulation of executive functions: beyond working memory. *Psychopharmacology (Berl).* Nov 2006;188(4):567-585.

219. Ernst M, Paulus MP. Neurobiology of Decision Making: A selective Review from a Neurocognitive and Clinical Perspective. *Biological Psychiatry.* 2005;58:597-604.

220. Krain AL, Wilson AM, Arbuckle R, Castellanos FX, Milham MP. Distinct neural mechanisms of risk and ambiguity: a meta-analysis of decision-making. *NeuroImage.* Aug 1 2006;32(1):477-484.

221. Rao H, Korczykowski M, Pluta J, Hoang A, Detre JA. Neural correlates of voluntary and involuntary risk taking in the human brain: An fMRI Study of the Balloon Analog Risk Rask (BART). *NeuroImage.* 2008;42:902-910.

222. Berntson GG, Norman GJ, Bechara A, Bruss J, Tranel D, Cacioppo JT. The insula and evaluative processes. *Psychol Sci.* Jan 2011;22(1):80-86.

223. Niv Y, Edlund JA, Dayan P, O'Doherty JP. Neural prediction errors reveal a risk-sensitive reinforcement-learning process in the human brain. *J Neurosci.* Jan 11 2012;32(2):551-562.

224. Gold JI, Shadlen MN. The neural basis of decision making. *Annu Rev Neurosci.* 2007;30:535-574.

225. Dayan P, Daw ND. Decision theory, reinforcement learning, and the brain. *Cogn Affect Behav Neurosci.* Dec 2008;8(4):429-453.

226. Lejuez CW, Read JP, Kahler CW, et al. Evaluation of a behavioral measure of risk taking: the Balloon Analogue Risk Task (BART). *J Exp Psychol Appl.* Jun 2002;8(2):75-84.

227. Dean AC, Sugar CA, Hellemann G, London ED. Is all risk bad? Young adult cigarette smokers fail to take adaptive risk in a laboratory decision-making test. *Psychopharmacology (Berl).* Jun 2011;215(4):801-811.

228. Ashenhurst JR, Jentsch JD, Ray LA. Risk-taking and alcohol use disorders symptomatology in a sample of problem drinkers. *Exp Clin Psychopharmacol.* Oct 2011;19(5):361-370.

229. Kahneman D, Tversky A. Choices, Values, and Frames. *American Psychologist.* 1984;39(4):341-350.

230. Tobler PN, Fiorillo CD, Schultz W. Adaptive coding of reward value by dopamine neurons. *Science.* Mar 11 2005;307(5715):1642-1645.

231. Schott BH, Minuzzi L, Krebs RM, et al. Mesolimbic functional magnetic resonance imaging activations during reward anticipation correlate with reward-related ventral striatal dopamine release. *J Neurosci.* Dec 24 2008;28(52):14311-14319.

232. Mata R, Hau R, Papassotiropoulos A, Hertwig R. DAT1 polymorphism is associated with risk taking in the Balloon Analogue Risk Task (BART). *PLoS One.* 2012;7(6):e39135.

233. Salamone JD, Correa M, Mingote SM, Weber SM. Beyond the reward hypothesis: alternative functions of nucleus accumbens dopamine. *Curr Opin Pharmacol.* Feb 2005;5(1):34-41.

234. Beaulieu JM, Gainetdinov RR. The physiology, signaling, and pharmacology of dopamine receptors. *Pharmacol Rev.* Mar 2011;63(1):182-217.

235. Alexander GE, DeLong MR, Strick PL. Parallel organization of functionally segregated circuits linking basal ganglia and cortex. *Annu Rev Neurosci.* 1986;9:357-381.

236. Bechara A, Damasio H, Tranel D, Anderson SW. Dissociation Of working memory from decision making within the human prefrontal cortex. *J Neurosci.* Jan 1 1998;18(1):428-437.

237. Mukherjee J, Yang ZY, Das MK, Brown T. Fluorinated benzamide neuroleptics--III. Development of (S)-N-[(1-allyl-2-pyrrolidinyl)methyl]-5-(3-[18F]fluoropropyl)-2, 3-dimethoxybenzamide as an improved dopamine D-2 receptor tracer. *Nucl Med Biol.* Apr 1995;22(3):283-296.

238. Fitzmaurice GM, Laird NM, Ware JH. *Applied Longitudinal Analysis*. Hoboken, NJ: John Wiley; 2004.

239. Laird NM. Missing data in longitudinal studies. *Stat Med.* Jan-Feb 1988;7(1-2):305-315.

240. Little RJA, Rubin DB. *Statistical Analysis with Missing Data*. 2nd ed. New York: John Wiley; 2002.

241. Jenkinson M, Bannister P, Brady M, Smith S. Improved optimization for the robust and accurate linear registration and motion correction of brain images. *Neuroimage.* Oct 2002;17(2):825-841.

242. Andersson J, Jenkinson M, Smith S. Non-linear registration, aka Spatial normalisation *in FMRIB technical report*. 2007.

243. Buchel C, Holmes AP, Rees G, Friston KJ. Characterizing stimulus-response functions using nonlinear regressors in parametric fMRI experiments. *NeuroImage.* Aug 1998;8(2):140-148.

244. Ardekani BA, Braun M, Hutton BF, Kanno I, Iida H. A fully automatic multimodality image registration algorithm. *J Comput Assist Tomogr.* Jul-Aug 1995;19(4):615-623.

245. Lammertsma AA, Hume SP. Simplified reference tissue model for PET receptor studies. *Neuroimage.* Dec 1996;4(3 Pt 1):153-158.

246. Mukherjee J, Christian BT, Dunigan KA, et al. Brain imaging of 18F-fallypride in normal volunteers: blood analysis, distribution, test-retest studies, and preliminary assessment of sensitivity to aging effects on dopamine D-2/D-3 receptors. *Synapse.* Dec 1 2002;46(3):170-188.

247. Wu Y, Carson RE. Noise reduction in the simplified reference tissue model for neuroreceptor functional imaging. *J Cereb Blood Flow Metab.* Dec 2002;22(12):1440-1452.

248. Benjamini Y, Hochberg Y. Controlling the False Discovery Rate - a Practical and Powerful Approach to Multiple Testing. *Journal of the Royal Statistical Society Series B-Methodological.* 1995;57(1):289-300.

249. Sokol-Hessner P, Camerer CF, Phelps EA. Emotion regulation reduces loss aversion and decreases amygdala responses to losses. *Soc Cogn Affect Neurosci.* Feb 15 2012.

250. De Martino B, Camerer CF, Adolphs R. Amygdala damage eliminates monetary loss aversion. *Proc Natl Acad Sci U S A.* Feb 23 2010;107(8):3788-3792.

251. Ferbinteanu J, Shapiro ML. Prospective and retrospective memory coding in the hippocampus. *Neuron.* Dec 18 2003;40(6):1227-1239.

252. Burgess N, Maguire EA, O'Keefe J. The human hippocampus and spatial and episodic memory. *Neuron.* Aug 15 2002;35(4):625-641.

253. Mason WA, Capitanio JP, Machado CJ, Mendoza SP, Amaral DG. Amygdalectomy and responsiveness to novelty in rhesus monkeys (Macaca mulatta): generality and individual consistency of effects. *Emotion.* Feb 2006;6(1):73-81.

254. Cools R, D'Esposito M. Inverted-U-shaped dopamine actions on human working memory and cognitive control. *Biol Psychiatry.* Jun 15 2011;69(12):e113-125.

255. Seamans JK, Yang CR. The principal features and mechanisms of dopamine modulation in the prefrontal cortex. *Prog Neurobiol.* Sep 2004;74(1):1-58.

256. Cummings JL. Anatomic and behavioral aspects of frontal-subcortical circuits. *Ann N Y Acad Sci.* Dec 15 1995;769:1-13.

257. Doll BB, Jacobs WJ, Sanfey AG, Frank MJ. Instructional control of reinforcement learning: a behavioral and neurocomputational investigation. *Brain Res.* Nov 24 2009;1299:74-94.

258. Frank MJ. Computational models of motivated action selection in corticostriatal circuits. *Curr Opin Neurobiol.* Jun 2011;21(3):381-386.

259. Grace AA. Phasic versus tonic dopamine release and the modulation of dopamine system responsivity: a hypothesis for the etiology of schizophrenia. *Neuroscience.* 1991;41(1):1-24.

260. Frank MJ, Loughry B, O'Reilly RC. Interactions between frontal cortex and basal ganglia in working memory: a computational model. *Cogn Affect Behav Neurosci.* Jun 2001;1(2):137-160.

261. Cepeda C, Radisavljevic Z, Peacock W, Levine MS, Buchwald NA. Differential modulation by dopamine of responses evoked by excitatory amino acids in human cortex. *Synapse.* Aug 1992;11(4):330-341.

262. Cepeda C, Buchwald NA, Levine MS. Neuromodulatory actions of dopamine in the neostriatum are dependent upon the excitatory amino acid receptor subtypes activated. *Proc Natl Acad Sci U S A.* Oct 15 1993;90(20):9576-9580.

263. Levine MS, Cepeda C. Dopamine modulation of responses mediated by excitatory amino acids in the neostriatum. *Adv Pharmacol.* 1998;42:724-729.

264. Frank MJ. Hold your horses: a dynamic computational role for the subthalamic nucleus in decision making. *Neural Netw.* Oct 2006;19(8):1120-1136.

265. Cepeda C, Hurst RS, Altemus KL, et al. Facilitated glutamatergic transmission in the striatum of D2 dopamine receptor-deficient mice. *J Neurophysiol.* Feb 2001;85(2):659-670.

266. Gonzalez S, Rangel-Barajas C, Peper M, et al. Dopamine D4 receptor, but not the ADHD-associated D4.7 variant, forms functional heteromers with the dopamine D2S receptor in the brain. *Mol Psychiatry.* Jun 2012;17(6):650-662.

267. Cohen JD, Braver TS, O'Reilly RC. A computational approach to prefrontal cortex, cognitive control and schizophrenia: recent developments and current challenges. *Philos Trans R Soc Lond B Biol Sci.* Oct 29 1996;351(1346):1515-1527.

268. St Onge JR, Stopper CM, Zahm DS, Floresco SB. Separate prefrontal-subcortical circuits mediate different components of risk-based decision making. *J Neurosci.* Feb 22 2012;32(8):2886-2899.

269. Volkow ND, Chang L, Wang GJ, et al. Low level of brain dopamine D2 receptors in methamphetamine abusers: association with metabolism in the orbitofrontal cortex. *Am J Psychiatry.* Dec 2001;158(12):2015-2021.

270. Floresco SB, Tse MT, Ghods-Sharifi S. Dopaminergic and glutamatergic regulation of effort- and delay-based decision making. *Neuropsychopharmacology.* Jul 2008;33(8):1966-1979.

271. Jensen J, McIntosh AR, Crawley AP, Mikulis DJ, Remington G, Kapur S. Direct activation of the ventral striatum in anticipation of aversive stimuli. *Neuron.* Dec 18 2003;40(6):1251-1257.

272. Poldrack RA. Can cognitive processes be inferred from neuroimaging data? *Trends Cogn Sci.* Feb 2006;10(2):59-63.

273. Gossop M, Griffiths P, Powis B, Strang J. Severity of heroin dependence and HIV risk. II. Sharing injecting equipment. *AIDS Care.* 1993;5(2):159-168.

274. Gossop M, Griffiths P, Powis B, Strang J. Severity of heroin dependence and HIV risk. I. Sexual behaviour. *AIDS Care.* 1993;5(2):149-157.

275. Gossop M, Griffiths P, Powis B, Strang J. Severity of dependence and route of administration of heroin, cocaine and amphetamines. *Br J Addict.* Nov 1992;87(11):1527-1536.

276. Fishbein DH, Eldreth DL, Hyde C, et al. Risky decision making and the anterior cingulate cortex in abstinent drug abusers and nonusers. *Brain Res Cogn Brain Res.* Apr 2005;23(1):119-136.

277. Kohno M, Ghahremani DG, Morales AM, et al. Risk-Taking Behavior: Dopamine D2/D3 Receptors, Feedback, and Frontolimbic Activity. *Cereb Cortex.* Aug 21 2013.

278. Jentsch JD, Taylor JR. Impulsivity resulting from frontostriatal dysfunction in drug abuse: implications for the control of behavior by reward-related stimuli. *Psychopharmacology (Berl).* Oct 1999;146(4):373-390.

279. Paulus MP, Hozack, N. E., Zauscher, B. E., Frank, L., Brown, G. G., Braff, D. L., Schuckit, M.A. Behavioral and functional neuroimaging evidence for prefrontal dysfunction in methamphetamine-dependent subjects. *Neuropsychopharmacology.* Jan 2002;26(1):53-63.

280. Baicy K, London ED. Corticolimbic dysregulation and chronic methamphetamine abuse. *Addiction.* Apr 2007;102 Suppl 1:5-15.

281. Hong LE, Gu H, Yang Y, et al. Association of nicotine addiction and nicotine's actions with separate cingulate cortex functional circuits. *Arch Gen Psychiatry.* Apr 2009;66(4):431-441.

282. Kelly C, Zuo XN, Gotimer K, et al. Reduced interhemispheric resting state functional connectivity in cocaine addiction. *Biol Psychiatry.* Apr 1 2011;69(7):684-692.

283. Sutherland MT, McHugh MJ, Pariyadath V, Stein EA. Resting state functional connectivity in addiction: Lessons learned and a road ahead. *NeuroImage.* Oct 1 2011;62(4):2281-2295.

284. Wilcox CE, Teshiba TM, Merideth F, Ling J, Mayer AR. Enhanced cue reactivity and fronto-striatal functional connectivity in cocaine use disorders. *Drug Alcohol Depend.* May 1 2010;115(1-2):137-144.

285. Bornovalova MA, Cashman-Rolls A, O'Donnell JM, et al. Risk taking differences on a behavioral task as a function of potential reward/loss magnitude and individual differences in impulsivity and sensation seeking. *Pharmacology, Biochemistry, and Behavior.* 2009.

286. Galvan A, Schonberg T, Mumford J, Kohno M, Poldrack RA, London ED. Greater risk sensitivity of dorsolateral prefrontal cortex in young smokers than in nonsmokers. *Psychopharmacology (Berl).* May 5 2013.

287. Kohno M, Ghahremani D, Morales AM, et al. Risk-taking behavior: dopamine D2/D3 receptors, feedback and frontolimbic activity. *Cerebral Cortex* 2013.

288. St Onge JR, Ahn S, Phillips AG, Floresco SB. Dynamic fluctuations in dopamine efflux in the prefrontal cortex and nucleus accumbens during risk-based decision making. *J Neurosci.* Nov 21 2012;32(47):16880-16891.

289. Krasnova IN, Justinova Z, Ladenheim B, et al. Methamphetamine self-administration is associated with persistent biochemical alterations in striatal and cortical dopaminergic terminals in the rat. *PLoS One.* 2010;5(1):e8790.

290. Schwendt M, Rocha A, See RE, Pacchioni AM, McGinty JF, Kalivas PW. Extended methamphetamine self-administration in rats results in a selective reduction of dopamine transporter levels in the prefrontal cortex and dorsal striatum not accompanied by marked monoaminergic depletion. *J Pharmacol Exp Ther.* Nov 2009;331(2):555-562.

291. Bechara A, Dolan S, Hindes A. Decision-making and addiction (part II): myopia for the future or hypersensitivity to reward? *Neuropsychologia.* 2002;40(10):1690-1705.

292. Konova AB, Moeller SJ, Tomasi D, Volkow ND, Goldstein RZ. Effects of Methylphenidate on Resting-State Functional Connectivity of the Mesocorticolimbic Dopamine Pathways in Cocaine Addiction. *JAMA Psychiatry.* Jun 26 2013:1-11.

293. Power JD, Barnes KA, Snyder AZ, Schlaggar BL, Petersen SE. Spurious but systematic correlations in functional connectivity MRI networks arise from subject motion. *NeuroImage.* Feb 1 2011;59(3):2142-2154.

294. Kim SJ, Lyoo IK, Hwang J, et al. Prefrontal grey-matter changes in short-term and long-term abstinent methamphetamine abusers. *Int J Neuropsychopharmacol.* Apr 2006;9(2):221-228.

295. Nakama H, Chang L, Fein G, Shimotsu R, Jiang CS, Ernst T. Methamphetamine users show greater than normal age-related cortical gray matter loss. *Addiction.* Aug 2011;106(8):1474-1483.

296. Schwartz DL, Mitchell AD, Lahna DL, et al. Global and local morphometric differences in recently abstinent methamphetamine-dependent individuals. *NeuroImage.* May 1 2010;50(4):1392-1401.

297. Volkow ND, Fowler JS, Wolf AP, et al. Changes in brain glucose metabolism in cocaine dependence and withdrawal. *Am J Psychiatry.* May 1991;148(5):621-626.

298. London ED, Simon SL, Berman SM, et al. Mood disturbances and regional cerebral metabolic abnormalities in recently abstinent methamphetamine abusers. *Arch Gen Psychiatry.* Jan 2004;61(1):73-84.

299. Salo R, Ursu S, Buonocore MH, Leamon MH, Carter C. Impaired prefrontal cortical function and disrupted adaptive cognitive control in methamphetamine abusers: a functional magnetic resonance imaging study. *Biol Psychiatry.* Apr 15 2009;65(8):706-709.

300. Simon SL, Dean AC, Cordova X, Monterosso JR, London ED. Methamphetamine dependence and neuropsychological functioning: evaluating change during early abstinence. *J Stud Alcohol Drugs.* May 2010;71(3):335-344.

301. Scott JC, Woods SP, Matt GE, et al. Neurocognitive effects of methamphetamine: a critical review and meta-analysis. *Neuropsychol Rev.* Sep 2007;17(3):275-297.

302. Jentsch JD, Woods JA, Groman SM, Seu E. Behavioral characteristics and neural mechanisms mediating performance in a rodent version of the Balloon Analog Risk Task. *Neuropsychopharmacology.* Jul 2010;35(8):1797-1806.

303. Tanaka SC, Doya K, Okada G, Ueda K, Okamoto Y, Yamawaki S. Prediction of immediate and future rewards differentially recruits cortico-basal ganglia loops. *Nat Neurosci.* Aug 2004;7(8):887-893.

304. Bamford NS, Zhang H, Joyce JA, et al. Repeated exposure to methamphetamine causes long-lasting presynaptic corticostriatal depression that is renormalized with drug readministration. *Neuron.* Apr 10 2008;58(1):89-103.

305. Boileau I, Dagher A, Leyton M, et al. Modeling sensitization to stimulants in humans: an [11C]raclopride/positron emission tomography study in healthy men. *Arch Gen Psychiatry.* Dec 2006;63(12):1386-1395.

306. Lett BT. Repeated exposures intensify rather than diminish the rewarding effects of amphetamine, morphine, and cocaine. *Psychopharmacology (Berl).* 1989;98(3):357-362.

307. Vezina P. Sensitization of midbrain dopamine neuron reactivity and the self-administration of psychomotor stimulant drugs. *Neurosci Biobehav Rev.* Jan 2004;27(8):827-839.

308. Ward SJ, Lack C, Morgan D, Roberts DC. Discrete-trials heroin self-administration produces sensitization to the reinforcing effects of cocaine in rats. *Psychopharmacology (Berl).* Apr 2006;185(2):150-159.

309. Schonberg T, Fox CR, Poldrack RA. Mind the gap: bridging economic and naturalistic risk-taking with cognitive neuroscience. *Trends Cogn Sci.* Jan 2011;15(1):11-19.

310. Redish AD, Jensen S, Johnson A. A unified framework for addiction: Vulnerabilities in the decision process. *Behavioral and Brain Sciences.* 2008.

311. Kalivas PW. Recent understanding in the mechanisms of addiction. *Curr Psychiatry Rep.* Oct 2004;6(5):347-351.

312. Koob GF. Circuits, drugs, and drug addiction. *Adv Pharmacol.* 1998;42:978-982.

313. Volkow ND, Fowler JS, Wang GJ, Swanson JM, Telang F. Dopamine in drug abuse and addiction: results of imaging studies and treatment implications. *Arch Neurol.* Nov 2007;64(11):1575-1579.

314. Everitt BJ, Dickinson A, Robbins TW. The neuropsychological basis of addictive behaviour. *Brain Res Brain Res Rev.* Oct 2001;36(2-3):129-138.

315. Montague PR, Dayan P, Sejnowski TJ. A framework for mesencephalic dopamine systems based on predictive Hebbian learning. *J Neurosci.* Mar 1 1996;16(5):1936-1947.

316. Robinson TE, Berridge KC. Addiction. *Annu Rev Psychol.* 2003;54:25-53.

317. Bechara A. Risky business: emotion, decision-making, and addiction. *J Gambl Stud.* Spring 2003;19(1):23-51.

318. Salamone JD. Functional significance of nucleus accumbens dopamine: behavior, pharmacology and neurochemistry. *Behav Brain Res.* Dec 2 2002;137(1-2):1.

319. Salamone JD. Functions of mesolimbic dopamine: changing concepts and shifting paradigms. *Psychopharmacology (Berl).* Apr 2007;191(3):389.

320. Cools R. Role of dopamine in the motivational and cognitive control of behavior. *Neuroscientist.* Aug 2008;14(4):381-395.

321. Meltzer HY. Relevance of dopamine autoreceptors for psychiatry: preclinical and clinical studies. *Schizophr Bull.* 1980;6(3):456-475.

322. Dreyer JK, Hounsgaard J. Mathematical model of dopamine autoreceptors and uptake inhibitors and their influence on tonic and phasic dopamine signaling. *J Neurophysiol.* Jan 2012;109(1):171-182.

323. Divac I, Fonnum F, Storm-Mathisen J. High affinity uptake of glutamate in terminals of corticostriatal axons. *Nature.* Mar 24 1977;266(5600):377-378.

324. Kim JS, Hasller R, Hau P, Paik KS. Effect of frontal cortex ablation on striatal glutamic acid level in rat. *Brain Res.* Aug 26 1977;132(2):370-374.

325. McGeer PL, McGeer EG, Scherer U, Singh K. A glutamatergic corticostriatal path? *Brain Res.* Jun 10 1977;128(2):369-373.

326. Schultz W, Ungerstedt U. A method to detect and record from striatal cells of low spontaneous activity by stimulating the corticostriatal pathway. *Brain Res.* Feb 24 1978;142(2):357-362.

327. Grace AA, Floresco SB, Goto Y, Lodge DJ. Regulation of firing of dopaminergic neurons and control of goal-directed behaviors. *Trends Neurosci.* May 2007;30(5):220-227.

328. MacKenzie RG, Zigmond MJ. Chronic neuroleptic treatment increases D-2 but not D-1 receptors in rat striatum. *Eur J Pharmacol.* Jul 17 1985;113(2):159-165.

329. Grace AA. The tonic/phasic model of dopamine system regulation and its implications for understanding alcohol and psychostimulant craving. *Addiction.* Aug 2000;95 Suppl 2:S119-128.

330. Anzalone A, Lizardi-Ortiz JE, Ramos M, et al. Dual control of dopamine synthesis and release by presynaptic and postsynaptic dopamine D2 receptors. *J Neurosci.* Jun 27 2012;32(26):9023-9034.

331. Zapata A, Shippenberg TS. D(3) receptor ligands modulate extracellular dopamine clearance in the nucleus accumbens. *J Neurochem.* Jun 2002;81(5):1035-1042.

332. Joseph JD, Wang YM, Miles PR, et al. Dopamine autoreceptor regulation of release and uptake in mouse brain slices in the absence of D(3) receptors. *Neuroscience.* 2002;112(1):39-49.

333. Volkow ND, Wang GJ, Begleiter H, et al. High levels of dopamine D2 receptors in unaffected members of alcoholic families: possible protective factors. *Arch Gen Psychiatry.* Sep 2006;63(9):999-1008.

334. Cox RW, Jesmanowicz A, Hyde JS. Real-time functional magnetic resonance imaging. *Magn Reson Med.* Feb 1995;33(2):230-236.

335. Cohen MS. Real-time functional magnetic resonance imaging. *Methods.* Oct 2001;25(2):201-220.

336. Weiskopf N, Scharnowski F, Veit R, Goebel R, Birbaumer N, Mathiak K. Self-regulation of local brain activity using real-time functional magnetic resonance imaging (fMRI). *J Physiol Paris.* Jul-Nov 2004;98(4-6):357-373.

337. Turkington TG. Introduction to PET instrumentation. *J Nucl Med Technol.* Mar 2001;29(1):4-11.

338. Rohren EM, Turkington TG, Coleman RE. Clinical applications of PET in oncology. *Radiology.* May 2004;231(2):305-332.

339. Verel I, Visser GW, van Dongen GA. The promise of immuno-PET in radioimmunotherapy. *J Nucl Med.* Jan 2005;46 Suppl 1:164S-171S.

340. Muller B, Thoma MH. Vacuum polarization and the electric charge of the positron. *Phys Rev Lett.* Dec 14 1992;69(24):3432-3434.

341. Rousset OG, Ma Y, Evans AC. Correction for partial volume effects in PET: principle and validation. *J Nucl Med.* May 1998;39(5):904-911.

342. Soret M, Bacharach SL, Buvat I. Partial-volume effect in PET tumor imaging. *J Nucl Med.* Jun 2007;48(6):932-945.

343. Slifstein M, Kegeles LS, Xu X, et al. Striatal and extrastriatal dopamine release measured with PET and [(18)F] fallypride. *Synapse.* May 2010;64(5):350-362.

344. Vandehey NT, Moirano JM, Converse AK, et al. High-affinity dopamine D2/D3 PET radioligands 18F-fallypride and 11C-FLB457: a comparison of kinetics in extrastriatal regions using a multiple-injection protocol. *J Cereb Blood Flow Metab.* May 2010;30(5):994-1007.